## ABSTRACT

Title of Dissertation: Transition Metal Polypnictides from Zintl Ions

Scott Charles, Doctor of Philosophy, 1995

Dissertation directed by: Associate Professor Bryan W. Eichhorn

Department of Chemistry & Biochemistry

The chemistry of the soluble $E_7^{3-}$ ions (E = P, As, Sb) with various transition metal complexes has been investigated. Alloys of $K_3E_7$ react with (arene)$M(CO)_3$ (M = Cr, Mo, W) complexes in the presence of three equivalents of 2,2,2-crypt in ethylenediamine to give $[K(2,2,2\text{-crypt})]_3[E_7M(CO)_3]$ complexes. Nine $[E_7M(CO)_3]^{3-}$ compounds (E = P, As, Sb; M = Cr, Mo, W) have been prepared. The compounds have norbornadiene-like $E_7$ fragments, with a formal negative charge associated with the unique two-coordinate pnictogen furthest from the transition metal. The bonding is described as $E_7$ $\pi$–type interactions with the metal center. $^{31}P$ NMR studies show that these compounds undergo an intramolecular wagging process in solution. The $[E_7M(CO)_3]^{3-}$ ions are modestly basic and highly nucleophilic. The complexes react with weak acids, tetraalkylammonium salts and (arene)$M'(CO)_3$ complexes to form the $[K(2,2,2\text{-crypt})]_2[HE_7M(CO)_3]$, $[K(2,2,2\text{-crypt})]_2[RE_7M(CO)_3]$ and $[K(2,2,2\text{-crypt})]_3[(L_2)(CO)_3M'E_7M(CO)_3]$ compounds, respectively. Each of the structures contains a norbornadiene-like $E_7$ fragment bound $\eta^4$ to the $M(CO)_3$ fragment and $\eta^1$ to the appended moiety [$H^+$, $R^+$, $M(CO)_3(en)$] that

is attached to the pnictogen atom furthest from the $M(CO)_3$ center. The $[K(2,2,2\text{-crypt})]_3[\eta^4\text{-}E_7M(CO)_3]$ complexes also react with carbon monoxide at the $M(CO)_3$ center and reversible binds CO to form $[K(2,2,2\text{-crypt})]_3[\eta^2\text{-}E_7M(CO)_4]$ complexes. These complexes are more easily protonated and undergo faster alkylations of the $E_7$ cages than the parent $[K(2,2,2\text{-crypt})]_3[\eta^4\text{-}E_7M(CO)_3]$ compounds. Each of these structures contains an $E_7$ fragment bound $\eta^2$ to the $M(CO)_4$ center. Products were characterized by various physical and spectroscopic techniques including UV-vis, IR, $^1H$, $^{13}C$, and $^{31}P$ NMR spectroscopies, mass spectrometry, elemental analyses, and single crystal X-ray diffraction studies.

# TRANSITION METAL POLYPNICTIDES FROM ZINTL IONS

by

Scott Charles

Dissertation submitted to the Faculty of the Graduate School
of The University of Maryland in partial fulfillment
of the requirements for the degree of
Doctor of Philosophy
1995



Advisory Committee:

Associate Professor Bryan W. Eichhorn, Chairman/Advisor
Professor Samuel Grim
Professor Philip DeShong
Professor Christopher Lobb
Assistant Professor Robert Pilato

## DEDICATION

To Dean Y. Charles

No father has ever been prouder of his son than I am of mine.

## ACKNOWLEDGMENT

I would like to express my sincere gratitude to Bryan Eichhorn for the guidance and suggestions he provided throughout this thesis. Thank you! I hope someone come along to pick up the project, because it is truly exciting and rewarding.

I owe my gratitude to the "younger generation", Lou Tranchitella and D. Web Keogh, for the personal support and companionship they have so unselfishly provided and to the "new generation" of labmates; Bryan Pratt, Jan Danis and Brian Litteer, for helping me put my work here at Maryland into perspective.

I am deeply indebted to Yiu-Fai Lam for his assistance with NMR experiments. He gave freely of his time and expertise.

It was a pleasure to know the ladies of the Business Office. They are the pearl of the Chemistry Department and have earned my respect and admiration with their patience and pleasant smiles.

And lastly, I would like to express my sincere thanks to my wife, Leslie, for providing me with the motivation and emotion necessary to complete a project such as this. The completion of this dissertation signals the end of our being apart and a whisper of "promises of things to come".

## TABLE OF CONTENTS

## LIST OF TABLES

## LIST OF FIGURES

## LIST OF SCHEMES

## ABBREVIATIONS

| | |
|---|---|
| en | ethylenediamine |
| tol | toluene |
| DMF | dimethylformamide |
| DMSO | dimethylsulfoxide |
| pip | piperidine |
| bipy | bipyridine |
| py | pyridine |
| HMPA | hexamethylphosphoric triamide |
| 2,2,2-crypt | 4,7,13,16,21,24-hexaoxa-1,10-diazabicyclo[8.8.8]hexacosane |
| IR | infrared |
| NMR | nuclear magnetic resonance |
| s | second |
| min | minute |
| h | hour |
| ORTEP | Oakridge thermal ellipsoid parameters |
| FAB-MS | fast atom bombardment mass spectroscopy |
| FH MO | Fenske-Hall molecular orbital |
| HOMO | highest occupied molecular orbital |
| SHOMO | second highest occupied molecular orbital |
| mM | millimolar |
| ε | molar absoptivity |
| ppm | parts per million |
| ppt | precipitant |
| Me | methyl |

| | |
|---|---|
| Et | ethyl |
| Pr | propyl |
| Bu | butyl |
| Ph | phenyl |
| equiv | equivalent |

# CHAPTER 1

## Introduction

### 1.1 Objective

The long range goals of this project are to develop a new class of ligand-free main group / transition metal polyhedral clusters ("molecular alloys") and study their solution dynamics, electronic structures, and reactivities towards small molecules. These polyhedral clusters could find uses similar to those of established main group / transition metal binary and ternary solid state materials used in a wide variety of technological applications such as catalysts (Pt-Sn reforming catalysts),[1,2] ceramic coatings (WC, TiN coatings),[3] ionic conductors ($TiS_2$)[4] and superconductors ($Nb_3Ge$ and $PbMo_6S_8$).[5]

However, before the materials applications of these "molecular alloys" can be advanced in the production of new solids, the molecular chemistry must first be understood. Therefore, besides being of academic interest, the short term goals are to 1) investigate the chemistry of the parent polypnictide anions, 2) develop new classes of transition metal polypnictides, 3) probe the structural and electronic relationships between the polypnictide anions and the transition metal fragments, 4) investigate the reactivity of these new transition metal polypnictides, and 5) investigate the structures, solution dynamics and redox properties of the various types of transition metal polypnictides developed.

## 1.2 Background

The first main group polyanions were prepared over 100 years ago by Joannis.[6,7] He observed that ammonia solutions of sodium and metallic lead precipitated sodium plumbides having the compositions $NaPb_4 \cdot 2NH_3$ or $NaPb_2$ depending on the reaction conditions. In 1907 subsequent work by Kraus showed that these plumbides behaved as electrolytes in liquid ammonia suggesting that they were dissociating like salts to give the $Na^+$ and $Pb_n^-$ (n = 2, 4) species.[8,9] He also observed that the lead solute would plate out on an anode, that the lead solute could be precipitated on addition of normal lead(II) salts, and that tin showed similar reactions with sodium solutions. For the lead solute, Kraus observed that there appeared to be two lead atoms per charge and concluded that the solute was $NaPb_2$. In 1917, more thorough measurements by Smyth of the plumbides demonstrated that 2.26 moles of Pb per Faraday of current plated out on the anode from the saturated liquid ammonia solutions.[10] He suggested that there was an equilibrium between $Pb_2^-$ and $Pb_3^-$ in liquid ammonia. A related study by Peck yielded maximum solubilities of 4.0 Te/Na and 2.33 Sb/Na.[11] These observations by Smyth and Peck led Kraus to speculate that the polyanionic salts in equilibrium with the metals were $Na_4Pb \cdot Pb_8$, $Na_3Sb \cdot Sb_6$ and $Na_2Te \cdot Te_3$ and that as electrolytes they contained the anions $Pb_9^{4-}$, $Sb_7^{3-}$ and $Te_4^{2-}$, respectively.

The next information on this type of polyanion was an extensive study conducted by Zintl and co-workers in the early 1930's.[12-15] Using extractions of binary alloys and potentiometric titrations of sodium or potassium in liquid ammonia with a normal-valent salt of the metal (*e.g.*, $PbI_2$, $BiI_3$, etc), Zintl and co-workers identified the solution species of many homopolyatomic anions including $Pb_7^{4-}$, $E_9^{4-}$ (E = Sn, Pb), $E_m^{3-}$ (E = As, Sb, Bi; m = 3, 7), $E_5^{3-}$ (E = As, Bi) and $E_n^{2-}$ (E = Se, Te; n

= 2, 3, 4) in solution. This thorough investigation and its discoveries led Laves to label this type of highly charged polyanion as "Zintl ions".[16] The potentiometric measurements monitored oxidation of the alkali metal and, subsequently, of any polymetal anions until a permanent precipitate of metal occurred. For example, the early

$$(4 + 2x)Na + xPbI_2 \longrightarrow Na_4Pb_x + 2xNaI \qquad (1.1)$$

stages of the Na/Pb reaction could be described by eq. 1.1. The alloy extraction studies were carried out by investigating the direct solution of binary alloys and their mixtures in liquid ammonia. Extraction of composition E/Na = 2.25 to ~ 2.75 (E = Sn, Pb) gave pure solutions and excellent analyses for the homoatomic $E_9^{3-}$ compositions. The composition NaSb readily yielded a saturated solution analyzed to be $NaSb_{2.33}$ ($Na_3Sb_{6.99}$) while the composition $NaBi_{1.95}$ yielded only unsaturated solutions after several months.

Zintl and co-workers also attempted to isolate crystalline salts from the metal-saturated polylead, -tin, -antimony and -bismuth solutions at low temperatures in liquid ammonia by evaporation of the solvent. Evaporations of the solvent initially gave amorphous solids that were apparently the $Na(NH_3)_n^+$ salts of the indicated anions (eq. 1.2) or reverted to the corresponding binary intermetallic phases of the alkali metal and

$$xNa^+_{(NH_3)} + E_n^{m-}{}_{(NH_3)} + NH_{3\,(l)} \longrightarrow [Na(NH_3)_y]_mE_{n\,(s)} \qquad (1.2)$$

E = Sn, Pb, Sb, Bi

the element. Loss of ammonia yielded metallic compounds that were identical to the starting alloys. It is important to note that phase composition (and structures) in the corresponding binary alloy systems show no relationship to the compositions for the

solutes in ammonia. The instability of simple solid derivatives of the polymetal anions formed in liquid ammonia solution seemingly results from a pronounced tendency for the electrons on the anions to transfer back onto the alkali metal cations in the dense solid state and thus to yield structures and bonding chracteristics of intermetallic phases.

In 1970 Kummer and Diehl[17] isolated the first solid derivative of a Zintl anion, $Na_4Sn_9 \cdot 6\text{-}8en$. They found the alloy composition $NaSn_{2.4\text{-}2.5}$ slowly dissolved in ethylenediamine or other polyamines on warming, and that $Na_4Sn_9$ precipitated on the addition of monoglyme or THF. Magnetic measurements of $Na_4Sn_9 \cdot 6\text{-}8en$ showed it to be highly diamagnetic. The incomplete crystal study identified a distorted and somewhat disordered $Sn_9$ polyhedron. The $Na_4(en)_5Ge_9$ and $Na_3(en)_4Sb_7$ "polyanionic salts" were also isolated by similar techniques and identified by elemental analyses. Diehl,[17,18] von Schnering[19,20] and others[21,22] have subsequently isolated various Zintl salts and determined the crystal structures of several naked metal clusters including $E_9^{4-}$ (E = Ge,Sn),[17,23] $E_7^{3-}$ (E = P,[24,25] As[26]), $P_{11}^{3-}$ [27]and $P_{16}^{2-}$.[20] The $E_9^{4-}$ (E = Ge, Sn) ions were isolated by extraction of binary alloys into polar solvents (*e.g.*, en, DMF) similar to the method discussed above. The $E_7^{3-}$ (E = P, As) ions were isolated as alkaline earth salts (*e.g.*, $Ba_3E_{14}$, $Sr_3P_{14}$) by reacting metallic alkaline earth metals with pnictogens in the ratio of 1:4 to 1:5 at temperatures from 850 °C to 1150 °C in quartz ampoules. Also at increased temperature, as described previously, the $P_{11}^{3-}$ ion was isolated as $Na_3P_{11}$ from the reaction of elemental sodium and phosphorus in a 2-3 P/Na ratio. Hönle and co-workers surprisingly isolated the remarkably stable $P_{16}^{2-}$ ion as the $PPh_4^+$ salt when $Na_3P_7$ suspended in THF reacted with $PPh_4Cl$ (eq. 1.3). The reaction is quite reproducible, however, the actual synthetic pathway is unknown at this time.

$$Na_3P_7 + PPh_3Cl \xrightarrow{THF} (PPh_4)_2P_{16} + NaCl \qquad (1.3)$$

More recently, Corbett and co-workers have used the macrocyclic ligand, 2,2,2-crypt (**1.I**), as a sequestering agent for the alkali metal cations of the binary alloys.[22]

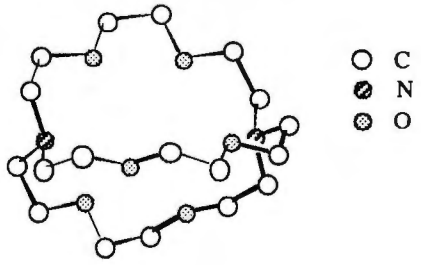


**1.I**

The sequestration of the alkali metal cations prevents electron transfer from the Zintl polyanions back onto the cations thus preventing the formation of the generally more stable intermetallic phases and allows the isolation of crystalline salts on solvent removal. The 2,2,2-crypt cavity diameter (d = 2.80 Å) is ideal for an ion the size of $K^+$ (d = 2.66 Å), but works with $Na^+$ (d = 1.90 Å) as well.[28,29] Corbett and co-workers also found that the presence of 2,2,2-crypt increased the solubility of sodium and potassium alloys of antimony, bismuth, tin and lead in ammonia and ethylenediamine.[30] This follows the observations of Dye and co-workers who previously demonstrated that the addition of 2,2,2-crypt gave a considerable enhancement of the solubility of the alkali metals in a diversity of solvents (*e.g.*, HMPA, en, ethylamine, diglyme, THF, diethyl ether, diethylamine) and had allowed for the isolation and structural determination of the salt $[Na(2,2,2\text{-crypt})^+]Na^-$.[31]

The large "cryptated" cations often dominate the crystalline packing and sometimes allow for disorder among the anions.[22] The use of 2,2,2-crypt has lead to the isolated of such stable Zintl anions as $Ge_9^{m-}$ (m = 2, 3, 4),[32] $Ge_4^{2-}$, $Sn_9^{m-}$ (m = 3,[33] 4[34]), $Sn_5^{2-}$,[35] $Pb_5^{2-}$,[35] $Sb_4^{2-}$,[36] and $Sb_7^{3-}$.[30,36] Other interesting homopolyatomic anions that have been isolated with the aid of 2,2,2-crypt include

$As_{11}^{3-}$,[21] $As_{22}^{4-}$ [37] and $Sb_{11}^{3-}$.[38] All anions were prepared by extraction of the appropriate alloy into ethylenediamine in the presence of 2,2,2-crypt. Haushalter and others have shown that mixed elemen: Zintl ions can also be prepared such as $Tl_2Te_2^{2-}$,[39] $As_2Se_6^{3-}$,[40] and $TlSn_9^{3-}$,[39] with even more remarkable and diverse structures.

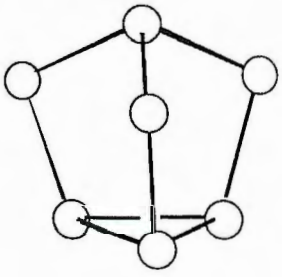

**1.II**

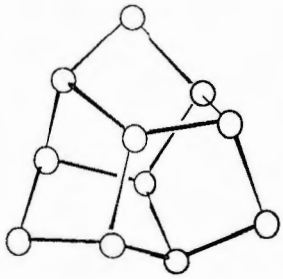

**1.III**

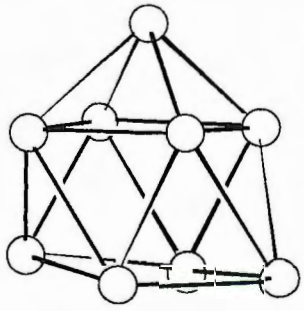

**1.IV**

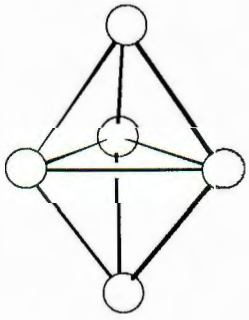

**1.V**

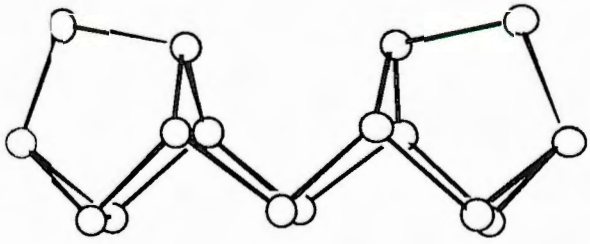

**1.VI**

The structural diversity among the homoatomic Zintl ions is illustrated by the structures of $E_7^{3-}$ (E = P, As, Sb) (**1.II**), $E_{11}^{3-}$ (E = P, As, Sb) (**1.III**), $Sn_9^{4-}$ (**1.IV**), $Pb_5^{2-}$ (**1.V**), and $P_{16}^{2-}$ (**1.VI**) as shown above. The Group 14 polyatomic anions form electron-deficient boron-hydride-like polyhedral clusters which follow Wade's rules.[41] Examples include the $Ge_9^{2-}$ and $Pb_5^{2-}$ (**1.V**) ions that have *closo*-structures (2n + 2 electrons) and the $Sn_9^{4-}$ ion (**1.IV**) (2n + 4 electrons)[34] that has a *nido*-structure. Rudolph has provided the most informative insights into the solution chemistry of the

Group 14 Zintl ions using NMR studies.[42,43] He investigated the $Sn_9^{4-}$, $Pb_9^{4-}$, $Sn_xPb_{9-x}^{4-}$ and $Sn_xGe_{9-x}^{4-}$ families by the appropriate $^{119}Sn$ or $^{207}Pb$ NMR spectroscopy. He found that all nine of the atoms of each cluster were averaged in an intramolecular manner on the NMR time scale. For example, the $Sn_9^{4-}$ ion gave a single $^{119}Sn$ resonance in en at *ca.* -1230 ppm (upfield from $Me_4Sn$) that was split by $^{119}Sn$-$^{117}Sn$ coupling into the multiplet predicted for a nine-atom cluster. The spectrum was unchanged at -40 °C in liquid $NH_3$. He also witnessed the effects of ion-pairing as a function of the cation for both the homogeneous ions, $Sn_9^{4-}$ and $Pb_9^{4-}$. In en the $^{119}Sn$ resonance for $Sn_9^{4-}$ shifts smoothly from -1115 ppm for $Cs^+$ to -1241 ppm for $Li^+$ and -1253 ppm for $[Na(2,2,2\text{-crypt})]^+$. The comparable range for $Pb_9^{4-}$ is -891 to -1224 ppm.[42,43]

In contrast to the boron-hydride-like structures of the Group 14 Zintl ions, the Group 15 polyatomic anions tend to form polycyclic hydrocarbon-like structures such as the nortricyclane $E_7^{3-}$ (E = P, As, Sb) (**1.II**) and trishomocubane $E_{11}^{3-}$ (E = P, As, Sb) (**1.III**) compounds. The structural analogies reside in the fact that E and $E^-$ are electronically equivalent to CH and $CH_2$, respectively. In a valence bond formalism, one can assign a localized -1 charge to each two-coordinate pnictogen atom.[44] Baudler has extensively studied the phosphorus Zintl ions by $^{31}P$ NMR spectroscopy.[45-47] She found the "bare" anions are highly fluxtional in solution and usually give rise to second order $^{31}P$ NMR spectra. In particular, she found that $Li_3P_7$ dissolved in THF gives a single $^{31}P$ resonance at -118 ppm (upfield from $H_3PO_4$) at room temperature by averaging of the phosphorus atoms in an intramolecular manner on the NMR time scale. However, at low temperature the $P_7^{3-}$ spectrum shows three separate groups of signals at -57, -103 and -162 ppm in the intensity ratio of 1:3:3, corresponding to the three different types of phosphorus atoms; the apex, the bridging and the basal phosphorus atoms, respectively. Also at low temperature, the bridging resonance is a pseudo triplet

produced by the P-nuclei bound to the lithium ($J_{P\text{-}Li}$ = ~ 6 Hz), illustrating the ion-pairing involved in the molecule.[45]

Another aspect of the solution dynamics exhibited by these phosphorus Zintl ions is their ability to invert at phosphorus. The first example of inversion at phosphorus for a polycyclophosphane was reported for P9*t*-Bu3 by Baudler.[47-49] She has subsequently reported inversion at phosphorus for other polycyclic organophosphanes such as $P_9Et_3$, $P_{11}i\text{-}Pr_3$, $P_{12}i\text{-}Pr_4$, $P_{13}i\text{-}Pr_5$ and $P_{14}i\text{-}Pr_4$.[47]

Dahl,[50,51] Scherer[52] and others[53] have investigated the reactivity of various transition metal complexes with the main group *elements*, but the chemistry of the true Zintl *anions* with transition metals has been rather limited. The first record of a transition metal fragment bonded to a naked Zintl ion was reported by Rudolph[54] when $^{119}Sn$ and $^{207}Pb$ NMR spectroscopic evidence of $(PPh_3)_2PtM_9^{4-}$ (M = Sn, Pb) were obtained in 1983. The only other reported transition metal / Group 14 Zintl ion complexes are the [*closo*-$E_9Cr(CO)_3]^{4-}$ (E = Sn, Pb)[55,56] complexes and the $[Sn_6\{Cr(CO)_5\}_6]^{2-}$ (**1.VII**) complex containing the octahedral $Sn_6^{2-}$ ion.[57]

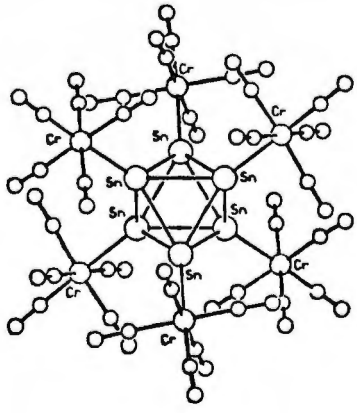


**1.VII**

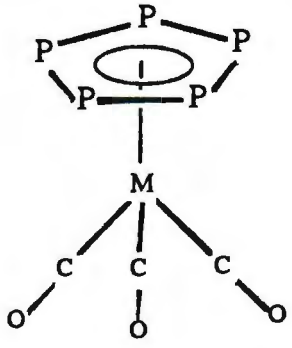


**1.VIII**

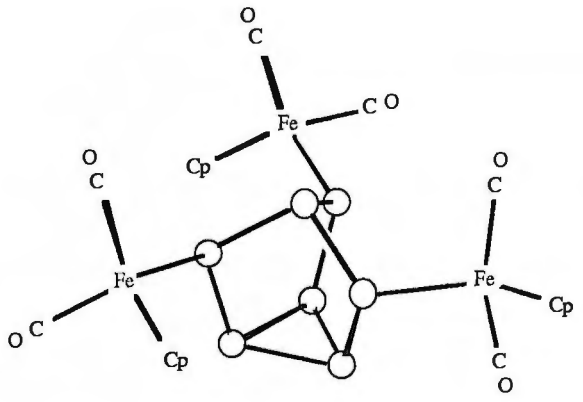


**1.IX**

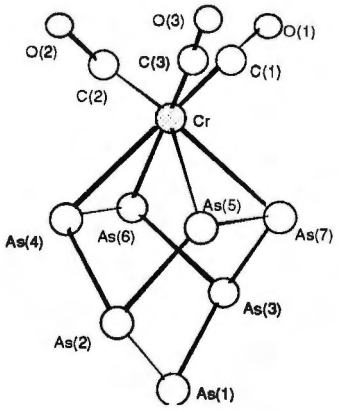


**1.X**

The transition metal / Group 15 Zintl ion complexes reported prior to this work include $[\eta^5\text{-}P_5M(CO)_3]^n$ (M = Cr, Mo, W; n = -1: M = Mn; n = 0) (**1.VIII**),[58] $[P_7\{Fe(CO)_2(Cp)\}_3]$ (**1.IX**),[59] $[As_7Cr(CO)_3]^{3-}$(**1.X**),[60] and $^1_\infty[Rb{\bullet}NbAs_8]^{2-}$ (**1.XI**).[61] Fritz *et al.*[62-65] have recently investigated the coordination ability of some tricycloheptaphosphanes $P_7R_3$ (R = Et, *i*-Pr, $SiMe_3$) toward metal carbonyl fragments of chromium and iron and have isolated such compounds as $P_7R_3[Cr(CO)_5]_n$ (n = 1, 2) and $P_7R_3[Cr(CO)_5]_n[Cr(CO)_4]$ (n = 1, 2, 3). And finally, $[P_{14}\{Ni(P\textit{n}\text{-}Bu_3)_2\}_4]$ has been recently sythesized and structurally characterized by Fenske.[66]

Some of the transition metal polypnictide compounds presented above are prepared in a "rational" manner and are analogous to their hydrocarbon analogues. For example, the $[(\eta^5\text{-}P_5)M(CO)_3]^{1-}$ ions (M = Cr, Mo, W) (**1.VIII**)[58] are prepared from $LiP_5$ and $M(CO)_6$ precursors and are isostructural to the $[(\eta^5\text{-}C_5H_5)M(CO)_3]^{1-}$ compounds (eq. 1.4). Similarly, $P_7^{3-}$ reacts with three equiv of $CpFe(CO)_2Br$ to form $[P_7\{Fe(CO)_2(Cp)\}_3]$ (**1.IX**) in a simple metathesis reaction.[59] Other compounds, such

$$LiP_5 + M(CO)_6 \longrightarrow [(\eta^5\text{-}P_5)M(CO)_3]^{1-} + Li^+ + 3\,CO \qquad (1.4)$$

M = Cr, Mo, W

$$P_7^{3-} + 3\ CpFe(CO)_2Br \longrightarrow [P_7\{Fe(CO)_2(Cp)\}_3] + 3\ Br^- \qquad (1.5)$$

as the crown-shaped $^1_\infty[Rb{\bullet}NbAs_8]^{2-}$ (**1.XI**)[61] and the boron-hydride-like $[Sb_7\{Ni(CO)\}_3]^{3-}$ (**1.XII**--without carbonyls)[67] have unprecedented structural types, and their synthetic pathways are not as obvious. The [Rb(2,2,2-crypt)]$^+$ salt of $^1_\infty[Rb{\bullet}NbAs_8]^{2-}$ was obtained initially during the synthesis of $Rb_3As_7$ in a sealed Nb

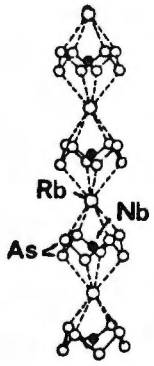


**1.XI**

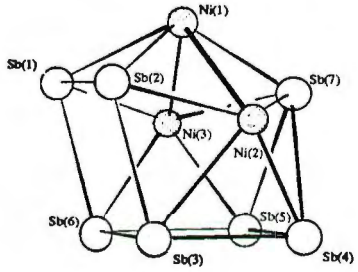


**1.XII**

tube when Rb was mistakenly added in too large an excess. A "direct" synthesis was obtained by fusing $Nb_2O_5$, Rb and As under argon in an Nb ampoule followed by extraction of the alloy into ethylenediamine with 3 equiv of 2,2,2-crypt. The [K(2,2,2-crypt)]$^+$ salt of $[Sb_7\{Ni(CO)\}_3]^{3-}$ was obtained when the ethylenediamine solution of $K_3Sb_7$ reacted with 1 equiv of $Ni(CO)_2(PPh_3)_2$ in the presence of 3 equiv of 2,2,2-crypt (eq. 1.6).

$$Sb_7^{3-} + Ni(CO)_2(PPh_3)_2 \xrightarrow{3\ 2,2,2\text{-crypt}} [Sb_7\{Ni(CO)\}_3]^{3-} + CO + 2\ PPh_3 \qquad (1.6)$$

The systematical development of the area of transition metal polypnictide chemistry to determine the structural and chemical diversity of these systems is the focus of this study. Of particular interest are the reactions of $E_7^{3-}$ ions (E = P, As, Sb) with various unsaturated transition metal fragments and the reactivities of the resultant transition metal polypnictide complexes. The synthesis of polypnictide metal carbonyl complexes was initially investigated because the CO ligands help stablize the high negative charge on the compounds and provide excellent spectroscopic handles with which to study the main group / transition metal interactions.

This thesis is organized as follows. Chapter 2 describes the synthesis, structure and characterization of the $[K(2,2,2\text{-crypt})]_3[E_7M(CO)_3]$ compounds (E = P, As, Sb; M = Cr, Mo, W).[44] Chapter 3 describes the synthesis, structure and characterization of the $[K(2,2,2\text{-crypt})]_2[HP_7M(CO)_3]$ (M = Cr, W) compounds.[68] Chapter 4 describes the synthesis, structure and characterization of the $[K(2,2,2\text{-crypt})]_2[RP_7W(CO)_3]$ (R = Me, Et, *n*-Bu, $CH_2Ph$) compounds.[69] Chapter 4 also describes the formation of the symmetrical $[R_2P_7]^-$ ions and the subsequent alkylated symmetric and asymmetric $R_2R'P_7$ compounds.[69] Chapter 5 describes the synthesis, structure and characterization of the $[K(2,2,2\text{-crypt})]_3[P_7M(CO)_4]$ (M = Mo, W) compounds, of the $[K(2,2,2\text{-crypt})]_2[HP_7M(CO)_4]$ (M = Mo, W) compounds and of $[K(2,2,2\text{-crypt})]_2[(CH_2Ph)P_7W(CO)_4]$.[70] Chapter 6 describes the synthesis, structure and characterization of the $[K(2,2,2\text{-crypt})]_3[(L_2)(CO)_2WP_7M(CO)_3]$ (M = Cr, W; $L_2$ = en, $DMF_2$) compounds.[71]

Other compounds prepared in the course of this study that are not described herein include $[P_7Ni(CO)]^{3-}$ (**1.XIII**)[72] and $[E_7HPt(PPh_3)]^{2-}$ (E = P, As) (**1.XIV**).[72]

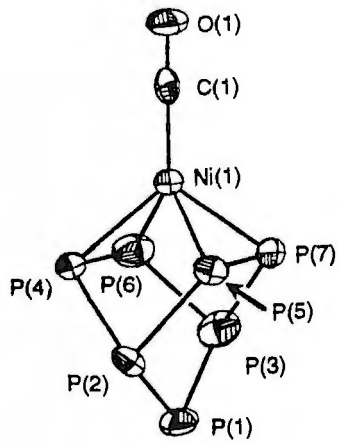


**1.XIII**

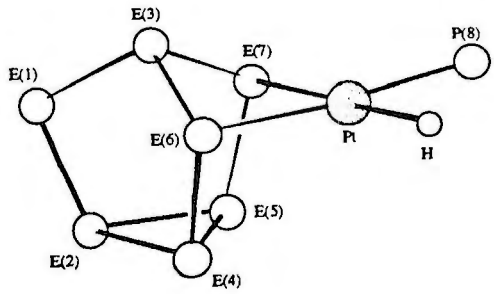


**1.XIV**

## 1.3 References


(1) Burch, R. *J. Catalysis* **1981**, *71*, 348.

(2) Keim, W. *New J. Chem.* **1994**, *18*, 93-96.

(3) *Refractory Materials*; Margrave, J. L., Ed.; Academic Press: New York, 1971.

(4) Clement, R. P.; Davies, W. B.; Green, M. L. H.; Jacobson, A. J. *Inorg. Chem.* **1978**, *17*, 2754 and references therein.

(5) *Chemistry of Oxide Superconductors*; Rao, C. N. R., Ed.; Blackwell Scientific Publications, Inc.: Palo Alto, 1988.

(6) Joannis, A. *Comp. Rend.* **1891**, *113*, 795-798.

(7) Joannis, A. *Comp. Rend.* **1892**, *114*, 585-587.

(8) Kraus, C. A. *J. Am. Chem. Soc.* **1907**, *29*, 1557-1571.

(9) Kraus, C. A. *J. Am. Chem. Soc.* **1922**, *44*, 1216-1239.

(10) Smyth, F. H. *J. Am. Chem. Soc.* **1917**, *39*, 1299-1312.

(11) Peck, E. B. *J. Am. Chem. Soc.* **1918**, *40*, 335-347.

(12) Zintl, E.; Harder, A. *Z. Phys. Chem. Abt. A* **1931**, *154*, 47.

(13) Zintl, E.; Goubeau, J.; Dullenkopf, W. *Z. Phys. Chem. Abt. A* **1931**, *154*, 1.

(14) Zintl, E.; W, D. *Z. Phys. Chem. Abt. B* **1932**, *16*, 183.

(15) Zintl, E.; Kaiser, H. *Z. Anorg. Allg. Chem.* **1933**, *211*, 113.

(16) Laves, F. *Naturwissenschaften* **1941**, *29*, 244.

(17) Diehl, L.; Khodadedeh, K.; Kummer, D.; Strahle, J. *Z. Naturforsch* **1976**, *318*, 522-524.

(18) Diehl, L.; Kummer, D. *Angew. Chem. Int. Ed. Engl.* **1970**, *9*, 895.

(19) von Schnering, H. G.; Hönle, W. *Chem. Rev.* **1988**, *88*, 243-273.

(20) von Schnering, H. G.; Manriquez, V.; Hönle, W. *Angew. Chem. Int. Ed. Engl.* **1981**, *20*, 594-595.

(21) Belin, C. H. E. *J. Am. Chem. Soc.* **1980**, *102*, 6036-6040.

(22) Corbett, J. D. *Chem. Rev.* **1985**, *85*, 383-397.

(23) Teller, R. G.; Krause, L. J.; Haushalter, R. C. *Inorg. Chem.* **1983**, *22*, 1809-1812.

(24) Dahlmann, W.; von Schnering, H. G. *Naturwissenschaften* **1972**, *59*, 420.

(25) Dahlmann, W.; von Schnering, H. G. *Naturwissenschaften* **1973**, *60*, 429.

(26) Schmettow, W.; von Schnering, H. G. *Angew. Chem. Int. Ed. Engl.* **1977**, *16*, 857.

(27) Wichelhaus, W.; von Schnering, H. G. *Naturwissenschaften* **1973**, *60*, 104.

(28) Hilgenfeld, R.; Saenger, W. R. *Top. Curr. Chem.* **1982**, *101*, 1-82.

(29) Vögtle, F.; Weber, E. *Angew. Chem. Int. Ed. Engl.* **1979**, *18*, 753-776.

(30) Adolphson, D. G.; Corbett, J. D.; Merryman, D. J. *J. Am. Chem. Soc.* **1976**, *98*, 7234-7239.

(31) Tehan, F. J.; Barnett, B. L.; Dye, J. L. *J. Am. Chem. Soc.* **1974**, *96*, 7203-7208.

(32) Belin, C. H. E.; Corbett, J. D.; Cisar, A. *J. Am. Chem. Soc.* **1977**, *99*, 7163-7169.

(33) Critchlow, S. C.; Corbett, J. D. *J. Am. Chem. Soc.* **1983**, *105*, 5715-5716.

(34) Corbett, J. D.; Edwards, P. A. *J. Am. Chem. Soc.* **1977**, *99*, 3313-3317.

(35) Edwards, P. A.; Corbett, J. D. *Inorg. Chem.* **1977**, *16*, 903-907.

(36) Critchlow, S. C.; Corbett, J. D. *Inorg. Chem.* **1984**, *23*, 770-774.

(37) Haushalter, R. C.; Eichhorn, B. W.; Rheingold, A. L.; Geib, S. J. *J. Chem. Soc., Chem. Commun.* **1988**, 1027.

(38) Bolle, U.; Tremel, W. *J. Chem. Soc., Chem. Commun.* **1992**, 91-93.

(39) Burns, R. C.; Corbett, J. D. *J. Am. Chem. Soc.* **1982**, *104*, 2804-2810.

(40) Belin, C. H. E.; Charbonnel, M. M. *Inorg. Chem.* **1982**, *21*, 2504-2506.

(41) Wade, K. *J. Chem. Soc., Chem. Commun.* **1971**, 792-793.

(42) Rudolph, R. W.; Wilson, W. L.; Taylor, R. C. *J. Am. Chem. Soc.* **1981**, *103*, 2480-2481.

(43) Rudolph, R. W.; Wilson, W. L.; Parker, F.; Taylor, R. C.; Young, D. C. *J. Am. Chem. Soc.* **1978**, *100*, 4629-4630.

(44) Charles, S.; Eichhorn, B. W.; Rheingold, A. L.; Bott, S. G. *J. Am. Chem. Soc.* **1994**, *116*, 8077-8086.

(45) Baudler, M. *Angew. Chem. Int. Ed. Engl.* **1982**, *21*, 492-512.

(46) Baudler, M. *Angew. Chem. Int. Ed. Engl.* **1987**, *26*, 419-441.

(47) Baudler, M.; Glinka, K. *Chem. Rev.* **1993**, *93*, 1623-1667.

(48) Baudler, M.; Aktalay, Y.; Kazmierezak, K.; Hahn, J. *Z. Naturforsch* **1982**, *38b*, 428-433.

(49) Baudler, M.; Hahn, J.; Arndt, V.; Koll, B.; Kazmierczak, K.; Därr, E. *Z. Anorg. Allg. Chem.* **1986**, *538*, 7-20.

(50) Barr, M. E.; Adams, B. R.; Weller, R. R.; Dahl, L. F. *J. Am. Chem. Soc.* **1991**, *113*, 3052-3060.

(51) Foust, A. S.; Foster, M. S.; Dahl, L. F. *J. Am. Chem. Soc.* **1969**, *91*, 5631-5633.

(52) Scherer, O. J.; Winter, R.; Heckmann, G.; Wolmershauser, G. *Angew. Chem. Int. Ed. Engl.* **1991**, *30*, 850-852.

(53) Capozzi, G.; Chiti, L. D. V., M.; Peruzzini, M.; Stoppioni, P. *J. Chem. Soc., Chem. Commun.* **1986**, 1799-1800.

(54) Teixidor, F.; Leutkens, M. L., Jr.; Rudolph, R. W. *J. Am. Chem. Soc.* **1983**, *105*, 149-150.

(55) Eichhorn, B. W.; Haushalter, R. C.; Pennington, W. T. *J. Am. Chem. Soc.* **1988**, *110*, 8704-8706.

(56) Eichhorn, B. W.; Haushalter, R. C. *J. Chem. Soc., Chem. Commun.* **1990**, 937-938.

(57) Schiemenz, B.; Huttner, G. *Angew. Chem. Int. Ed. Engl.* **1993**, *32*, 297-298.

(58) Baudler, M.; Etzbach, T. *Angew. Chem. Int. Ed. Engl.* **1991**, *30*, 580-582.

(59) Fritz, G.; Hoppe, K. D.; Hönle, W.; Weber, D.; Mujica, C.; Manriquez, V.; von Schnering, H. G. *J. Organomet. Chem.* **1983**, *249*, 63-80.

(60) Eichhorn, B. W.; Haushalter, R. C.; Huffman, J. C. *Angew. Chem. Int. Ed. Engl.* **1989**, *28*, 1032-1033.

(61) von Schnering, H. G.; Wolf, J.; Weber, D.; Ramirez, R.; Meyer, T. *Angew. Chem. Int. Ed. Engl.* **1986**, *25*, 353-354.

(62) Fritz, G.; Schneider, H.-W.; Hönle, W.; von Schnering, H. G. *Z. Anorg. Allg. Chem.* **1990**, *584*, 21.

(63) Fritz, G.; Mayer, B.; Matern, E. *Z. Anorg. Allg. Chem.* **1992**, *608*, 7.

(64) Fritz, G.; Layher, E.; Hönle, W.; von Schnering, H. G. *Z. Anorg. Allg. Chem.* **1991**, *595*, 67.

(65) Hönle, W.; von Schnering, H. G.; Fritz, G.; Schneider, H.-W. *Z. Anorg. Allg. Chem.* **1990**, *584*, 51.

(66) Fenske, D., **1995**, personal communication with Dr. Bryan W. Eichhorn.

(67) Charles, S.; Eichhorn, B. W.; Bott, S. G. *J. Am. Chem. Soc.* **1993**, *115*, 5837-5838.

(68) Charles, S. C.; Eichhorn, B. W.; Fettinger, J. C. **1995**, in preparation.

(69) Charles, S.; Fettinger, J. C.; Eichhorn, B. W. *J. Am. Chem. Soc.* **1995**, *117*, 5303-5311.

(70) Charles, S.; Eichhorn, B. W.; Fettinger, J. C.; Bott, S. G. *Inorg. Chem.* **1995**, submitted.

(71) Charles, S.; Eichhorn, B. W.; Fettinger, J. C.; Bott, S. G. **1995**, in preparation.

(72) Charles, S.; Eichhorn, B. W.; Bott, S. G.; Fettinger, J. C. *Angew. Chem. Int. Ed. Engl.* **1995**, submitted.

# CHAPTER 2

## Synthesis, Structure, and Properties of $[E_7M(CO)_3]^{3-}$ Complexes where E = P, As, Sb and M = Cr, Mo, W.

### 2.1 Introduction

The reactivity of the group 15 Zintl ions with transition metal complexes has been virtually unexplored with only a few compounds reported to date. The products isolated thus far are quite different from those obtained from elemental precursors under similar reaction conditions. Some of the compounds are prepared in a "rational" manner and are analogous to their hydrocarbon analogues. For example, the $[(\eta^5\text{-}P_5)M(CO)_3]^{1-}$ ions (M = Cr, Mo, W) (**1.VIII**)[1] are prepared from $LiP_5$ and $M(CO)_6$ precursors and are isostructural to the $[(\eta^5\text{-}C_5H_5)M(CO)_3]^{1-}$ compounds. Similarly, $P_7^{3-}$ reacts with three equiv. of $(\eta^5\text{-}C_5H_5)Fe(CO)_2Br$ to form $[(\eta^5\text{-}C_5H_5)Fe(CO)_2]_3P_7$ (**1.IX**)[2] in a simple metathesis reaction. Other compounds, such as $^1_\infty[Rb{\bullet}NbAs_8]^{2-}$ (**1.XI**)[3] and $[Sb_7Ni_3(CO)_3]^{3-}$ (**1.XII**)[4] have unprecedented structural types and their synthetic pathways are not as obvious. The structure of the former has an $As_8^{8-}$ ring that is reminiscent of $S_8$; whereas the latter contains a *nido*-$Sb_7Ni_3$ core that is a new type of 10 atom polyhedron.

The reactions of the $E_7^{3-}$ ions (**1E**, where E = P, As, Sb) (**1.II**) with various unsaturated transition metal fragments have been investigated. In this chapter, the synthesis, structure and properties of the $[E_7M(CO)_3]^{3-}$ complexes where E = P, As, Sb and M = Cr, Mo, W are described. Accounts of the synthesis and structure of $[As_7Cr(CO)_3]^{3-}$ [5] and the structure and bonding of $[Sb_7Mo(CO)_3]^{3-}$ [6,7] have appeared.

## 2.2 Results and Discussion

### 2.2.1 Synthesis

Ethylenediamine (en) solutions of $K_3E_7$ (E = P, As, Sb) react with toluene solutions of $LM(CO)_3$ (M = Cr, W; L = mesitylene; M = Mo; L = cycloheptatriene) in the presence of three equiv. of 2,2,2-crypt to give $[K(2,2,2\text{-crypt})]_3[E_7M(CO)_3]$ complexes according to eq. 2.1.[8] Nine $[E_7M(CO)_3]^{3-}$ compounds have been prepared and are generically described by the symbol **2EM** where E denotes the main group element and M denotes the transition metal. The compounds crystallize from solution in

$$K_3E_7 + LM(CO)_3 + 3\ 2,2,2\text{-crypt} \xrightarrow{\text{en / tol}} [K(2,2,2\text{-crypt})]_3[E_7M(CO)_3] + L \quad (2.1)$$

E = P, As, Sb

M = Cr, Mo, W

L = mesitylene (M = Cr, W), cycloheptatriene (M = Mo)

reasonable yields (30-80%) with the exceptions of the **2AsMo** and **2SbMo** compounds which were obtained in lower crystalline yields (~ 3 %). No attempts were made to optimize crystalline yields. $^{31}P$ NMR spectra of the crude reaction mixtures involving $K_3P_7$ show virtually quantitative conversions to the **2PM** compounds.

Microanalyses and single crystal X-ray analyses of the crystalline solids revealed solvate molecules (en or toluene) for some of the crystalline compounds (see Sections 2.2.3 and 2.4). The colors of the complexes vary from bright orange for E = P, dark red-orange for E = As and dark red-brown for E = Sb. The W compounds are slightly darker in color than the Mo or Cr complexes. The crystals and their solutions are very air and moisture sensitive. The nine **2EM** compounds have been characterized by elemental analyses, electronic absorption, IR spectroscopy, $^{13}C$ and $^{31}P$ NMR

spectroscopies, and representative single crystal X-ray diffraction studies. The 2EM compounds have a distorted (norbornadiene)$Fe(CO)_3$-type structure (**2.I**). A qualitative analysis of the electronic structure and bonding was performed with the aid of Fenske-Hall molecular orbital calculations.

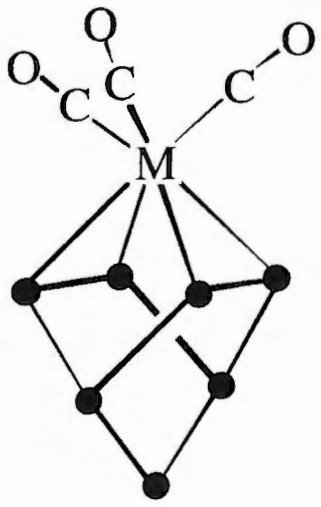


**2.I**

It was previously noted,[5] the chemistry outlined by eq. 2.1 and similar reactions involving the synthesis of $[E_9Cr(CO)_3]^{4-}$ ions (E = Sn, Pb) [9,10] do not occur in the absence of 2,2,2-crypt. Structural and NMR spectroscopic studies on $K_4Sn_9$ • HMPA[11,12,13] and $^{31}P$ NMR spectroscopic studies on $Li_3P_7$ [14,15] clearly reveal significant ion pairing (coordination) between the main group polyanions and the alkali ions in solution and in the solid state. Subsequent investigations revealed that the chemistry outlined by eq. 2.1 **does** occur in the absence of 2,2,2-crypt, but is transition metal dependent. For example, $^{31}P$ NMR monitoring shows that ethylenediamine solutions of $K_3P_7$ and (mesitylene)$W(CO)_3$ quatitatively give the $[P_7W(CO)_3]^{3-}$ ion according to eq. 2.2. However, the chemistry outlined by eq. 2.2 does **not** proceed

$$K_3P_7 + (\text{mesitylene})W(CO)_3 \xrightarrow{\text{en}} [P_7W(CO)_3]^{3-} + 3\,K^+ + \text{mesitylene} \quad (2.2)$$

when M = Cr. When M = Cr, the ion pairing of $K_3P_7$ must first be broken by a reagent that can sequester $K^+$ (*e.g.* 2,2,2-crypt, 18-crown-6, etc) before the $Cr(CO)_3$ moiety can complex with $P_7^{3-}$ to form the $[P_7Cr(CO)_3]^{3-}$ ion. Eqs. 2.1 and 2.2 chemistry proceeds slowly at room temperature at approximately equal rates ($t_{1/2} \approx 3$ h).

### 2.2.2 Reactivity

$^{13}C$ and $^{31}P$ NMR spectroscopic studies on compounds **2EM** show that $E_7$ - $M(CO)_3$ dissociation is not occurring on the NMR time scale at room temperature. Carbonyl-phosphorus coupling is observed for the **2PM** compounds and the three phosphorus environments remain distinct from -60 to 30 °C (see Section 2.2.7). Furthermore, in the absence of external oxidants or $H^+$ sources, compounds **2EM** do not exchange with added $E'_7^{3-}$ ions or $M'(CO)_3$ fragments (E≠E'; M≠M').

The reactions between the **2ECr** compounds and other $E'_7^{3-}$ ions (eq. 2.3) were monitored by $^{13}C$ NMR spectroscopy and showed no signs of exchange after several days at room temperature or 2 h at 70 °C. In the presence of protio impurities or external oxidants, however, exchange is facile and mixed main- group complexes are formed.[16]

$$\underset{\textbf{2ECr}}{[E_7Cr(CO)_3]^{3-}} + \underset{\textbf{1E'}}{E'_7{}^{3-}} \not\longrightarrow \underset{\textbf{2E'Cr}}{[E'_7Cr(CO)_3]^{3-}} + \underset{\textbf{1E}}{E_7{}^{3-}} \quad (2.3)$$

E or E' = P, As, Sb; E ≠ E'

Similar reactions between **2EM** compounds and other $M'(CO)_3$ precursors do not give exchange products **2EM'** and $M(CO)_3$. Instead, bimetallic products are

formed of general formula $[(L_2)(CO)_3M'E_7M(CO)_3]^{3-}$, where M and M' are Cr, Mo or W; E = P, As, Sb; and $L_2$ is en or $(DMF)_2$ (*e.g.*, $[(en)(CO)_3WP_7W(CO)_3]^{3-}$) (eq. 2.4).[8,17,18] The synthesis, structure and properties of these compounds will be described in Chapter 6.[18]

$$[P_7W(CO)_3]^{3-} + W(CO)_3 \xrightarrow{en} [(en)(CO)_3WP_7W(CO)_3]^{3-} \qquad (2.4)$$

**Scheme 2.1**

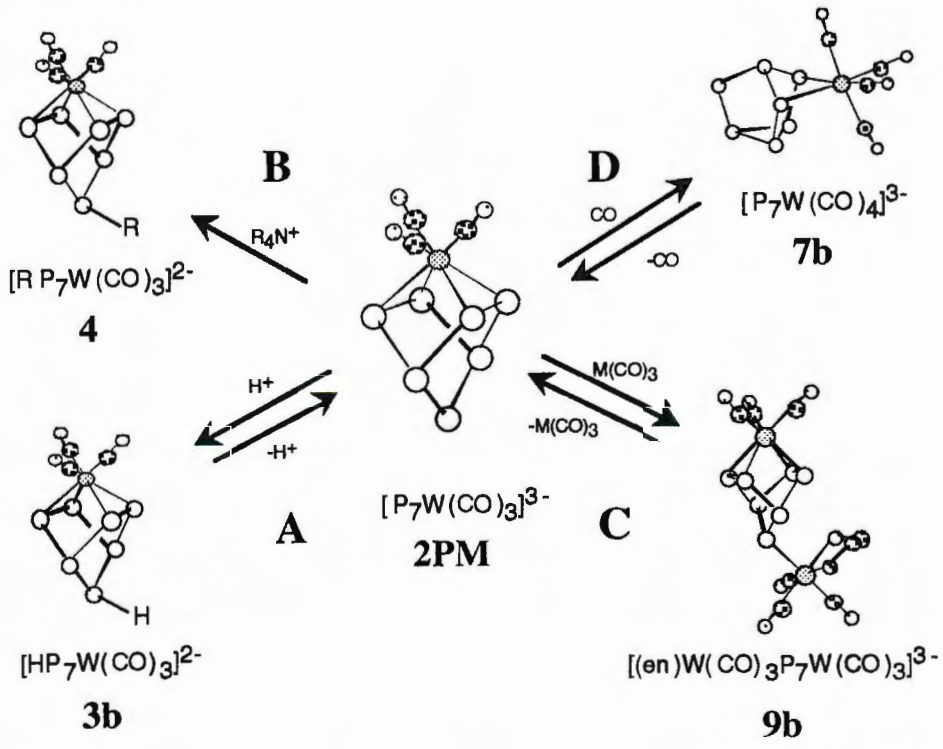


The $[E_7M(CO)_3]^{3-}$ ions react with both electrophiles and nucleophiles. As an example, the reactivity of the $[P_7W(CO)_3]^{3-}$ ion is described in Scheme 2.1. The electrophilic reactivity is ligand based, whereas the nucleophilic reactivity is metal based. The $[E_7M(CO)_3]^{3-}$ ions have a formal negative charge associated with the unique two-coordinate pnictogen atom furthest from the transition metal (the E(1) site). This pnictogen atom remains highly nucleophilic and is the site of attack by various

electrophiles (*e.g.*, $H^+$, $R^+$, $W(CO)_3(en)$, etc).[8,17,18,19] These reactions will be described in Chapters 3, 4 and 6. Under more forcing conditions, CO reacts at the metal center.[20] This reaction will be discussed in Chapter 5.

### 2.2.3 Solid State Structures

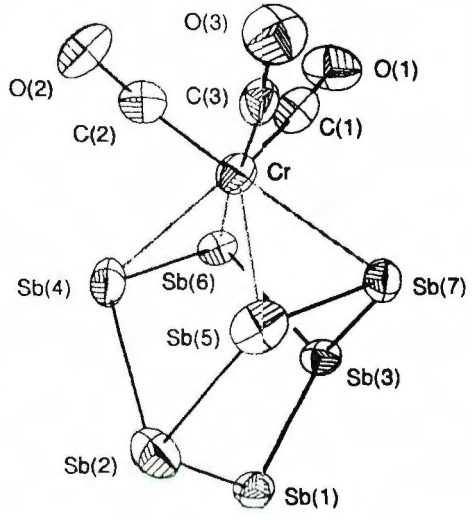


**Figure 2.1.** ORTEP drawing of the $[Sb_7Cr(CO)_3]^{3-}$ ion, **2SbCr**, using the common atomic numbering scheme.

The $[K(2,2,2\text{-crypt})]^+$ **2PCr** and **2SbCr** have been characterized by single crystal X-ray diffraction. The single crystal X-ray structures of **2AsCr** and **2SbMo** were reported previously.[5,6,7] An ORTEP drawing of **2SbCr** is given in Figure 2.1 as an example of the $E_7M(CO)_3^{3-}$ structure type. The crystallographic data are summarized in Table 2.1 and pertinent bond distances and angles for the three crystallographically characterized **2EM** compounds are reported in Table 2.2.

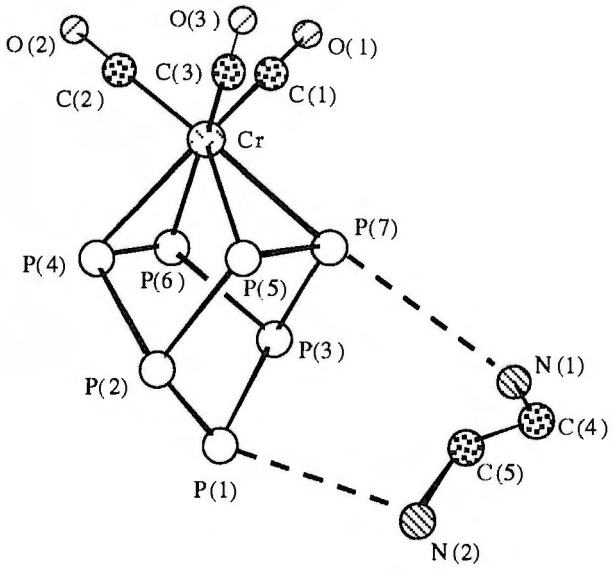


**Figure 2.2.** Ball-and-stick drawing of the $[P_7Cr(CO)_3]^{3-}$ ion, **2PCr**, using the common atomic numbering scheme. Dotted lines represent hydrogen bonding interactions.

The $[E_7M(CO)_3]^{3-}$ structure type contains a $C_s$ $\eta^4$-$E_7^{3-}$ group attached to a $C_{3v}$ $M(CO)_3$ center. The ions have $C_s$ molecular symmetry with one mirror plane defined by E(1), M and C(1). The [K(2,2,2-crypt)]$^+$ salts of the **2PCr** and **2AsCr** ions crystallize in space group $P\bar{1}$ ; the latter with a toluene solvate and the former with an en molecule hydrogen bonded to the $P_7$ cage as shown in Figure 2.2. The two N-P separations average 3.57 Å which are consistent with hydrogen bonding interactions.[21] The [K(2,2,2-crypt)]$^+$ salts of the $[Sb_7M(CO)_3]^{3-}$ ions where M = Cr, W are isomorphic and crystallize in the monoclinic space group *C2/c* although molecular $C_s$ symmetry is not crystallographically imposed. The refinement of the $[Sb_7W(CO)_3]^{3-}$ complex was hampered by lack of observed data and will not be reported here.

The Cr-C distances are slightly shorter and the C-O distances slightly longer than those of the neutral ($\eta^6$-benzene)$Cr(CO)_3$ precursor [$d_{Cr-C}$ = 1.841 Å, $d_{C-O}$ = 1.58 Å][22] as one would expect from charge considerations and π-backbonding effects. The

virtual $C_s$ symmetry observed in the **2EM** complexes leave two carbonyl ligands [C(2) and C(3)] in positions *trans* to E(7) and E(6), respectively (average C-M-E angle = 175°). Therefore, there is a slight lengthening of the Cr-E contacts to E(6) and E(7) relative to E(4) and E(5) due to the high *trans* influence of the CO ligands.

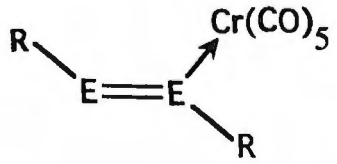


**2.II**

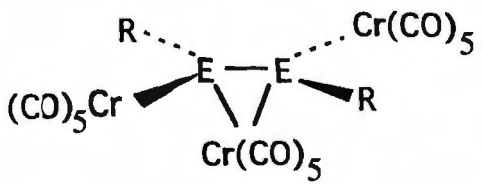


**2.III**

It is informative to compare the E-E and M-E contacts for compounds **2EM** to those observed in the $R_2E_2[Cr(CO)_5]_n$ series where E = P, As, Sb and n = 0, 1, 2, 3.[23,24] The n = 0 members are the well known RE=ER compounds with unbridged E-E double bonds. Schematic drawings of the n = 1 and n = 3 structure types are given in **2.II** and **2.III**. Representative bond distances for these compounds and the **2ECr** ions are listed in Table 2.3. The E-Cr contacts in the type **2.II** compounds are simple dative bonds with distances quite similar to the E-Cr contacts in the $Cr(ER_3)_3(CO)_3$ and related compounds.[25-28] Moreover, the E-E distances (and $^1J_{P-P}$ values) are virtually unchanged from the RE=ER type compounds.[23] In contrast, the E-E distances and the E-Cr contacts to the bridging $Cr(CO)_5$ fragments in type **2.III** compounds are substantially longer than those in type **2.II**. The E-Cr and E-E distances observed for compounds **2ECr** are quite similar to those found for type **2.III** compounds. These similarities are suggestive of a diene-like model in which the $E_7^{3-}$ fragment is attached through π-type interactions. These interactions are discussed in Section 2.2.4 below.

**Chart 2.1**

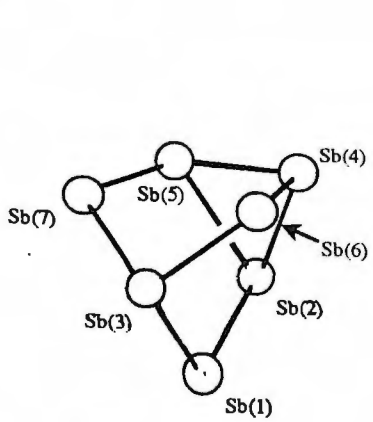


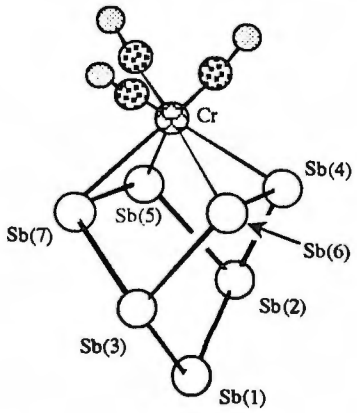


| Bond (Å)/Angle ( ° ) | $Sb_7^{3-}$ [a] | $[Sb_7Cr(CO)_3]^{3-}$ |
|---|---|---|
| Sb(4)-Sb(5) | 2.895 | 3.331 |
| Sb(6)-Sb(7) | 4.296 | 3.715 |
| Sb(4)-Sb(6) | 2.727 | 2.700 |
| Sb(1)-Sb(3) | 2.769 | 2.723 |
| Cr-C (ave) | --- | 1.80 |
| C-O (ave) | --- | 1.18 |
| Sb(6)-Sb(3)-Sb(7) | 100.5 | 81.3 |
| Sb(4)-Sb(2)-Sb(5) | 60.0 | 71.7 |

[a] Data are averaged.

In general, the E-E bonds in the $E_7^{3-}$ fragments of the $[E_7Cr(CO)_3]^{3-}$ ions fall into three categories: four short bonds between E(1)-E(2), E(1)-E(3), E(4)-E(6) and E(5)-E(7); four single bond contacts between E(3)-E(6), E(3)-E(7), E(2)-E(4), and E(2)-E(5); and a long secondary bond[36] between E(4)--E(5). The structural changes that occur in the $E_7^{3-}$ fragment upon complexation are best illustrated by the $Sb_7^{3-}$ [37,38] / $[Sb_7Cr(CO)_3]^{3-}$ pair (Chart 2.1). The primary distortion occurs by significant lengthening of the Sb(4)-Sb(5) bond of 2.895 Å in $Sb_7^{3-}$ to a secondary bonding distance of 3.331(4) Å in $[Sb_7Cr(CO)_3]^{3-}$. In turn, the nonbonding Sb(6)--Sb(7) contact of 4.296(4) Å in $Sb_7^{3-}$ is significantly decreased to 3.715(4) Å in the Cr complex. The changes in bond angles E(4)-E(2)-E(5) [60.0° → 71.7°] and E(6)-E(3)-E(7) [100.5° → 81.3°] also illustrate the $E_7$ cage distortions upon coordination. The $Cr(CO)_3$ moiety seems to fit the best into the $As_7^{3-}$ fragment in that **2AsCr** displays the

smallest overall distortions from the parent $E_7^{3-}$ cluster and shows the least relative E(4)--E(5) / E(6)--E(7) asymmetry of the three structurally characterized compounds. Despite this fact, the E(4)--E(5) / E(6)--E(7) bond asymmetries are quite pronounced for all compounds in the solid state ($\Delta$ E-E $\approx$ 0.20 - 0.35 Å) yet the fluxional nature of the compounds in solution renders the four E atoms equivalent on the NMR time scale (see Section 2.2.7).

### 2.2.4 Electronic Structure of $[E_7M(CO)_3]^{3-}$

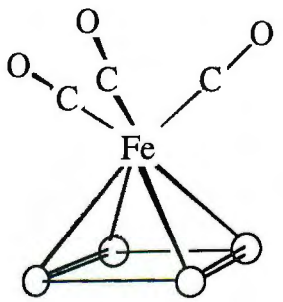


**2.IV**

With the aid of Fenske-Hall molecular orbital (FH MO) calculations,[39-42] molecular orbital diagrams for the **2EM** complexes have been constructed from the constituent $C_{3v}$ $Cr(CO)_3$ and $E_7^{3-}$ fragments with and without E(4)--E(5) / E(6)--E(7) asymmetries. As with any system studied by FH MO method, one can gain insight into the trends in orbital interactions between compounds, but absolute energies and specific orbital orderings are of little value.

The electronic structures of $C_{3v}$ $M(CO)_3$ fragments are well known.[43] As previously mentioned, the **2EM** structure type is similar to that of (norbornadiene)$Fe(CO)_3$. Accordingly, the metal - ligand interactions in the **2EM** compounds are reminiscent of those in ($\eta^4$-$C_4H_4$)$Fe(CO)_3$, (**2.IV**), with a rectangular

distortion of the cyclobutadiene ligand.[43] Using this formalism, one obtains an 18-electron configuration at Cr through coordination of a 6-electron $E_4^{2-}$ fragment to the 12-electron $Cr(CO)_3$ center. The other -1 charge of $E_7^{3-}$ is formally localized on the $E_7$ cage (discussed below).

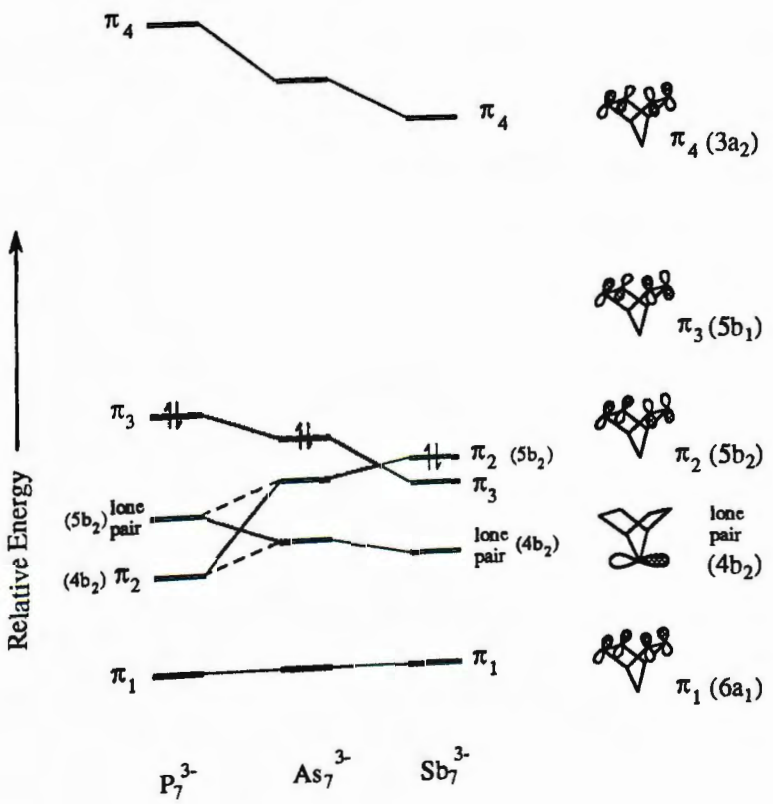


**Figure 2.3.** Qualitative molecular orbital diagram for the idealized $C_{2v}$ $E_7^{3-}$ fragments of the $[E_7M(CO)_3]^{3-}$ ions where E = P, As, Sb. The energies of the $\pi_1$ molecular orbitals were normalized to illustrate the trends in the series.

It is informative to first examine the changes in electronic structure of the $E_7^{3-}$ fragments as one progresses from Sb → As → P. These are shown diagrammatically in Figure 2.3. In order to illustrate the bonding trends within the $E_7^{3-}$ series, the fragment energies were normalized such that the energy of the $\pi_1$ orbitals were equivalent. The

$P_7^{3-}$ fragment represents one limiting case of a cyclobutadiene type system with a rectangular distortion. The two π-bonding orbitals, $\pi_1$ ($6a_1$) and $\pi_2$ ($4b_2$), fall below the π-antibonding orbitals, $\pi_3$ ($5b_1$) and $\pi_4$ ($3a_2$), as expected. The lone pair on P(1) is primarily localized in the $5b_2$ fragment orbital with some contribution from the $4b_2$. Due to the relatively strong π interactions between the phosphorus atoms, the $\pi_2$ orbital is well below the $\pi_3$ orbital. The π bonding diminishes in the $E_7^{3-}$ fragments as one progresses from P → As → Sb as is observed in the RE=ER compounds (E = P, As, Sb).[23,24] Accordingly, the stabilization of $\pi_2$ and destabilization of the $\pi_3$ decrease such that the two orbitals are virtually degenerate for $Sb_7^{3-}$. This $\pi_2$-$\pi_3$ degeneracy

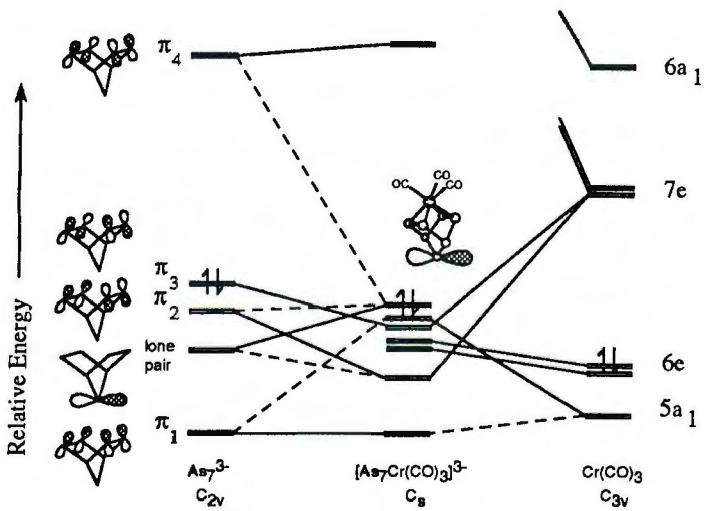


**Figure 2.4.** Qualitative molecular orbital diagram for the $[As_7Cr(CO)_3]^{3-}$ complex showing the interactions of the $As_7^{3-}$ and $Cr(CO)_3$ fragments.

represents the undistorted limit for cyclobutadiene , but in this case, the degeneracy is due to the lack of p-orbital interaction. For the $As_7^{3-}$ and $Sb_7^{3-}$ fragments, the E(1) lone pairs are almost exclusively associated with the $4b_2$ orbitals and drop below the $\pi_2$ orbitals.

The $[E_7Cr(CO)_3]^{3-}$ interaction diagrams were calculated from both atomic basis sets and transformed basis sets of the fragment molecular orbitals in order to trace the origins of the orbital interactions. The molecular orbital diagram for $[As_7Cr(CO)_3]^{3-}$ was the least complicated by mixing and is shown in Figure 2.4. Again, the energies of the $\pi_1$-derived orbitals were normalized to that of **2AsCr** in order to illustrate the bonding trends across the series. Because of the low symmetry of the complexes ($C_s$) and the large number of high lying pnictogen lone pairs, significant orbital mixing was observed in all the $E_7^{3-}$ fragments. However, the major interactions involve the four "π-type orbitals" of the $E_7^{3-}$ fragment in analogy to $(\eta^4\text{-}C_4H_4)Fe(CO)_3$. The primary orbital interactions involve the stabilization of the $\pi^2$ and $\pi^3$ $E_7^{3-}$ fragment molecular orbitals upon complexation by interactions with the 7e fragment orbitals of $Cr(CO)_3$. These interactions transfer significant charge onto the $Cr(CO)_3$ fragment, resulting in the destabilization of the filled $5a_1$ and 6e $Cr(CO)_3$ fragment orbitals upon complexation. The $\pi_1$ and $\pi_4$ orbitals essentially come straight across, the latter as the LUMO of the three **2ECr** complexes. It is interesting to note that, in the $E_7^{3-}$ field, the $5a_1$ orbital of the $Cr(CO)_3$ fragment is artificially stablized[43] relative to the 6e oribtal due to the high charge on the complex. Interaction with the $E_7^{3-}$ fragment brings this orbital back up to its "expected" position.[43]

The As(1) lone pair of the $As_7^{3-}$ fragment remains highly localized and comes across as the HOMO of the **2AsCr** ion whereas the lone pair of **2SbCr** is distributed between the HOMO, SHOMO, and a lower lying orbital. In contrast, the lone pair on **2PCr** is stabilized relative to the other two compounds and is found below the predominantly metal-based HOMO and $\pi_2$. This trend can be attributed to the higher electronegativity of P relative to the other pnictogens that allows for increased stabilization of the negative charge associated with the E(1) lone pair (see below). The changes in HOMO orbital type in this series are also consistent with the trends in

electronic spectra, as discussed in the next section, but the nature of the lowest energy transitions suggest that the exact orderings of orbitals in Figure 2.4 are most likely incorrect. The second-order orbital mixing is more pronounced for **2SbCr** relative to the other two, but the general bonding is quite similar.

The Mulliken atomic charges on the E(1) atoms are *ca.* -0.7 and are twice as large as the charges on the $\eta^4$-E atoms (*ca.* -0.35). This observation is in accord with the valence bond formalism that leaves a negative charge on two coordinate pnictogens and is consistent with the reactivity of the compounds. For example, electrophiles such as $H^+$, $R^+$ and $M(CO)_3$ attack compounds **2EM** at E(1) to form compounds **3**, **4** and **9** respectively (see Scheme 2.1).

Finally, the effect of distortion of the $E_7^{3-}$ fragments was examined by monitoring the changes in orbital interactions occurring when the fragment symmetry was lowered from the idealized $C_{2v}$ to the observed ground state $C_s$ fragment structure with E(4)--E(5) / E(6)--E(7) asymmetries. In all three $[E_7Cr(CO)_3]^{3-}$ analyses, the distorted structures gave lower total energies. The most prominent stabilizations occurred for those orbitals with σ-like character across the shortened E(4)-E(5) contact. Additional mixing occurs upon distortion and, in general, the E(1) lone pair orbitals mixed with lower lying orbitals which also leads to some stabilization. The distortion of the $E_7^{3-}$ cage may be ascribed to a second-order Jahn-Teller effect. The Mulliken atomic charges associated with the four metal-bound E atoms become inequivalent upon distortion with higher charges associated with the E(6) and E(7) (*ca.* -0.4) and lower charges on E(4) and E(5) (*ca.* -0.2). These charges nicely explain the occurrence of hydrogen bonding of the en solvate molecule to the P(7) and P(1) atoms in the crystal structure of $[K(2,2,2\text{-crypt})]_3[P_7Cr(CO)_3]\bullet en$ (Fig. 2.2).

In a recent paper by Bolle and Tremel,[7] the electronic structure of $[Sb_7Mo(CO)_3]^{3-}$, **2SbMo**, was studied by the extended Hückel method. In their

analysis, the $Sb_7^{3-}$ fragment of the complex was modeled after the unperturbed $Sb_7^{3-}$ ion with the basal bonds fixed at 2.9 Å. Their analysis showed a similar mechanism of electron transfer from the $Sb_7^{3-}$ fragment to the metal center; however, the analogy to a coordinated diene was not considered. Their viewpoint was based on the decreased elongation of the Sb(4)-Sb(5) bond relative to **2AsCr**. The authors suggested[6] that this decrease in elongation was due to poorer M-E overlap relative to As-Cr interactions, thus reducing the tendency to "cleave" the E(4)-E(5) bond as effectively as was observed in **2AsCr**. This trend may reflect a relative size effect in which the large $Sb_7^{3-}$ ion does not have to distort (elongate the E(4)-E(5) contact) as much as the smaller $E_7^{3-}$ ions in order to "fit" in the $M(CO)_3$ coordination sphere.

### 2.2.5 Electronic Spectra

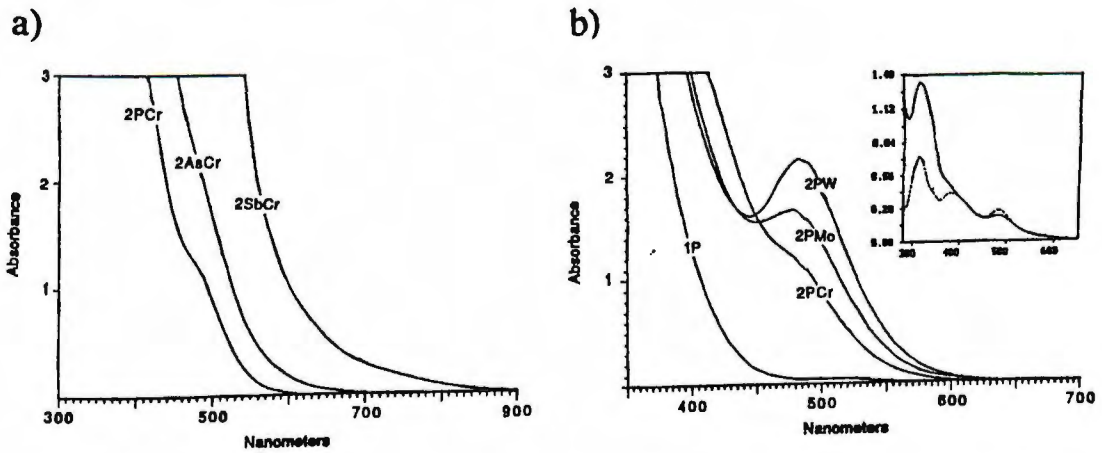


**Figure 2.5.** (a) Electronic absorption spectra for the $[E_7Cr(CO)_3]^{3-}$ ions, **2ECr**, where E = P, As, Sb. Spectra were recorded at room temperature from 1.0 mM en solutions. (b) Electronic absorption spectra for the $[P_7M(CO)_3]^{3-}$ ions, **2PM**, where M = Cr, Mo, W. Spectra were recorded at room temperature from 1.0 mM en solutions. The spectrum of $P_7^{3-}$ at the same concentration is given for comparison. The inset shows spectra of $[P_7W(CO)_3]^{3-}$ (solid line) and $[HP_7W(CO)_3]^{2-}$ (dashed line) recorded from 0.1 mM en solutions.

The electronic absorption spectra for the three chromium compounds **2ECr** and the three phosphorus compounds **2PM** are shown in Figures 2.5a and 2.5b, respectively. The spectrum of **1P** (with 3 equiv 2,2,2-crypt) is included in Figure 2.5b for comparison. A listing of the $\lambda_{max}$ values for compounds **2EM** and their molar absorptivities are given in Table 2.4.

The tails of the intense charge transfer bands ($\varepsilon$ >10,000 $L \cdot mol^{-1} \cdot cm^{-1}$) in the **2ECr** series (Figure 2.5a) are red shifted as E changes from P→As→Sb and are relatively insensitive to the nature of the transition metal. Because this behavior is also consistent with the *trend* observed in the **1E** parent clusters, we have assigned these absorbances as intraligand charge transfer bands. A low-energy shoulder is observed in the **2PCr** spectrum that appears to be buried beneath the charge transfer bands in the other two spectra. In the **2PM** series (Fig. 2.5b), the lowest energy transition is almost invariant in energy as M changes from Cr→Mo→W with $\lambda_{max} \approx 480$ nm. Instead, only an increase in molar absorptivity is observed with values of 1230, 1671, and 2163 $L \cdot mol^{-1} \cdot cm^{-1}$, respectively. It is also informative to compare the spectrum of **2PW** to its protonated analog, **4b** (see insert of Figure 2.5b). The 480-nm absorbance does not significantly change upon protonation, indicating that the transition is not $n \rightarrow \pi^4$ in character. On the basis of these data, we assign the 480-nm band as the $\pi^3 \rightarrow \pi^4$ transition.

On the basis of the qualitative orbital analysis above, one might expect low energy metal-ligand charge transfer ($M \rightarrow \pi^4$) and $n \rightarrow \pi^4$ type transitions in the electronic absorption spectra of the **2ECr** compounds. As mentioned previously, the exact ordering of orbitals shown in Figure 2.4 are probably incorrect and should only be used as a guide in examining trends. In addition, the $n \rightarrow \pi^4$ transition should be characteristically weak and may be hidden beneath the tails of the other transitions.

### 2.2.6 IR Spectroscopic Studies

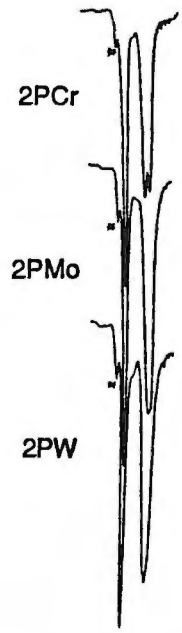


**Figure 2.6.** Solid-state IR spectra (KBr pellets) showing the carbonyl regions of the $[P_7M(CO)_3]^{3-}$ complexes, **2PM**, where M = Cr, Mo, W. The high-energy bands marked with the asterisks arise from $[HP_7M(CO)_3]^{2-}$ impurities. See Table 2.4 for $\nu$(CO) values.

The IR spectra (KBr pellet) for compounds **2EM** show ν(C-O) stretching vibrations between 1845 $cm^{-1}$ and 1708 $cm^{-1}$ (see Table 2.4). The ν(C-O) region for the **2PM** series is shown in Figure 2.6. The low ν(C-O) values reflect the high negative formal charge on the ion and significant CO π-backbonding.

In $C_s$ symmetry, the ν(C-O) modes have 2a'+ a" symmetry and are IR allowed. In most low-symmetry organometallic compounds containing a $C_{3v}$ $M(CO)_3$ fragment, such as (cyclooctatetraene)$Fe(CO)_3$[44] with $C_s$ point symmetry, the observed ν(C-O) modes reflect the local $C_{3v}$ symmetry of the $M(CO)_3$ fragment showing only two bands

($a_1$ + e). The true molecular symmetry is not reflected in the C-O vibrations due to the low effective mass of the fragment relative to the $M(CO)_3$ fragment. In contrast, compounds with $C_s$ symmetry and massive attendant groups on the $M(CO)_3$ fragments (*i.e.*, $Pb_9Cr(CO)_3^{4-}$)[10] show the expected three well resolved ν(C-O) modes reflecting their true point symmetries. Compounds **2EM** are intermediate between these extremes showing virtual $C_{3v}$ ν(C-O) patterns for the heaviest M and lightest E combination, **2PW**, with splitting of the e band into its a' + a" components for the other E-M combinations.

### 2.2.7 NMR Spectroscopic Studies

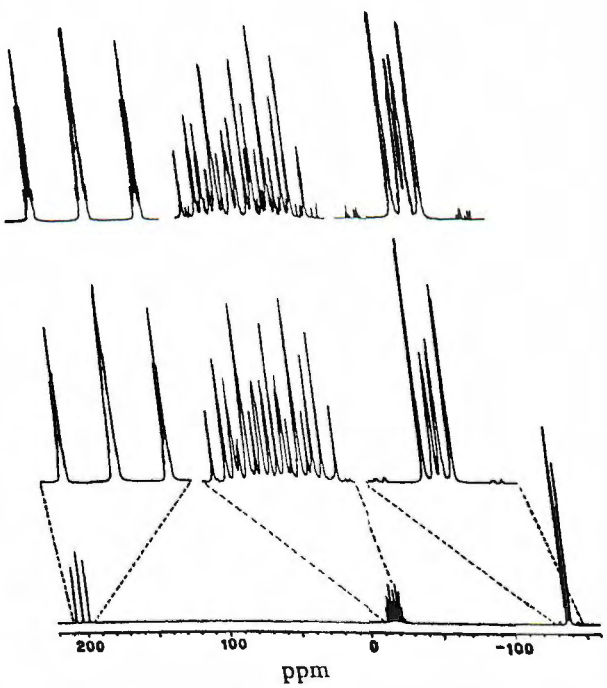


**Figure 2.7.** Calculated (top) and observed (middle and bottom) $^{31}P$ NMR spectra for $[P_7Cr(CO)_3]^{3-}$ recorded at 27 °C and 81.0 MHz from DMF-$d_7$ solutions. See Table 2.4 for chemical shifts and coupling constants.

The calculated and observed $^{31}P$ NMR spectra of **2PCr** are shown in Figure 2.7 and are representative of the **2PM** series. The $^{31}P$ NMR data are summarized in Table 2.4. The spectra show three resonances in a 4:2:1 integral ratio corresponding to the four metal-bound atoms [P(4), P(5), P(6), P(7)], the two bridging atoms [P(2) and P(3)], and the unique phosphorus P(1), respectively. On the basis of the solid-state structures, AA'BB'MM'X spin systems would be anticipated. However, the spectra are consistent with AA'A"A'"MM'X spin systems, indicating that the compounds are fluxional on the NMR time scale at room temperature. That is, the asymmetries in the P(4)--P(5) / P(6)--P(7) separations observed in the solid state are time averaged in solution (an intramolecular wagging process as shown in Scheme 2.2). Coupled with the rapid rotation of the $M(CO)_3$ fragment in the $P_4$ face, the wagging process generates virtual $C_{2v}$ symmetries in the $P_7$ fragments. Exchange remains rapid on the NMR time scale (no signal broadening) at -60 °C in DMF.

**Scheme 2.2**

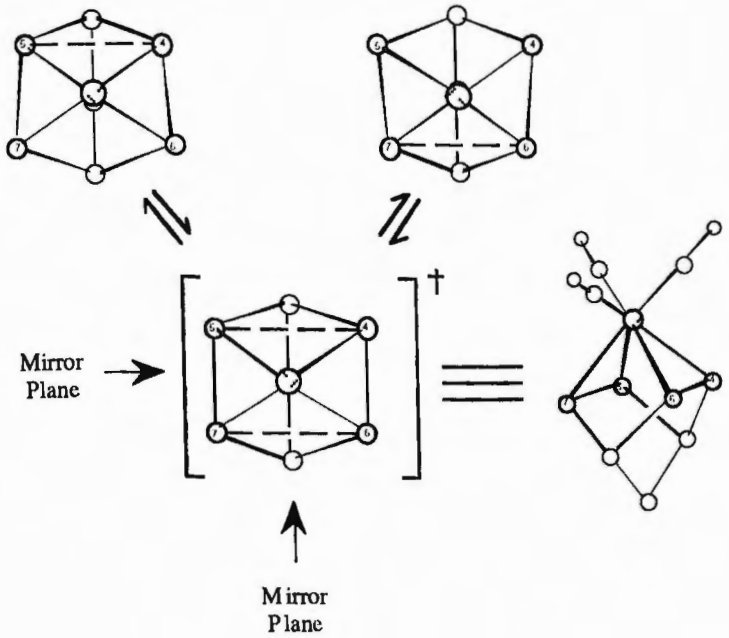

The $^{31}P$ NMR spectra of the **2PM** compounds were simulated in order to extract the P-P coupling constants. The P(4)-P(6) and P(5)-P(7) contacts (2.121 Å, ave), which presumably have multiple bond character, are among the shortest observed in the crystal structure of **2PCr**. Although the P(1)-P(2) and P(1)-P(3) contacts are also quite short (2.135 Å, ave), the P-P coupling constants are indicative of P-P single bonds. The calculated $^{1}J_{P\text{-}P}$ values for the P(4)-P(6) [or P(5)-P(7)] interactions are 478 Hz (ave) for the **2PM** compounds. As expected, these values are less than the $^{1}J_{P\text{-}P}$ coupling constants observed for the RP=PR diphosphene complexes (550-670 Hz)[23] but larger than the coupling constants associated with short P-P single bonds in related polyphosphorus compounds (200 - 430 Hz).[2,45]

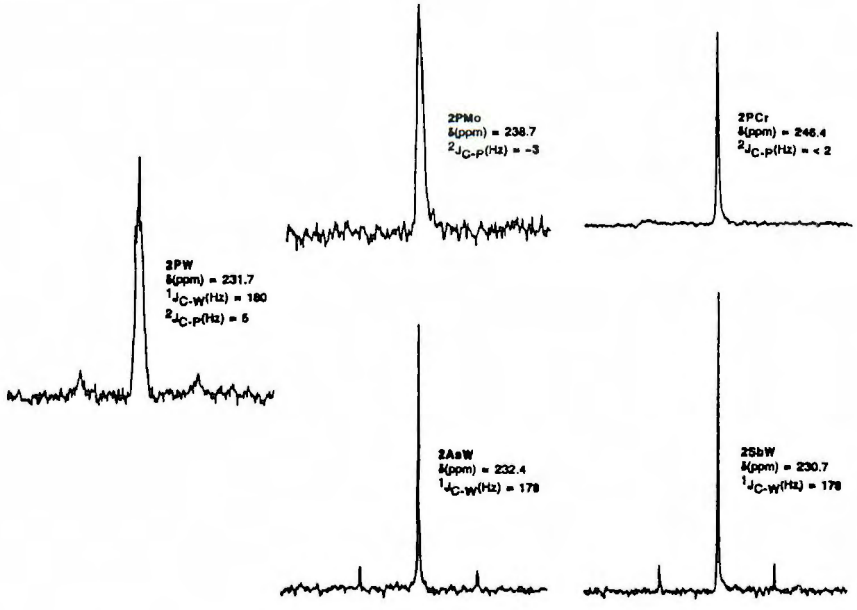


**Figure 2.8.** $^{13}C$ NMR spectra showing the carbonyl resonances of representative $[E_7M(CO)_3]^{3-}$ complexes, **2EM**, where E = P, As, Sb and M = Cr, Mo, W. Spectra were recorded at 27 $^{o}C$ and 100.6 MHz from DMF-$d_7$ solutions.

The $^{13}C$ NMR data for compounds **2EM** are summarized in Table 2.4 and representative $^{13}C$ carbonyl resonances are shown in Figure 2.8. The chemical shifts range from 230 to 247 ppm with deshielding increasing as **2EW < 2EMo < 2ECr** as the transition metal is varied and **2SbM < 2PM < 2AsM** as the $E_7^{3-}$ group is varied. The influence of the transition metals on the carbonyl chemical shifts parallels that of the $M(CO)_6$ compounds where M = W ($\delta$ = 192.1), Mo ($\delta$ = 202.0), and Cr ($\delta$ = 212.1)[46] and the related $[HM(CO)_5]^{1-}$ ions.[47] The relative shifts in these series do not correlate with $\nu$(CO) values and are presumably governed by paramagnetic terms to the chemical shift equation.[46] In general, however, there is a downfield shift of the carbonyl resonances relative to the $M(CO)_6$ and $[HM(CO)_5]^{1-}$ series where M = Cr, Mo, W that is consistent with increased carbyne-like character due to M-C multiple bonding.

The carbonyl resonances for the **2EW** and **2PM** compounds show coupling to $^{183}W$ (I = 1/2, 14 % abundance) and $^{31}P$, respectively, as shown in Figure 2.8. The $^1J_{W\text{-}C}$ values range from 176 to 180 Hz and increase as **2SbW < 2AsW < 2PW** which parallels the trends in $\nu$(CO) values, but is opposite to expectations based on electronegativity. The $^2J_{P\text{-}C}$ coupling constants for the **2PM** compounds range from 5 to $\leq$ 2 Hz according to the series **2PW < 2PMo < 2PCr**.

## 2.3 Conclusions

A series of $[E_7M(CO)_3]^{3-}$ ions (**2EM** where E = P, As, Sb and M = Cr, Mo, W) has been prepared from $E_7^{3-}$ Zintl ions and (arene)$M(CO)_3$ precursors. The compounds contain distorted norbornadiene-like $E_7^{3-}$ units bound $\eta^4$ to the $M(CO)_3$ fragments. They are fluxional in solution but do not dissociate into the parent $LM(CO)_3$ and $E_7^{3-}$ fragments. The formation of the **2EM** complexes affects structural rearrangements of the $E_7^{3-}$ clusters generating $\pi$-type character (diene-like) between the

two pairs of metal-bound pnictogens. The compounds have been studied by electronic absorption, NMR and IR spectroscopies as well as bonding analyses. The bonding is reminiscent to that in $(\eta^4\text{-}C_4H_4)Fe(CO)_3$ where the frontier $M(CO)_3$ orbitals interact with the diene-like $\pi$ system. The structural and spectroscopic features of the metal-ligand interaction are quite similar to those of the $E_2R_2[M(CO)_5]_3$ complexes where the bridging $M(CO)_5$ fragments insert into the E=E double bonds.

The reactivity of compounds **2EM** remains ligand based throughout the series. The lone pair on E(1) is quite nucleophilic and the site of attack by various electrophiles (*e.g.*, $H^+$, $R^+$, $(en)W(CO)_3$)[8,17,18,19] and will be described in Chapters 3 through 6. Studies on the isoelectronic $[E_7ML]^{3-}$ series of compounds (where M = Pt, L = $PPh_3$; M = Ni, L = CO and E = P, As) show metal based reactivity that is in sharp contrast to the chemistry of the **2EM** compounds (*e.g.*, the formation $[E_7Pt\mathit{H}(PPh_3)]^{2-}$ versus $[\mathit{H}E_7M(CO)_3]^{2-}$).[18] These transition metal Zintl ion complexes provide an excellent opportunity to systematically study the interactions of main group atoms with transition metals. Further studies are in progress.

## 2.4 Experimental Section

### 2.4.1 General Data

All reactions were performed in a Vacuum Atmospheres Company drybox under dinitrogen atmospheres. All IR spectra were recorded from KBr pellets on a Nicolet Model 5DXC FTIR spectrophotometer under dinitrogen purge. IR spectral data are listed individually below (s = strong, m = medium and w = weak). Elemental analyses were performed under inert atmospheres by Schwarzkopf Microanalytical Laboratories, Woodside, N.Y. and Desert Analytics, Tucson, AZ. Ambient temperature $^{13}C$ (100.614 MHz) and $^{31}P$ (81.015 MHz) NMR spectra were recorded on Bruker AM400

and WP200 spectrometers, respectively. The $^{31}P$ NMR data were referenced against an external 85% $H_3PO_4/CD_2Cl_2$ standard (0 ppm). Instruments were run unlocked for samples in ethylenediamine (en) and locked for samples in DMF-$d_7$. Negative line broadening was used to extract coupling constants from some $^{13}C$ NMR data. Spectral simulations were performed with the NMR-II simulation software package on a Macintosh computer. Electronic absorption spectra were recorded on a Milton Roy Spectronic 3000 Array spectrophotometer or a Perkin Elmer Lambda 2S spectrometer at ambient temperature using matching, modified anaerobic quartz cells with ethylenediamine as the solvent.

The following IR spectral data are common to all compounds containing $[K(2,2,2\text{-crypt})]^+$: IR (KBr pellet), $cm^{-1}$: 3126 (m), 2960 (m), 2879 (m), 2813 (m), 1659 (w), 1478 (m), 1459 (m), 1438 (m), 1403 (m), 1387 (s), 1360 (s), 1352 (s), 1296 (m), 1261 (m), 1231 (w), 1173 (w), 1129 (s), 1099 (s), 1082 (s), 1055 (m), 1027 (w), 947 (m), 932 (m), 829 (m), 806 (m), 750 (w), 669 (m), 629 (w), 614 (w), 572 (w), 525 (w). The following NMR spectral data are common to all compounds containing $[K(2,2,2\text{-crypt})]^+$ and/or en: $^1H$ NMR (DMF-$d_7$) δ(ppm): 3.61 (s, 12 H, 2,2,2-crypt), 3.58 (t, 12 H, 2,2,2-crypt), 2.57 (t, 12 H, 2,2,2-crypt), 2.54 (s, en), 1.28 (br s, en). $^{13}C\{^1H\}$ NMR (DMF-$d_7$) δ(ppm): 71.0 (s, 2,2,2-crypt), 68.3 (s, 2,2,2-crypt), 54.6 (s, 2,2,2-crypt), 46.3 (s, en).

### 2.4.2 Materials

The $K_3E_7$ (E = P, As, Sb) reagents were prepared by fusing stoichiometric ratios of the elements in evacuated, sealed silica tubes. **CAUTION:** alkali polyphosphorus compounds are known to spontaneously detonate even under rigorously anaerobic conditions. These materials should only be prepared in small quantities and should be handled with caution. Ethylenediamine solutions of the $E_7^{3-}$

ions were prepared by extracting finely ground powders of the $K_3E_7$ alloys. The $K_3P_7$ and $K_3As_7$ reagents dissolved completely, but the $K_3Sb_7$ powders were only partially soluble (~80 %) under the conditions given below. Mesitylene chromium tricarbonyl, cycloheptatetriene molybdenum tricarbonyl, mesitylene tungsten tricarbonyl, and 4,7,13,16,21,24-hexaoxa-1,10-diazabicyclo[8.8.8]hexacosane (2,2,2-crypt) were purchased from Aldrich and used without further purification. Ethylenediamine (en) was purchased from Fisher (Anhydrous), distilled from $CaH_2$ under dinitrogen, then from $K_4Sn_9$ under dinitrogen and finally stored under dinitrogen over molecular sieves. Toluene was distilled from sodium / benzophenone under dinitrogen and stored under dinitrogen over molecular sieves. DMF-$d_7$ was purchased from Cambridge Isotope Laboratories and degassed.

### 2.4.3 Syntheses

#### 2.4.3.1 Preparation of $[K(2,2,2\text{-crypt})]_3[P_7Cr(CO)_3]\cdot en$.

In vial 1, $K_3P_7$ (29.6 mg, 0.089 mmol) and 2,2,2-crypt (100 mg, 0.27 mmol) were dissolved in en (~3 mL) producing a yellow-orange solution. In vial 2, $[C_6H_3(CH_3)_3]Cr(CO)_3$ (22.7 mg, 0.089 mmol) was dissolved in toluene (~1 mL) producing a yellow solution. The contents of vial 2 were added dropwise to the contents of vial 1 yielding a red solution. The reaction mixture was stirred for 4 h, concentrated *in vacuo* to 2 mL and filtered through *ca.* one quarter inch of tightly packed glass wool in a pipet. After 24 h, the reaction vessel contained rectangular red-orange crystals that were removed from the mother liquor, washed with toluene and dried *in vacuo* (crystalline yield, 109 mg, 74%). IR (KBr pellet), $cm^{-1}$: 1829 (s), 1738 (s), 1716 (s). Anal. Calcd for $C_{59}H_{116}N_8O_{21}K_3P_7Cr$: C, 42.70; H, 7.04; N, 6.75; P, 13.06. Found: C,

42.35; H, 6.51; N, 5.21; P, 12.08. Two additional microanalyses did not produce better values.

### 2.4.3.2 Preparation of $[K(2,2,2\text{-crypt})]_3[As_7Cr(CO)_3]\cdot tol$.

A procedure identical to that described earlier for $[Rb(2,2,2\text{-crypt})]_3[As_7Cr(CO)_3]\cdot tol$ was followed except $K_3As_7$ (56.8 mg, 0.089 mmol) was used in the reaction instead of $Rb_3As_7$.[5] After 24 h, the reaction vessel contained rectangular, dark red crystals. The crystals were removed from the mother liquor, washed with toluene and dried *in vacuo* (crystalline yield, 54 mg, 31%). IR (KBr pellet), $cm^{-1}$: 1824 (s), 1741 (s), 1708 (s).

### 2.4.3.3 Preparation of $[K(2,2,2\text{-crypt})]_3[Sb_7Cr(CO)_3]$.

A procedure identical to that described for $[K(2,2,2\text{-crypt})]_3[P_7Cr(CO)_3]\cdot en$ above was followed except $K_3Sb_7$ (85.8 mg, 0.089 mmol) was used in the reaction. After 24 h, the reaction vessel contained rectangular dark red crystals. The crystals were removed from the mother liquor, washed with toluene and dried *in vacuo* (crystalline yield, 77 mg, 38%). IR (KBr pellet), $cm^{-1}$: 1823 (s), 1748 (s), 1718 (s). Anal. Calcd for $C_{57}H_{108}N_6O_{21}K_3Sb_7Cr$: C, 30.63; H, 4.87; N, 3.76; Sb, 38.13; Cr, 2.33. Found: C, 31.44; H, 5.24; N, 5.33; Sb, 36.66; Cr, 2.12.

### 2.4.3.4 Preparation of $[K(2,2,2\text{-crypt})]_3[P_7Mo(CO)_3]\cdot en$.

In vial 1, $K_3P_7$ (29.6 mg, 0.089 mmol) and 2,2,2-crypt (100 mg, 0.27 mmol) were dissolved in en (~3 mL) producing a yellow-orange solution. In vial 2, $(C_7H_8)Mo(CO)_3$ ( 24.1 mg, 0.089 mmol) was dissolved in toluene (~2 mL) and gently heated to give a red solution. Not all of the molybdenum complex dissolved into the toluene. The contents of vial 2, including the undissolved molybdenum complex, were

added dropwise to the contents of vial 1 producing a red solution. The reaction mixture was stirred for 4 h during which time the remaining $(C_7H_8)Mo(CO)_3$ dissolved. The volume was concentrated *in vacuo* to 1 mL and filtered through *ca.* one quarter inch of tightly packed glass wool in a pipet. After 12 h the reaction vessel contained small red crystals. The crystals were removed from the mother liquor, washed with toluene and dried *in vacuo* (crystalline yield, 67 mg, 44%). IR (KBr pellet), $cm^{-1}$: 1841 (s), 1732 (s), 1721 (s). Anal. Calcd for $C_{59}H_{116}N_8O_{21}K_3P_7Mo$: C, 41.60; H, 6.86; N, 6.58; P, 12.73. Found: C, 42.05; H, 6.99; N, 6.99; P, 12.47.

### 2.4.3.5 Preparation of $[K(2,2,2\text{-crypt})]_3[As_7Mo(CO)_3]$.

A procedure identical to that described for $[K(2,2,2\text{-crypt})]_3[P_7Mo(CO)_3]\cdot en$ was followed except $K_3As_7$ (56.8 mg, 0.089 mmol) was used in the reaction. After 24 h the reaction vessel contained a few very small red crystals. The crystals were removed from the mother liquor, washed with toluene and dried *in vacuo* (crystalline yield, *ca.* 5 mg, 3%). Yields were not optimized. IR (KBr pellet), $cm^{-1}$: 1840 (s), 1744 (s), 1720 (s).

### 2.4.3.6 Preparation of $[K(2,2,2\text{-crypt})]_3[Sb_7Mo(CO)_3]$.

A procedure identical to that described for $[K(2,2,2\text{-crypt})]_3[P_7Mo(CO)_3]\cdot en$ was followed except $K_3Sb_7$ (85.8 mg, 0.089 mmol) was used in the reaction. After 24 h, the reaction vessel contained very small dark red crystals. The crystals were removed from the mother liquor, washed with toluene and dried *in vacuo* (crystalline yield, *ca.* 7 mg, 3%). Yields were not optimized. IR (KBr pellet), $cm^{-1}$: 1845 (s), 1759 (s), 1730 (s).

### 2.4.3.7 Preparation of $[K(2,2,2\text{-crypt})]_3[P_7W(CO)_3]\cdot en$.

In vial 1, $K_3P_7$ (29.6 mg, 0.089 mmol) and 2,2,2-crypt (100 mg, 0.27 mmol) were dissolved in en (~3 mL ) producing a yellow-orange solution. In vial 2, $[C_6H_3(CH_3)_3]W(CO)_3$ (34.4 mg, 0.089 mmol) was dissolved in toluene (~1 mL) producing an orange solution. The contents of vial 2 were added dropwise to the contents of vial 1 yielding a red solution. The reaction mixture was stirred for 2 h, concentrated *in vacuo* to 1.5 mL and filtered through *ca.* one quarter inch of tightly packed glass wool in a pipet. After 3 h, the reaction vessel contained rectangular red crystals. The crystals were removed from the mother liquor, washed with toluene and dried *in vacuo* (crystalline yield, 140 mg, 88%). IR (KBr pellet), $cm^{-1}$: 1839 (s), 1729 (s). Anal. Calcd for $C_{59}H_{116}N_8O_{21}K_3P_7W$: C, 39.55; H, 6.53; N, 6.25. Found: C, 39.53; H, 6.79; N, 6.50.

### 2.4.3.8 Preparation of $[K(2,2,2\text{-crypt})]_3[As_7W(CO)_3]\cdot en$.

A procedure identical to that described for $[K(2,2,2\text{-crypt})]_3[P_7W(CO)_3]\cdot en$ was followed except $K_3As_7$ (56.8 mg, 0.089 mmol) was used in the reaction. After 12 h, the reaction vessel contained rectangular red crystals. The crystals were removed from the mother liquor, washed with toluene and dried *in vacuo* (crystalline yield, 54 mg, 31%). IR (KBr pellet), $cm^{-1}$: 1836 (s), 1744 (s), 1713 (s). Anal. Calcd for $C_{59}H_{116}N_8O_{21}K_3As_7W$: C, 33.76; H, 5.57; N, 5.34. Found: C, 33.53; H, 5.59; N, 5.61.

### 2.4.3.9 Preparation of $[K(2,2,2\text{-crypt})]_3[Sb_7W(CO)_3]$.

A procedure identical to that described for $[K(2,2,2\text{-crypt})]_3[P_7W(CO)_3]\cdot en$ was followed except $K_3Sb_7$ (85.8 mg, 0.089 mmol) was used in the reaction. The reaction mixture was stirred for 2 h, concentrated *in vacuo* to 2 mL and filtered through *ca.* one

quarter inch of tightly packed glass wool in a pipet. While filtering, rectangular dark red crystals began to form in the reaction vessel. The crystals were removed from the mother liquor, washed with toluene and dried *in vacuo* (crystalline yield, 61 mg, 29%). IR (KBr pellet), $cm^{-1}$: 1842 (s), 1760 (s), 1728 (s). Anal. Calcd for $C_{57}H_{108}N_6O_{21}K_3Sb_7W$: C, 28.93; H, 4.60; N, 3.55. Found: C, 27.89; H, 4.81; N, 3.97.

### 2.4.3.12 Preparation of UV/Vis Samples.

In a drybox, crystalline $[K(2,2,2\text{-crypt})]^+$ salts of **2ECr** (E = P, As, Sb) and **2PM** (M = Cr, Mo, W) ions were dissolved in en in 10 mL volumetric flasks to produce 2.5 mM stock solutions. Stepwise dilutions were then performed to obtain 1.0 mM and 0.10 mM sample solutions which were stored in a drybox. For analysis, an aliquot of each dilute solution was placed in a quartz cell which was stoppered with a rubber septum.

### 2.4.3.13 Preparation of Ligand Exchange Samples.

The crystalline $[K(2,2,2\text{-crypt})]^+$ salts of **2ECr** (E = P, As, Sb) ions were dissolved in DMF-$d_7$ (~1/2 mL). Separately, an equiv. of $K_3E'_7$ (E≠E'=P,As,Sb) and three equiv. of 2,2,2-crypt were dissolved in en (~1/2 mL) and allowed to react for at least 24 h. The $E'_7{}^{3-}$ solution was then combined with the **2ECr** solution. Reactions were monitored by $^{13}C$ NMR spectroscopy over 7-day periods.

## 2.4.4 X-ray Crystallography for [K(2,2,2-crypt)]$_3$[$Sb_7Cr(CO)_3$] and [K(2,2,2-crypt)]$_3$ [$P_7Cr(CO)_3$]•en.

Single crystal X-ray diffraction studies for [K(2,2,2-crypt)]$_3$ [$P_7Cr(CO)_3$]•en and [K(2,2,2-crypt)]$_3$[$Sb_7Cr(CO)_3$] were done by Dr. Arnold L. Rheingold, University

of Delaware, and for $[K(2,2,2\text{-crypt})]_3[Sb_7W(CO)_3]$ by Dr. Simon G. Bott, University of North Texas.[8]

### 2.4.5 Computational Procedures.

Molecular orbital calculations were performed by Dr. Bryan W. Eichhorn using the Fenske-Hall method that has been described elsewhere.[39-42] SCF calculations were performed in the atomic basis on the $E_7^{3-}$ fragments, the $C_{3v}$ $Cr(CO)_3$ fragment and the $[E_7Cr(CO)_3]^{3-}$ complexes. To aid in the analysis of the orbital interactions, the converged wave functions were transformed into the appropriate fragment bases. The internuclear distances were obtained from crystal data and averaged where appropriate. A common $Cr(CO)_3$ fragment with $d_{C\text{-}O} = 1.20$ Å and $d_{Cr\text{-}C} = 1.76$ Å was used for all structural models. Calculations were performed on idealized symmetrical complexes as well as the observed unsymmetrical structures. The symmetrical models containing $C_{2v}$ $E_7^{3-}$ fragments were constructed by averaging the crystallographically determined Cr-E contacts and E(4)--E(5) / E(6)--E(7) distances and corresponding angles. The interatomic distances and angles for the unsymmetrical models were taken directly from the crystallographic data. All calculations were performed on a Macintosh IIcx personal computer using the Fenske-Hall program, version 5.1.[42]

The basis functions (single $\zeta$) were generated by the numerical $X\alpha$ atomic orbital program of Herman and Skillman[41] used in conjunction with the $X\alpha$-to-Slater basis program of Bursten and Fenske.[39,40] The Cr atoms were assumed to have cationic $d^{n+1}s^0$ configurations whereas the ground state atomic configurations were used for the remainder of the atoms.

**Table 2.1.** Crystallographic Data for $[K(2,2,2\text{-crypt})]_3[E_7Cr(CO)_3]$ where E = P, Sb.

| compound | $[K(2,2,2\text{-crypt})]_3[P_7Cr(CO)_3]\cdot en$ | $[K(2,2,2\text{-crypt})]_3[Sb_7Cr(CO)_3]$ |
|---|---|---|
| formula | $C_{59}H_{116}N_8O_{21}K_3P_7Cr$ | $C_{57}H_{108}N_6O_{21}K_3Sb_7Cr$ |
| formula weight | 1659.73 | 2235.06 |
| space group | $P\bar{1}$ | *C2/c* |
| *a*, Å | 14.236(5) | 50.300(9) |
| *b*, Å | 14.523(4) | 13,897(3) |
| *c*, Å | 20.895(7) | 28.433(5) |
| α, deg | 80.67(3) | --- |
| β, deg | 88.93(3) | 108.43(1) |
| γ, deg | 78.39(3) | --- |
| V, $Å^3$ | 4175.3(26) (Z = 2) | 18856(6) (Z = 8) |
| cryst dimens, mm | 0.27 x 0.31 x 0.36 | 0.36 x 0.40 x 0.46 |
| cryst color | red-orange | dark maroon |
| D(calc), g $cm^3$ | 1.318 | 1.574 |
| $\mu(MoK_\alpha)$, $cm^{-1}$ | 4.72 | 22.71 |
| temp, K | 296 | 243 |
| 2θ scan range, deg | 4.0 - 42.0 | 4.0 - 45.0 |
| rflns, collected | 9430 | 13220 |
| indpt. rflns | 9284 | 12174 |
| indpt obsvd rflns $F_o \geq n\sigma(F_o)$ | 3616 (n = 5) | 8158 (n = 4) |
| R(F), % | 10.33 | 6.75 |
| R(wF), % | 10.45 | 7.44 |

| | | |
|---|---|---|
| $\Delta/\sigma$(max) | 0.019 | 0.550 |
| GOF | 1.74 | 1.64 |

$^{a}R(F) = \Sigma \mid F_o - F_c \mid / \Sigma F_o$; $^{b}R(wF) = (\Sigma w \mid F_o - F_c \mid^2 / \Sigma w F_o^2)^{1/2}$

**Table 2.2.** Selected Bond Distances ( Å ) and Angles ( $^{o}$ ) for the $[E_7Cr(CO)_3]^{3-}$ ions.

| Distances | E = P | E = As[a] | E = Sb |
|---|---|---|---|
| E(1)-E(2) | 2.124(10) | 2.347(8) | 2.721(2) |
| E(1)-E(3) | 2.146(8) | 2.370(8) | 2.723(2) |
| E(2)-E(3) | 3.190(10) | 3.556(8) | 4.122(2) |
| E(2)-E(4) | 2.237(9) | 2.466(8) | 2.846(2) |
| E(2)-E(5) | 2.230(8) | 2.471(8) | 2.845(2) |
| E(3)-E(6) | 2.233(9) | 2.453(8) | 2.855(2) |
| E(3)-E(7) | 2.212(9) | 2.462(8) | 2.846(2) |
| E(4)--E(5) | 2.825(8) | 3.082(8) | 3.331(4) |
| E(6)--E(7) | 3.071(8) | 3.292(8) | 3.715(4) |
| E(4)-E(6) | 2.128(9) | 2.356(9) | 2.700(2) |
| E(5)-E(7) | 2.114(8) | 2.334(9) | 2.707(2) |
| E(1)-Cr | 4.736(9) | 5.107(9) | 5.644(2) |
| E(4)-Cr | 2.502(6) | 2.636(10) | 2.804(3) |
| E(5)-Cr | 2.487(6) | 2.630(11) | 2.807(3) |
| E(6)-Cr | 2.539(7) | 2.703(10) | 2.848(3) |
| E(7)-Cr | 2.527(6) | 2.685(10) | 2.850(3) |
| Cr-C(1) | 1.824(17) | 1.62(8) | 1.877(20) |
| Cr-C(2) | 1.754(20) | 1.82(16) | 1.812(15) |
| Cr-C(3) | 1.768(21) | 1.82(9) | 1.827(17) |
| C(1)-O(1) | 1.173(22) | 1.15(5) | 1.146(24) |
| C(2)-O(2) | 1.224(24) | 1.28(5) | 1.178(19) |
| C(3)-O(3) | 1.196(26) | 1.25(10) | 1.176(21) |

| Angles | E = P | E = As[a] | E = Sb |
|---|---|---|---|
| E(1)-E(2)-E(4) | 107.4(4) | 107.5(3) | 108.1(1) |
| E(1)-E(2)-E(5) | 107.8(3) | 107.06(26) | 106.7(1) |
| E(1)-E(3)-E(6) | 105.5(3) | 106.83(28) | 107.7(1) |
| E(1)-E(3)-E(7) | 107.0(3) | 105.5(3) | 106.2(1) |
| E(2)-E(1)-E(3) | 96.6(3) | 97.9(3) | 98.5(1) |
| E(2)-E(4)-E(6) | 104.0(3) | 104.76(28) | 105.9(1) |
| E(2)-E(5)-E(7) | 104.7(4) | 104.3(3) | 105.7(1) |
| E(3)-E(6)-E(4) | 103.2(3) | 103.3(3) | 102.7(1) |
| E(3)-E(7)-E(5) | 103.1(3) | 104.2(3) | 102.9(1) |
| E(4)-E(2)-E(5) | 78.5(3) | 77.29(24) | 71.7(1) |
| E(6)-E(3)-E(7) | 87.4(3) | 84.11(25) | 81.3(1) |
| E(4)-Cr-E(5) | 69.0(2) | 71.67(27) | 72.8(1) |
| E(4)-Cr-E(6) | 49.9(2) | 52.36(24) | 57.1(1) |
| E(4)-Cr-E(7) | 92.6(2) | 95.7(3) | 103.3(1) |
| E(5)-Cr-E(6) | 92.3(2) | 96.2(3) | 103.5(1) |
| E(5)-Cr-E(7) | 49.9(2) | 52.08(25) | 57.2(1) |
| E(6)-Cr-E(7) | 74.6(2) | 75.33(28) | 81.4(1) |
| E(2)-E(4)-Cr | 104.4(3) | 103.93(27) | 104.8(1) |
| E(2)-E(5)-Cr | 105.1(3) | 103.9(3) | 104.7(1) |
| E(3)-E(6)-Cr | 98.1(3) | 99.4(3) | 97.4(1) |
| E(3)-E(7)-Cr | 99.1(3) | 99.64(28) | 97.6(1) |
| E(4)-E(6)-Cr | 64.1(2) | 62.36(27) | 60.6(1) |
| E(5)-E(7)-Cr | 64.1(2) | 62.75(26) | 60.6(1) |
| E(6)-E(4)-Cr | 65.9(2) | 65.29(26) | 62.3(1) |
| E(7)-E(5)-Cr | 66.0(2) | 65.17(28) | 62.2(1) |

| Angles | E = P | E = As | E = Sb |
|---|---|---|---|
| E(4)-Cr-C(1) | 140.2(7) | 132.7(16) | 137.9(5) |
| E(4)-Cr-C(2) | 84.1(6) | 83.7(17) | 78.7(6) |
| E(4)-Cr-C(3) | 123.8(6) | 128.4(17) | 126.9(5) |
| E(5)-Cr-C(1) | 133.1(6) | 140.0(16) | 138.8(5) |
| E(5)-Cr-C(2) | 134.3(6) | 130.2(18) | 125.9(5) |
| E(5)-Cr-C(3) | 82.5(6) | 80.3(17) | 77.9(6) |
| E(6)-Cr-C(1) | 86.831 | 84.5(16) | 84.4(5) |
| E(6)-Cr-C(2) | 97.8(7) | 102.0(17) | 97.9(5) |
| E(6)-Cr-C(3) | 173.3(6) | 175.3(17) | 176.0(5) |
| E(7)-Cr-C(1) | 86.8(6) | 90.1(16) | 85.1(5) |
| E(7)-Cr-C(2) | 172.0(8) | 177.9(18) | 176.8(5) |
| E(7)-Cr-C(3) | 104.8(7) | 100.1(17) | 96.4(5) |
| C(1)-Cr-C(2) | 91.0(8) | 88.1(24) | 91.8(7) |
| C(1)-Cr-C(3) | 94.5(9) | 96.3(24) | 92.1(8) |
| C(2)-Cr-C(3) | 83.1(10) | 82.6(24) | 84.2(7) |
| Cr-C(1)-O(1) | 179.5(15) | 170.(4) | 175.5(15) |
| Cr-C(2)-O(2) | 174.1(19) | 168.(4) | 173.5(16) |
| Cr-C(3)-O(3) | 177.3(17) | 174.(5) | 176.0(15) |

[a] Data taken from reference 5.

**Table 2.3.** Comparison of Bond Distances of RE=ER, RE=ER[$Cr(CO)_5$], RE=ER[$Cr(CO)_5$]$_3$ with $E_4$-$E_6$/$E_5$-$E_7$ of the **2ECr** Complexes.[a]

| Compound | E-E (Å) | | | E-$Cr_b$ (Å) | | | E-$Cr_t$ (Å) | | |
|---|---|---|---|---|---|---|---|---|---|
| | P | As | Sb | P | As | Sb | P | As | Sb |
| RE=ER' | 2.034(2)[b] | 2.244(1)[c] | --- | --- | --- | --- | --- | --- | --- |
| RE=ER'[$Cr(CO)_5$] | 2.039(3)[d] | 2.246(1)[e] | --- | --- | --- | --- | 2.354(2) | 2.454(1) | --- |
| RE=ER'[$Cr(CO)_5$]$_3$ | 2.125(6)[f] | 2.371[g] | 2.720(3)[h] | 2.524(3) | 2.64 | 2.870(4) | 2.405(4) | 2.53 | 2.687(3) |
| | | | | 2.546(5) | | 2.924(5) | 2.411(4) | | 2.700(4) |
| **2ECr**[i] | 2.121 | 2.345 | 2.704 | 2.514 | 2.664 | 2.827 | --- | --- | --- |

[a]See **2.II** & **2.III** for schematic drawings of RE=ER[$Cr(CO)_5$] and RE=ER[$Cr(CO)_5$]$_3$. ($Cr_b$ and $Cr_t$ denote bridging and terminal chromium pentacarbonyl fragments, respectively). [b]R=R'=[2,4,6-$(Me_3C)_3C_6H_2$] [29] [c]R=R'=[$(Me_3Si)_3C$] [30] [d]R=[2,4,6-$(Me_3C)_3C_6H_2$], R'=[1,3,5-$(Me)_3C_6H_2$] [31] [e]R=[2,4,6-$(Me_3C)_3C_6H_2$], R'=[$CH(Me_3Si)_2$] [32] [f]R=R'=[$C_6H_5$] [33] [g]R=R'=[$C_6H_5$] [34] [h]R=R'=$Me_3C$ [35] [i]Bond distances are averaged. [this work]

**Table 2.4**. Spectroscopic Data of **2EM** Complexes.

| Compound | IR[a] | NMR[b] | | | | UV-Vis[c] | |
|---|---|---|---|---|---|---|---|
| | | $^{31}P$ | | $^{13}C$ | | | |
| | $\nu_{C-O}$ ($cm^{-1}$) | δ (ppm) | J (Hz)[d] | δ (ppm) | J (Hz)[e] | $\lambda_{max}$ | ε ($Lcm^{-1}mol^{-1}$) |
| **2PCr** | 1829,1738,1716 | 204,-20,-139 | A) $^1J_{P-P} = 483$ | 246.4 | $^2J_{C-P} = <2$ | 317 | ( 8,871) |
| | | | B) $^1J_{P-P} = 370$ | | | 363 | ( 6,600) |
| | | | C) $^1J_{P-P} = 238$ | | | 478 | ( 1,230) |
| **2PMo** | 1841,1732,1721 | 174,-12,-150 | A) $^1J_{P-P} = 473$ | 238.7 | $^2J_{C-P} = 3$ | 320 | (20,745) |
| | | | B) $^1J_{P-P} = 370$ | | | 350 | (10,635) |
| | | | C) $^1J_{P-P} = 241$ | | | 478 | ( 1,671) |
| **2PW** | 1837, 1728 | 184,-7,-159 | A) $^1J_{P-P} = 472$ | 231.7 | $^1J_{C-W} = 180$ | 319 | (18,453) |
| | | | B) $^1J_{P-P} = 369$ | | $^2J_{C-P} = 5$ | 370 | ( 5,100) |
| | | | C) $^1J_{P-P} = 238$ | | | 486 | ( 2,163) |
| **2AsCr** | 1824,1741,1708 | | | 247.1 | | 365 | (11,400) |
| **2AsMo** | 1840,1744,1720 | | | | | | |
| **2AsW** | 1836,1744,1714 | | | 232.4 | $^1J_{C-W} = 178$ | | |
| **2SbCr** | 1823,1748,1718 | | | 245.1 | | 365 | (16,000) |
| **2SbMo** | 1845,1759,1730 | | | | | | |
| **2SbW** | 1842,1756,1726 | | | 230.7 | $^1J_{C-W} = 176$ | | |

[a] KBr pellets. [b] $^{31}P$ NMR (DMF $d_7$), ambient temperature, 81.015 MHz; $^{13}C$ NMR (DMF $d_7$), ambient temperature, 100.614 MHz. [c] Solvent was ethylenediamine. [d] A) $J_{P_4-P_6}$, $J_{P_5-P_7}$; B) $J_{P_1-P_2}$, $J_{P_1-P_3}$; C) $J_{P_2-P_4}$, $J_{P_2-P_5}$, $J_{P_3-P_6}$, $J_{P_3-P_7}$. [e] Coupling constants were determined with negative line broadening. LB = 1 used for spectra in Figure 2.8.

## 2.5 References


(1) Baudler, M.; Etzbach, T. *Angew. Chem. Int. Ed. Engl.* **1991**, *30*, 580-582.

(2) (a) Fritz, G.; Hoppe, K. D.; Hönle, W.; Weber, D.; Mujica, C.; Manriquez, V.; von Schnering, H. G. *J. Organomet. Chem.* **1983**, *249*, 63-80. (b) Fenske, D. **1995**, personal communication with Dr. Bryan W. Eichhorn.

(3) von Schnering, H. G.; Wolf, J.; Weber, D.; Ramirez, R.; Meyer, T. *Angew. Chem. Int. Ed. Engl.* **1986**, *25*, 353-354.

(4) Charles, S.; Eichhorn, B. W.; Bott, S. G. *J. Am. Chem. Soc.* **1993**, *115*, 5837-5838.

(5) Eichhorn, B. W.; Haushalter, R. C.; Huffman, J. C. *Angew. Chem. Int. Ed. Engl.* **1989**, *28*, 1032-1033.

(6) Bolle, U.; Tremel, W. *J. Chem. Soc., Chem. Commun.* **1992**, 91-93.

(7) Bolle, U.; Tremel, W. *J. Chem. Soc., Chem. Commun.* **1994**, 217-219.

(8) Charles, S.; Eichhorn, B. W.; Bott, S. G.; Rheingold, A. L. *J. Am. Chem. Soc.* **1994**, *116*, 8077-8086.

(9) Eichhorn, B. W.; Haushalter, R. C.; Pennington, W. T. *J. Am. Chem. Soc.* **1988**, *110*, 8704-8706.

(10) Eichhorn, B. W.; Haushalter, R. C. *J. Chem. Soc., Chem. Commun.* **1990**, 937-938.

(11) Corbett, J. D. *Chem. Rev.* **1985**, *85*, 383-397.

(12) Teller, R. G.; Krause, L. J.; Haushalter, R. C. *Inorg. Chem.* **1983**, *22*, 1809-1812.

(13) Wilson, W. L.; Rudolph, R. W.; Lohr, L. L.; Taylor, R. C.; Pyykko, P. *Inorg. Chem.* **1986**, *25*, 1535-1541.

(14) Baudler, M. *Angew. Chem. Int. Ed. Engl.* **1982**, *21*, 492-512.

(15) Baudler, M.; Ternberger, H.; Faber, W.; Hahn, J. *Z. Naturforsch.* **1979**, *34B*, 1690-1697.

(16) Charles, S.; Eichhorn, B. W.; Fettinger, J. C. **1995**, unpublished results.

(17) Charles, S.; Fettinger, J. C.; Eichhorn, B. W. *J. Am. Chem. Soc.* **1995**, *117*, 5303-5311.

(18) Charles, S.; Fettinger, J. C.; Bott, S. G.; Eichhorn, B. W. *Angew. Chem. Int. Ed. Engl.* **1995**, submitted.

(19) Charles, S.; Eichhorn, B. W., Fettinger, J. C. **1995**, in preparation.

(20) Charles, S. B.; Fettinger, J.; Bott, S. G.; Eichhorn, B. W. *Inorg. Chem.* **1995**, submitted.

(21) Huheey, J. E.; Keiter, E. A.; Keiter, R. L. *Inorganic Chemistry; Principles of Structure and Reactivity;* 4th ed.; Harper & Row: New York, 1993, pp 300.

(22) Rees, B.; Coppens, P. *Acta. Cryst.* **1973**, *B29*, 2515-2528.

(23) Scherer, O. J. *Angew. Chem. Int. Ed. Engl.* **1985**, *24*, 924-943.

(24) Cowley, A. H. *Polyhedron* **1984**, *3*, 389-432 and references therein.

(25) Huttner, G.; Schelle, S. *J. Organomet. Chem.* **1973**, *47*, 383-390.

(26) Elmes, P. A.; Gatehouse, B. M.; Lloyd, D. J.; West, B. O. *J. Chem. Soc., Chem. Commun.* **1974**, 953-954.

(27) Plastas, H. J.; Stewart, J. M.; Grim, S. O. *Inorg. Chem.* **1973**, *12*, 265-272.

(28) Wieber, M.; Graf, N. *Z. Anorg. Allg. Chem.* **1993**, *619*, 1991-1997.

(29) Yoshifuji, M.; Shima, I.; Inamoto, N.; Hirotsu, K.; Higuchi, T. *J. Am. Chem. Soc.* **1981**, *103*, 4587-4589.

(30) Cowley, A. C.; Norman, N. C.; Pakulski, M. *J. Chem. Soc., Dalton Trans.* **1985**, 383-386.

(31) Yoshifuji, M.; Hashida, T.; Inamoto, N.; Kirotsu, K.; Horiuchi, T.; Higuchi, T.; Ito, K.; Nagase, S. *Angew. Chem. Int. Ed. Engl.* **1985**, *24*, 211-212.

(32) Cowley, A. H.; Lasch, J. G.; Norman, N. C.; Pakulski, M. *Angew. Chem. Int. Ed. Engl.* **1983**, *22*, 978-979.

(33) Borm, J.; Zsolnai, L.; Huttner, G. *Angew. Chem. Int. Ed. Engl.* **1983**, *22*, 977-978.

(34) Huttner, G.; Schmid, H. G.; Frank, A.; Orama, O. *Angew. Chem. Int. Ed. Engl.* **1976**, *15*, 224.

(35) Weber, U.; Huttner, G.; Scheidsteger, O.; Zsolnai, L. *J. Organomet. Chem.* **1985**, *289*, 357-366.

(36) Alcock, N. W. *Adv. Inorg. Chem. Radiochem.* **1972**, *15*, 1-53.

(37) Adolphson, D. G.; Corbett, J. D.; Merryman, D. J. *J. Am. Chem. Soc.* **1976**, *98*, 7234-7239.

(38) Critchlow, S. C.; Corbett, J. D. *Inorg. Chem.* **1984**, *23*, 770-774.

(39) Bursten, B. E.; Fenske, R. F. *J. Chem. Phys.* **1977**, *67*, 3138-3145.

(40) Bursten, B. E.; Jensen, R. J.; Fenske, R. J. *J. Chem. Phys.* **1978**, *68*, 3320.

(41) Herman, F.; Skillman, S. *Atomic Structure Calculations*; Prentice-Hall: Englewood Cliffs, N.J., 1963.

(42) Hall, M. B.; Fenske, R. F. *Inorg. Chem.* **1972**, *11*, 768-775.

(43) Albright, T. A.; Burdett, J. K.; Whangbo, M.-H. *Orbital Interactions in Chemistry*; John Wiley & Son, Inc.: New York, 1985, pp 218, 387.

(44) Deganello, G. *Transition Metal Complexes of Cyclic Polyolefins*; Academic Press: New York, 1979, pp 197-199.

(45) Ali, A. A. M.; Bocelli, G.; Harris, R. K.; Fild, M. *J. Chem. Soc., Dalton Trans.* **1980**, 638-644.

(46) Braterman, P. S.; Milne, D. W.; Randall, E. W.; Rosenberg, E. *J. Chem. Soc., Dalton Trans.* **1973**, 1027-1031.

(47) Darensbourg, M. Y.; Slater, S. *J. Am. Chem. Soc.* **1981**, *103*, 5914-5915.

# CHAPTER 3

## Synthesis, Structure and Characterization of the $[HP_7M(CO)_3]^{2-}$ Ions (M = Cr, W).

### 3.1 Introduction

The reactivity of the $[E_7M(CO)_3]^{3-}$ ions (**2EM**, where E denotes P, As or Sb and M denotes Cr, Mo or W) was discussed in Chapter 2. The $[E_7M(CO)_3]^{3-}$ compounds have norbornadiene-like $E_7$ fragments with a formal negative charge associated with the unique two-coordinate E atom furthest from the transition metal (the E(1) site). The pnictogen atom remains modestly basic and highly nucleophilic and is the site of attack by various electrophiles (*e.g.*, $H^+$, $R^+$, $Me_3Si^+$, etc). In this chapter, the basicity of the $[P_7M(CO)_3]^{3-}$ ions (**2PM**) is addressed and the synthesis, structure and characterization of the $[HP_7M(CO)_3]^{2-}$ ions (M = Cr, W) is described.

### 3.2 Results

#### 3.2.1 Synthesis

Ethylenediamine solutions of $[P_7M(CO)_3]^{3-}$ (M = Cr, W) react with weak acids with $pK_a$'s less than 18 to give $[HP_7M(CO)_3]^{2-}$ (**3**) compounds according to eq. 3.1.[1] The complexes were isolated as the dark red $[K(2,2,2\text{-crypt})]^+$ salts in *ca.* 76 %

$$[P_7M(CO)_3]^{3-} + \text{"}H^+\text{"} \longrightarrow [HP_7M(CO)_3]^{2-} \qquad (3.1)$$

**2PM** M = Cr (**3a**); M = W (**3b**)

crystalline yields and are moderately air and moisture sensitive in solution and the solid state. Eq. 3.1 chemistry also occurs in DMF and DMSO. $^{31}P$ NMR studies show fast rates of reaction ($t_{\infty} \approx 15$ min) and virtually quantitative conversions to **3** at ambient temperatures. Microanalysis and X-ray analyses of the crystalline solids revealed no solvate molecules for the crystalline compounds. Compounds **3** were characterized by IR, $^{1}H$, $^{13}C$ and $^{31}P$ NMR spectroscopic studies, elemental analyses and single crystal X-ray diffraction studies.

Compounds **3** have also been prepared by an alternative synthetic route. Ethylenediamine/toluene solutions of **2PM** react with one-half equiv of $I_2$ to give **3** according to eq. 3.2 (34 % crystalline yield for **3a**). Although $I_2$ appears to affect some

$$\underset{\textbf{2PM}}{[P_7M(CO)_3]^{3-}} + {}^1/_2\, I_2 \xrightarrow[\text{"H}\bullet\text{"}]{\text{en / tol}} \underset{\textbf{3}}{[HP_7M(CO)_3]^{2-}} + I^- \qquad (3.2)$$

type of transformation of **2PM** in DMF, it is clear that **3** are not formed in these reactions. The source of the hydrogen atom has not yet been determined, however, when eq. 3.2 chemistry is conducted using tol-$d_8$ instead of tol-$H_8$, $[DP_7W(CO)_3]^{2-}$ is not formed (eq. 3.3). This experiment indicates that toluene is not the hydrogen atom source.

$$\underset{\textbf{2PCr}}{[P_7Cr(CO)_3]^{3-}} + {}^1/_2\, I_2 \xrightarrow[\text{en / tol-}d_8]{} \not\rightarrow \underset{\textbf{d-3a}}{[DP_7Cr(CO)_3]^{2-}} + I^- \qquad (3.3)$$

Compounds **2PM** are not protonated by MeOH indicating that they are more acidic than MeOH. Subsequently, **3** are efficiently deprotonated by $MeO^-$ in en or DMF (eq. 3.4). In an attempt to quantify the basicity of **2PM** by competition experiments,

proton sources with various known $pK_a$ values in DMSO ($pK_{DMSO}$) were selected to combine with **2PW** (see Table 3.1).

$$\underset{\textbf{3}}{[HP_7M(CO)_3]^{2-}} + MeO^- \xrightarrow{\text{en or DMF}} \underset{\textbf{2PM}}{[P_7M(CO)_3]^{3-}} + MeOH \qquad (3.4)$$

**Table 3.1.** Acidities in DMSO Solution at 25 °C.

| Acid | $pK_{DMSO}$ | Reference |
|---|---|---|
| Acetic acid | 11.9 | 2 |
| 9-Phenylfluorene | 17.9 | 2 |
| 4-Chloro-2-nitroaniline | 18.9 | 2 |
| 4-Nitroaniline | 21.0 | 2 |
| Fluorene | 22.6 | 2 |
| Acetone | 26.5 | 2 |
| Methanol | 29.1 | 2 |
| Water | 31.4 | 3 |
| Dimethylsulfoxide | 35.1 | 3 |

When combined with dry, degassed water, methanol, acetone or fluorene ($pK_{DMSO}$ = 22.6), **2PW** remained unreacted. Further studies revealed that **2PW** reacts quickly (~ 15 min) to form **3b** when combined with 9-phenylfluorene ($pK_{DMSO}$ = 17.9). These studies provide a relative $pK_a$ range for **2PW** in DMSO from 17.9 to 22.6.

In attempts to narrow the $pK_a$ range, the obvious experiments would be to use 4-nitroaniline ($pK_{DMSO}$ = 21.0) and 4-chloro-2-nitroaniline ($pK_{DMSO}$ = 18.9) (see Table 3.1). However, when **2PW** was combined with these reagents and monitored by $^{31}P$ NMR spectroscopy, it was observed that **3b** was not formed. Instead, these reactions yielded products that have not yet been identified.

### 3.2.2 Structural Studies

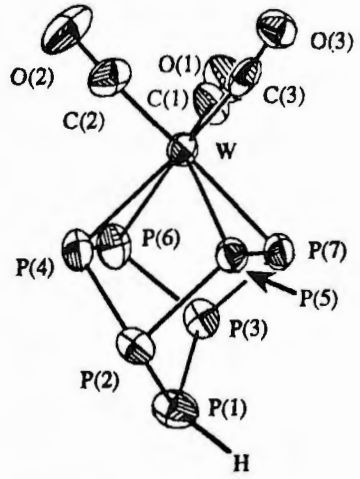


Figure 3.1. ORTEP drawing of the $[HP_7W(CO)_3]^{2-}$ ion, **3b**, using the common atomic numbering scheme. The hydrogen was not crystallographically located.

The structures of the $[K(2,2,2\text{-crypt})]^+$ salts of the $[HP_7M(CO)_3]^{2-}$ (M = Cr, W) were determined by single crystal X-ray diffraction studies. An ORTEP drawing of the $[P_7W(CO)_3]^{2-}$ anion (**3b**) is shown in Figure 3.1. A summary of the crystallographic data is given in Table 3.2 and a listing of selected bond distances and angles is given in Table 3.3.

The $[K(2,2,2\text{-crypt})]^+$ salts of the $[HP_7W(CO)_3]^{2-}$ ions (M = Cr, W) are triclinic, space group $P\bar{1}$, but are not isomorphic. The ions have virtual $C_s$ symmetry with a virtual mirror plane defined by M, P(1) and H. The $[HP_7M(CO)_3]^{2-}$ structure type contains an $\eta^4$-$P_7$ group attached to a $C_{3v}$ $M(CO)_3$ center and a hydrogen attached to the phosphorus atom furthest from the $M(CO)_3$ center. The Cr-P bond distances in **3a** (ave 2.51 Å) are virtually unchanged from the parent $[P_7Cr(CO)_3]^{3-}$ ion (ave 2.51 Å) and are typical for these types of compounds (*e.g.*, $Cr(CO)_3(PH_3)_3$, $Cr(CO)_4(PH_3)_2$).[4-

[6] The W-P bond distances in **3b** (ave 2.620 Å) are also similar to those observed for type **2PM** compounds and are virtually identical to those of $[EtP_7W(CO)_3]^{2-}$ (2.629 Å) (Chapter 4), $[(en)(CO)_2WP_7W(CO)_3]^{3-}$ (2.634 Å) (Chapter 6) and related compounds (*e.g.*, $W(CO)_4(PMe)_6$].[7] The virtual $C_s$ symmetry observed in **3** leaves two carbonyl ligands [C(2) and C(3)] in positions *trans* to P(7) and P(6), respectively [ave C-Cr-P angle = 177° (**3a**) and C-W-P angle = 176° (**3b**)]. Therefore, there is a slight lengthening of the M-P contacts to P(6) and P(7) relative to P(4) and P(5) due to the high *trans* influence of the CO ligands. The asymmetry observed in **2PCr**, **4b** and **9b** for the P(4)--P(5) and P(6)--P(7) separations is also observed in **3a** (2.81(1) Å and 3.25(2) Å, respectively) and **3b** (2.968(4) Å and 3.307(4) Å, respectively). The P-P bond distances for **3** range from 2.14 Å to 2.25 Å with a long secondary bond from P(4) to P(5) [2.81 Å (**3a**); 2.968 Å (**3b**)].[8] The shorter P-P bonds are the P(1)-P(2), P(1)-P(3), P(4)-P(6), P(5)-P(7) contacts and the typical single bonds are the P(2)-P(4), P(2)-P(5), P(3)-P(6), P(3)-P(7) contacts. The hydrogen atoms of **3** were not crystallographically located. The $[K(2,2,2\text{-crypt})]^+$ ions were crystallographically well behaved and were well separated from the anions. No solvates were located in the crystal lattices.

### 3.2.3 Spectroscopic Studies

The IR spectrum for **3b** (Figure 3.2) contains two $\nu$(HP) bands between 2235 and 2210 $cm^{-1}$ and is quite similar to **3a**. The two bands may be due to solid state effects, although it is unclear at this time. The IR spectra for **3** also contain three $\nu$(CO) bands between 1892 and 1755 $cm^{-1}$. These vibrations are blue shifted by *ca.* 40 $cm^{-1}$ from the parent trianion **2** due to the decrease in negative charge.[6]

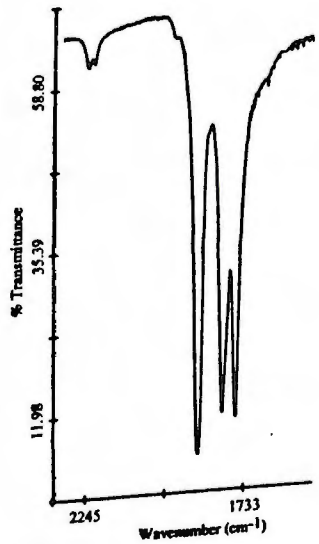


Figure 3.2. Solid-state IR spectrum (KBr pellet) showing the ν(HP) and ν(CO) regions of the $[HP_7W(CO)_3]^{2-}$ ion, **3b**.

The $^1H$ NMR spectrum for **3a** is shown in Figure 3.3 and is quite similar to **3b**. The $^1H$ NMR spectra for **3** show one resonance split into doubles of multiplets at 4.8 ppm for **3a** and 4.2 ppm for **3b**. The doublets result from one-bond hydrogen-phosphorus couplings of 168 Hz (**3a**) and 172 Hz (**3b**).

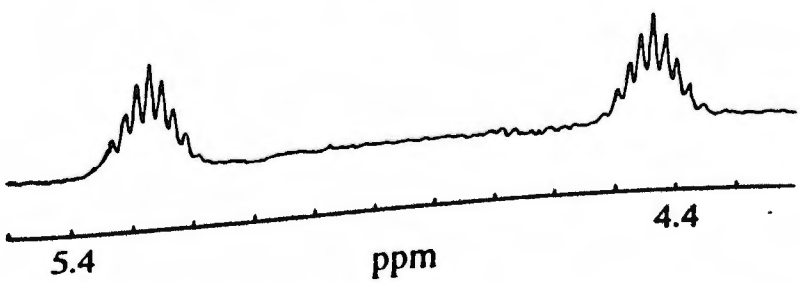


Figure 3.3. The *P-H* resonance of the $^1H$ NMR spectrum of $[HP_7Cr(CO)_3]^{2-}$, **3a**, recorded at 27 $^oC$ at 200.1 MHz in DMF-$d_7$ solution.

The $^{13}C$ NMR spectra show single carbonyl resonances at 242 ppm for **3a** and at 228 ppm for **3b**. The carbonyl resonance for **3b** shows $^{1}J_{C\text{-}W}$ = 179 Hz. This coupling is virtually identical to that exhibited for **2PW** ($^{1}J_{C\text{-}W}$ = 180 Hz).[6] The carbonyl resonance for **3b** is a broad singlet, but no carbon-phosphorus coupling could be determined. There is an upfield shift of the carbonyl resonances relative to **2PM** ($\delta$ = 246 ppm, M = Cr; $\delta$ = 232 ppm, M = W) and a downfield shift relative to the $M(CO)_6$ ($\delta$ = 212 ppm, M = Cr; $\delta$ = 192 ppm, M = W) compounds.[9]

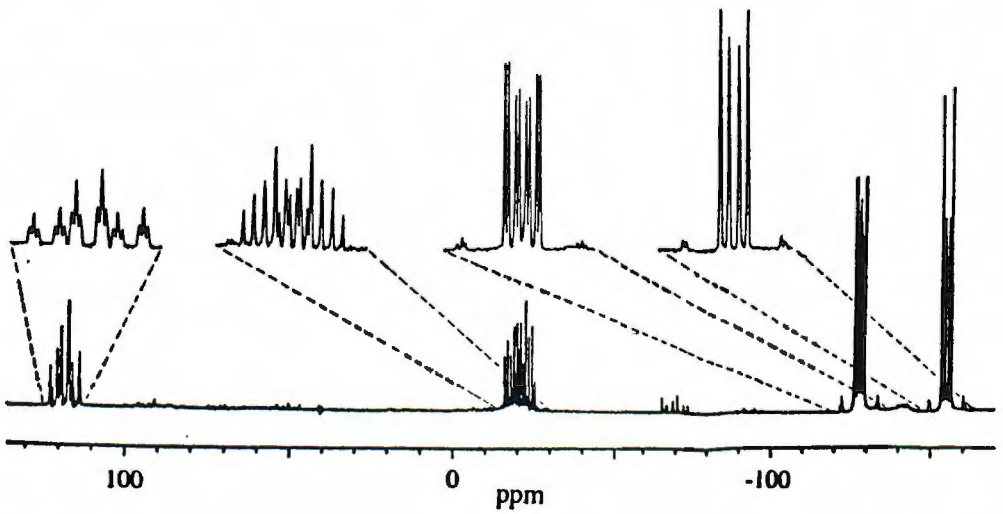


Figure 3.4. $^{31}P$ NMR spectrum for $[HP_7Cr(CO)_3]^{2-}$, **3a**, recorded at 27 °C and 81.0 MHz from DMF-$d_7$ solution.

The $^{31}P$ NMR spectrum for **3a** is shown in Figure 3.4 and is quite similar to **3b**. On the basis of the solid-state structures, seven phosphorus resonances would be anticipated due to the seven inequivalent phosphorus atoms. However, the $^{31}P$ NMR spectra for **3** show AA'BB'MM'X spin patterns in a 2:2:2:1 integral ratio corresponding to the two sets of pair-wise equivalent phosphorus atoms bound to the transition metal [P(4), P(6) and P(5), P(7)], the two bridging phosphorus atoms [P(2), P(3)] and the unique phosphorus atom [P(1)] bound to the hydrogen atom, respectively. The

**Scheme 3.1**

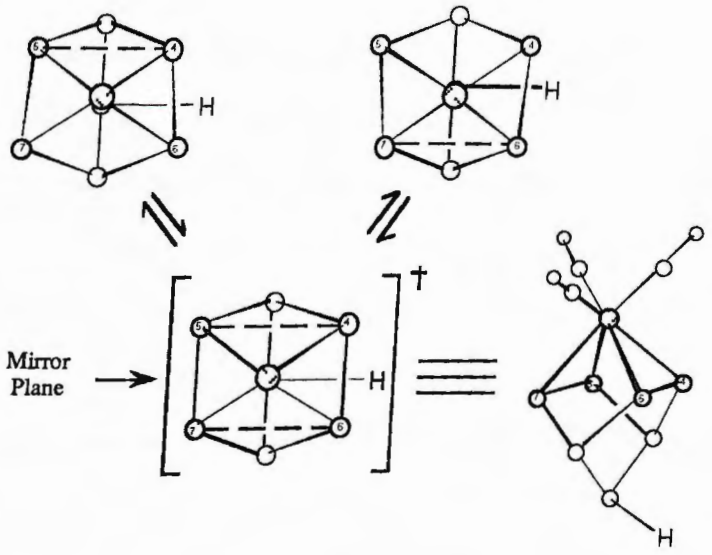


asymmetries in the P(4)--P(5) / P(6)--P(7) separations observed in the solid state are time averaged in solution due to an intramolecular wagging process. The compounds remain fluxional at -60 °C in DMF-$d_7$. The exchange process generates a virtual mirror plane that bisects the P(4)-P(6) and P(5)-P(7) bonds and makes atoms P(4) and P(5) chemically equivalent to atoms P(6) and P(7), respectively. However, inversion at P(1) is not observed on the NMR time scale. The intramolecular wagging process is based on the following: 1) rapid inversion at P(1) without the wagging process would render P(2) and P(3) **in**equivalent, which is not observed, and 2) rapid wagging **and** inversion at P(1) would make P(4), P(5), P(6), and P(7) all chemically equivalent, which is also not observed. The proton coupled spectra reveal P-H coupling identical to that observed in the $^1$H NMR spectra.

## 3.3 Discussion

Compounds **2PM** are potent nucleophiles in that extremely weak electrophiles such as $R_4N^+$ ions serve as efficient alkylating agents in the formation of $[RP_7W(CO)_3]^{2-}$ ions (**4**) at room temperature (Chapter 4).[10] In contrast to their high nucleophilicity, these compounds are only modestly basic. Compound **3** can be readily protonated and deprotonated (eqs. 3.1 and 3.2) and have a $pK_{DMSO}$ range of 17.9 to 22.6.

Although the mechanistic pathway of the eq. 3.2 chemistry is unknown at this time, it is not unrealistic to hypothesize that **3** initially undergoes a one-electron oxidation at the unique phosphorus [P(1)] upon addition of $I_2$ to form the $[\cdot P_7M(CO)_3]^{2-}$ radical. It is apparent that the "reaction" is not the transfer of a proton to **2PM** or the reaction would occur without the addition of $I_2$. However, the hydrogen radical source is yet unknown. The source is not toluene (eq. 3.3) but might be solvent or crypt. Supported by the qualitative Fenske-Hall calculations and the single crystal X-ray diffraction study of **2PCr** (Chapter 2), it is known that en is hydrogen-bond to the P(1) site. This hydrogen-bound en, through tight-ion pairing with the $[\cdot P_7M(CO)_3]^{2-}$ radical, *could* be the hydrogen atom source. This could explain why eq. 3.2 chemistry has only been observed in en.

The reactivity of the $E_7^{3-}$ (E = P, As, or Sb) Zintl ions with Group 6 and Group 10 low valent transition metal fragments has been explored.[6,10-12] The compounds formed (*i.e.*, $[E_7M(CO)_3]^{3-}$ (M = Cr, Mo, W), $[P_7Ni(CO)]^{3-}$, $[Sb_7Ni_3(CO)_3]^{3-}$, $[P_7HPt(PPh_3)]^{2-}$, etc.) contain the $E_7$ clusters bound $\eta^2$ or $\eta^4$ to the transition metal. In these compounds, the $E_7$ ligands appear to be *soft*. However, with the formation of **3** from the **2PM** precursors, the $E_7$ ligands appear to be *hard*. This "dual" character can be explained as follows: 1) soft ligands usually either have donor atoms from the

second or subsequent rows of the periodic table (*e.g.*, $Br^-$, $PPh_3$, etc.) or they have double or triple bonds (ethylene, acetylene, benzene, etc.) and 2) hard ligands usually are good donor ligands that may have lone pairs of electrons to use for donation. The complexation of the $E_7$ cluster to the Group 6 $M(CO)_3$ fragments has been described as diene-like attachment through $\pi$-type interactions.[6] Additionally, the $E_7$ ligands have donor atoms from the second or subsequent rows of the periodic table. It follows, then, that the $E_7$ ligands be classified as *soft* in their interaction with low valent transition metal fragments. The atom furthest from the transition metal fragment in **2EM** is a two-coordinate pnictogen that has two lone pairs of electrons and can be formally assigned a -1 charge. It is these lone-pairs of electrons that can be donated to various electrophiles that enable the $E_7$ ligand to be classified as *hard.*[13-15]

## 3.4 Experimental Section

### 3.4.1 General Data

General operating procedures used in this laboratory have been described in Chapter 2. General data not included in Chapter 2 follow. Proton ($^1H$) NMR spectra were recorded at ambient temperature on both Bruker WP200 (200.133 MHz) and AM400 (400.136 MHz) spectrometers. Elemental analyses were performed under inert atmosphere by Schwarzkopf Microanalytical Laboratories, Woodside, N.Y. and Desert Analytics, Tucson, AZ.

The IR and NMR spectral data common to all compounds containing $[K(2,2,2\text{-crypt})]^+$ and/or en were reported in Chapter 2.

### 3.4.2 Materials

All materials not included in Chapter 2 follow. Flourene, 9-phenylfluorene, 4-

chloro-2-nitroaniline, and 4-nitroaniline were purchased from Aldrich and used without further purification. DMF was purchased from Burdick & Jackson (High Purity) and distilled at reduced pressure from $K_4Sn_9$.

### 3.4.3 Synthesis

#### 3.4.3.1 Preparation of $[K(2,2,2\text{-crypt})]_2[HP_7Cr(CO)_3]$.

Method A: $K_3P_7$ (29.6 mg, 0.089 mmol), 2,2,2-crypt (100.0 mg, 0.27 mmol) and (mesitylene)$Cr(CO)_3$ (22.4 mg, 0.089 mmol) were dissolved in en (~ 3 mL) in a 5 Dram vial in a drybox and stirred for 12 h producing an orange solution. 9-Phenylflourene (21.6 mg, 0.089 mmol) was added as a solid and the reaction mixture was stirred for an additional 2 h producing a dark red solution. The reaction mixture was filtered through *ca.* one quarter in. of tightly packed glass wool in a pipet. After 4 h, the reaction vessel contained rectangular dark red crystals that were removed from the mother liquor, washed with toluene, and dried under vacuum (crystalline yield, 80 mg, 76 %). Method B: In vial 1, $K_3P_7$ (29.6 mg, 0.089 mmol) and 2,2,2-crypt (100 mg, 0.27 mmol) were dissolved into en (~ 3 mL) producing a yellow-orange solution. In vial 2, $[C_6H_3(CH_3)_3]Cr(CO)_3$ (22.4 mg, 0.089 mmol) was dissolved into toluene (~ 1 mL) producing a yellow solution. The contents of vial 2 were added dropwise to the contents of vial 1 producing an orange solution. The reaction mixture was stirred for 12 h. Iodine crystals (11.2 mg, 0.045 mmol) were added. The solution was stirred for an additional 15 min and filtered through *ca.* one quarter in. of tightly packed glass wool in a pipet. After 2 h, the reaction vessel contained rectangular dark red crystals. The crystals were removed from the mother liquor, washed with toluene and dried under vacuum (crystalline yield, 36 mg, 34 %). Anal. Calcd. for $C_{39}H_{73}N_4O_{15}K_2P_7Cr$ (Method B): C, 39.53; H, 6.21; N, 4.73. Found: C, 39.78; H, 6.21; N, 4.83. IR

(KBr pellet), $cm^{-1}$: 2219, 2210, 1872, 1799, 1755. $^{1}H$ NMR (DMF-$d_7$) δ(ppm): 4.8 (dm, $^{1}J_{H-P}$ = 168 Hz). $^{13}C$ NMR (DMF-$d_7$) δ(ppm): 242 (br s, *CO*). $^{31}P\{^{1}H\}$ NMR (DMF-$d_7$) δ(ppm): 119 [ttt, $^{1}J_{P-P}$ = 270 Hz, $^{2}J_{P-P}$ = 27 Hz, $^{2}J_{P-P}$ = 7.5 Hz; 1 P, P(1)], -20 [2nd order multiplet, 2 P, P(2,3)], -127 [2nd order multiplet, 2 P, P(4,6) or P(5,7)], -153 [2nd order multiplet, 2 P, P(4,6) or P(5,7)].

### 3.4.3.2 Preparation of $[K(2,2,2\text{-crypt})]_2[HP_7W(CO)_3]$.

A procedure identical to that described for $[K(2,2,2\text{-crypt})]_2[HP_7Cr(CO)_3]$ (Method A) was followed except (mesitylene)$W(CO)_3$ (34.4 mg, 0.089 mmol) was used in the reaction. The reaction mixture was filtered through *ca.* one quarter in. of tightly packed glass wool in a pipet. After 4 h, the reaction vessel contained rectangular dark red crystals that were removed from the mother liquor, washed with toluene, and dried under vacuum (crystalline yield, 89 mg, 76 %). Anal. Calcd for $C_{39}H_{73}N_4O_{15}K_2P_7W$: C, 35.57; H, 5.59; N, 4.25. Found: C, 35.94; H, 5.59; N, 4.48. IR (KBr pellet), $cm^{-1}$: 2235, 2212, 1880, 1800, 1758. $^{1}H$ NMR (DMF-$d_7$) δ(ppm): 4.2 (dm, $^{1}J_{H-P}$ = 172 Hz). $^{13}C$ NMR (DMF-$d_7$) δ(ppm): 228 (br s, $^{1}J_{C-W}$ = 179 Hz, *CO*). $^{31}P\{^{1}H\}$ NMR (DMF-$d_7$) δ(ppm): 111 [tt, $^{1}J_{P-P}$ = 263 Hz, $^{2}J_{P-P}$ = 29 Hz, 1 P, P(1)], 24 [2nd order multiplet, 2 P, P(2,3)], -149 [2nd order multiplet, 2 P, P(4,6) or P(5,7)], -181 [2nd order multiplet, 2 P, P(4,6) or P(5,7)].

### 3.4.3.3 Attempted Preparation of $[DP_7Cr(CO)_3]^{2-}$ with Toluene-$d_8$

A procedure identical to that described for $[K(2,2,2\text{-crypt})]_2[HP_7Cr(CO)_3]$ (Method B) was followed except toluene-$d_8$ was used. $^{31}P$ NMR analysis showed $[HP_7Cr(CO)_3]^{2-}$.

### 3.4.3.4 Attempts at Deprotonation of $[HP_7W(CO)_3]^{2-}$

$[K(2,2,2\text{-crypt})]_2[HP_7W(CO)_3]$ (0.089 mmol) was generated *in situ* as described above. Solid NaOMe (7.2 mg, 0.134 mmol) was added and the reaction mixture stirred for 4 h. $^{31}P$ NMR spectroscopic analysis of the mother liquor showed quantitative conversion to $[P_7W(CO)_3]^{3-}$.

### 3.4.3.5 Preparation of $pK_{DMSO}$-Determination Experiments

In a dry box $K_3P_7$ (29.6 mg, 0.089 mmol) and mesitylene$W(CO)_3$ (34.4 mg, 0.089 mmol) were combined in DMSO-$d_6$ (~ 2 mL) and stirred for 12 h yielding a dark red solution. Fluorene (14.8 mg, 0.089 mmol) or 9-phenylfluorene (21.6 mg, 0.089 mmol) were added as a solid. The reaction mixture was stirred for an additional 1/2 h. An aliquot was removed from each reaction mixture and monitored by $^{31}P$ NMR spectroscopy.

### 3.4.4 Crystallographic Experimental Details for $[K(2,2,2\text{-crypt})]_2[HP_7M(CO)_3]$ (M = Cr, W).

Single crystal X-ray diffraction study for $[K(2,2,2\text{-crypt})]_2[HP_7Cr(CO)_3]$ was done by Dr. Bryan W. Eichhorn and for $[K(2,2,2\text{-crypt})]_2[HP_7W(CO)_3]$ was done by Dr. James C. Fettinger, University of Maryland.[1]

**Table 3.2.** Crystallographic data for $[K(2,2,2\text{-crypt})]_2[HP_7M(CO)_3]$ (M = Cr, W).

| formula | $C_{39}H_{73}N_4O_{15}K_2P_7Cr$ | $C_{39}H_{73}N_4O_{15}K_2P_7W$ |
|---|---|---|
| fw | 1185.0 | 1316.9 |
| space group | $P\bar{1}$ | $P\bar{1}$ |
| *a*, Å | 12.000(3) | 10.9709(8) |
| *b*, Å | 14.795(3) | 13.9116(10) |
| *c*, Å | 17.421(4) | 19.6400(14) |
| α, deg | 93.01(2) | 92.435(6) |
| β, deg | 93.79(2) | 93.856(6) |
| γ, deg | 110.72(2) | 108.413(6) |
| V, $Å^3$ | 2877(2) (Z = 2) | 2831.2(4) (Z = 2) |
| D(calcd), g $cm^3$ | 1.37 | 1.544 |
| μ(Mo $K_\alpha$), $cm^{-1}$ (λ = 0.71073 Å) | 6.06 | 24.46 |
| temp, K | 296 | 153(2) |
| 2θ (max), deg | 45.0 | 22.50 |
| F(000) | 1244 | 1342 |
| no. of reflns, colld | 1516 | 7868 |
| no. of ind. reflns | unknown | 7400[$R_{int}$= .0344] |
| Data/restraints/parameters | unknown | 7400 / 136 / 657 |
| $F_o \geq n\sigma(F_o)$ | (n = 5) | (n = 4) [5733 data] |
| R(F), %[a] | 8.3 | 5.20 |
| $R_w(F^2)$, %[b] | 11.4 | 12.67 |
| Δ/σ(max) | 0.89 | ≤ 0.001 |
| GOF | 2.57 | 1.049 |

[a] $R(F) = \Sigma \mid F_o - F_c \mid / \Sigma F_o$. [b] $R_w(F^2) = (\Sigma w \mid F_o - F_c \mid^2 / \Sigma w F_o^2)^{1/2}$.

**Table 3.3**. Selected bond distances ( Å ) and angles ( $^{o}$ ) for the $[HP_7M(CO)_3]^{2-}$ (M = Cr, W) ions.

| Distances | M = Cr | M = W | Distances | M = Cr | M = W |
|---|---|---|---|---|---|
| P(1)-P(2) | 2.20(2) | 2.163(4) | P(1)-P(3) | 2.14(2) | 2.162(4) |
| P(2)-P(4) | 2.19(2) | 2.219(4) | P(2)-P(5) | 2.25(2) | 2.217(4) |
| P(3)-P(6) | 2.19(2) | 2.220(4) | P(3)-P(7) | 2.21(2) | 2.199(4) |
| P(4)--P(5) | 2.81(1) | 2.968(4) | P(6)--P(7) | 3.25(2) | 3.307(4) |
| P(4)-P(6) | 2.15(2) | 2.145(4) | P(5)-P(7) | 2.15(1) | 2.162(4) |
| P(4)-M | 2.46(1) | 2.565(3) | P(5)-M | 2.44(1) | 2.563(2) |
| P(6)-M | 2.56(1) | 2.674(3) | P(7)-M | 2.59(1) | 2.676(3) |
| M-C(1) | 1.90(5) | 1.971(10) | M-C(2) | 1.79(6) | 1.944(12) |
| M-C(3) | 1.80(4) | 1.975(11) | C(1)-O(1) | 1.16(4) | 1.153(11) |
| C(2)-O(2) | 1.15(5) | 1.184(13) | C(3)-O(3) | 1.15(3) | 1.164(11) |

| Angles | M = Cr | M = W | Angles | M = Cr | M = W |
|---|---|---|---|---|---|
| P(1)-P(2)-P(4) | 104.7(7) | 106.(2) | P(1)-P(3)-P(7) | 100.1(6) | 97.8(2) |
| P(2)-P(1)-P(3) | 100.8(7) | 100.0(2) | P(2)-P(4)-P(6) | 106.5(7) | 105.9(2) |
| P(3)-P(7)-P(5) | 104.1(6) | 103.74(14) | P(4)-P(2)-P(5) | 78.3(5) | 83.99(13) |
| P(6)-P(3)-P(7) | 95.6(6) | 96.9(2) | P(4)-M-P(5) | 70.1(4) | 70.73(8) |
| P(4)-M-P(6) | 50.8(4) | 48.28(9) | P(6)-M-P(7) | 78.6(4) | 76.36(9) |
| P(2)-P(4)-M | 104.8(5) | 101.65(12) | P(3)-P(7)-M | 92.3(5) | 93.52(11) |
| P(4)-P(6)-M | 62.1(4) | 63.20(10) | P(7)-P(5)-M | 68.4(4) | 68.38(10) |
| P(4)-M-C(1) | 130(1) | 129.2(3) | P(5)-M-C(1) | 140(1) | 136.9(3 |
| P(4)-M-C(2) | 85(2) | 84.2(3) | P(4)-M-C(3) | 129(1) | 133.1(3) |
| P(6)-M-C(3) | 177(1) | 175.9(3) | P(7)-M-C(2) | 176(2) | 176.9(3) |

## 3.5 References


(1) Charles, S. C.; Eichhorn, B. W.; Fettinger, J. C. **1995**, in preparation.

(2) *Solute-Solvent Interactions*; Coetzee, J. F.; Ritchie, C. D., Ed.; Marcel Dekker, Inc.: New York, 1976; Vol. 2, pp 232-233.

(3) Bordwell, F. G.; Olmstead, W. N.; Margolin, Z. *J. Org. Chem.* **1980**, *45*, 3295-3299.

(4) Guggenberger, L. S.; Klabunde, U.; Schunn, R. A. *Inorg. Chem.* **1973**, *12*, 1143-1148.

(5) Huttner, G.; Schelle, S. *J. Organomet. Chem.* **1973**, *47*, 383-390.

(6) Charles, S.; Eichhorn, B. W.; Rheingold, A. L.; Bott, S. G. *J. Am. Chem. Soc.* **1994**, *116*, 8077-8086.

(7) Elmes, P. S.; Gatehouse, B. M.; West, B. O. *J. Organomet. Chem.* **1974**, *82*, 235-241.

(8) Alcock, N. W. *Adv. Inorg. Chem. Radiochem.* **1972**, *15*, 1-53.

(9) Braterman, P. S.; Milne, D. W.; Randall, E. W.; Rosenberg, E. *J. Chem. Soc., Dalton Trans.* **1973**, 1027-1031.

(10) Charles, S.; Fettinger, J. C.; Eichhorn, B. W. *J. Am. Chem. Soc.* **1995**, *117*, 5303-5311.

(11) Charles, S.; Eichhorn, B. W.; Bott, S. G. *J. Am. Chem. Soc.* **1993**, *115*, 5837- 5838.

(12) Charles, S.; Eichhorn, B. W.; Bott, S. G.; Fettinger, J. C. *Angew. Chem. Int. Ed. Engl.* **1995**, submitted.

(13) Pearson, R. G. *J. Am. Chem. Soc.* **1963**, *85*, 3533-3539.

(14) Pearson, R. B. *Chem. Brit.* **1967**, *3*, 103-107.

(15) Pearson, R. B. *Hard and Soft Acids and Bases*; Hutchinson & Ross, Inc.: Stroudsburg, PA, 1973.

# CHAPTER 4

## Tetraalkylammonium Salts as Stereoselective Alkylating Agents for Highly Nucleophilic Polyphosphide Zintl Anions

### 4.1 Introduction

The polyphosphide Zintl ions represent a remarkable class of compounds that have a rich structural diversity and a unique chemistry.[1-3] For example, $K_3P_7$ dissolves in ethylenediamine (en) to give discrete $P_7^{3-}$ ions (**1P**) that adopt the nortricyclane structure (**1.II**).[3] Baudler,[4-6] Hönle,[7-9] von Schnering[2,7] and Fenske[10] have shown that $P_7^{3-}$ can be derivatized in a systematic fashion to give various alkylated, protonated, and metallated compounds (*e.g.*, $R_3P_7$, $H_3P_7$, $(PbMe_3)_3P_7$). Recently, the transition metal chemistry of the $E_7^{3-}$ polypnictide anions where E = P, As, Sb has been the subject of investigation.[11-19] These studies have yielded many new compounds that include the series of $[E_7M(CO)_3]^{3-}$ ions[11,13,19] where E = P, As, Sb and M = Cr, Mo, W as described in Chapter 2. The $[E_7M(CO)_3]^{3-}$ compounds have norbornadiene-like $E_7$ fragments, as shown in Figures 2.1 and 2.2, with a formal negative charge associated with the unique two-coordinate E atom futhest from the transition metal (the E(1) site). This pnictogen atom remains highly nucleophilic and is the site of attack by various electrophiles.[13,14,17,18]

During the course of studying the chemistry of the $[P_7M(CO)_3]^{3-}$ compounds, an unusual reaction with tetraalkylammonium salts was observed in which the $R_4N^+$ ions serve as alkylating agents. In this chapter the ambient temperature alkylations of the $[P_7M(CO)_3]^{3-}$ compounds and their $P_7^{3-}$ precursor using $R_4N^+$ salts (where R = Me, Et, *n*-Bu) as $R^+$ sources are described.

## 4.2 Results

### 4.2.1 Synthesis

Ethylenediamine solutions of $[P_7W(CO)_3]^{3-}$ (**2PW**) react with excess $R_4NBr$ to give dark red $[RP_7W(CO)_3]^{2-}$ compounds where R = Me (**4a**), Et (**4b**), *n*-Bu (**4c**) in 37-69 % crystalline yields (eq. 4.1) as the $[K(2,2,2\text{-crypt})]^+$ salts. $^{31}P$ NMR spectroscopic

$$\underset{\textbf{2PW}}{[P_7W(CO)_3]^{3-}} + \text{xs } R_4N^+ \xrightarrow{\text{en}} \underset{\begin{array}{l}\textbf{4a (R = Me)}\\ \textbf{4b (R = Et)}\\ \textbf{4c (R = } n\text{-Bu)}\end{array}}{[RP_7W(CO)_3]^{2-}} + NR_3 \qquad (4.1)$$

studies show modest rates of reaction ($t_\infty \approx 1$ h) and virtually quantitative conversions to **4** at ambient temperatures when R = Et, *n*-Bu. Because of the limited solubility of the $Me_4N^+$ ion in en, the formation of **4a** required gentle heating (*ca.* 40 °C) to obtain similar reaction rates. Like the protonation reactions discussed in Chapter 3, alkylation occurs at the P(1) site (see Figure 4.1) which is the most nucleophilic site on the precursor **2PW**. The mixed alkylammonium ions $Me(n\text{-}C_8H_{17})_3N^+$ and $(CH_2Ph)Me_3N^+$ gave quantitative conversions to the $[MeP_7W(CO)_3]^{2-}$ and $[(CH_2Ph)P_7W(CO)_3]^{2-}$ ions, respectively, as shown in eqs. 4.2 and 4.3. Equation 4.2 chemistry affords a higher yield of **4a** (49 % crystalline yield) than that obtained from eq. 4.1. Reactions of **3** with excess olefin did not give **4** (eq. 4.4). Attempted alkyations of **2PW** with alkyl halides were also unsuccessful. The implications of reactions 4.2-4.4 will be presented in Section 4.3.

$$[P_7W(CO)_3]^{3-} + \text{xs } Me(n\text{-}C_8H_{17})_3N^+ \xrightarrow{\text{en}} [MeP_7W(CO)_3]^{2-} + (n\text{-}C_8H_{17})_3N \quad (4.2)$$

**2PW** **4a**

$$[P_7W(CO)_3]^{3-} + \text{xs } (CH_2Ph)Me_3N^+ \xrightarrow{\text{en}} [(CH_2Ph)P_7W(CO)_3]^{2-} + Me_3N \quad (4.3)$$

**2PW** **4d**

$$[HP_7W(CO)_3]^{2-} + \text{xs olefin} \not\longrightarrow [RP_7W(CO)_3]^{2-} \quad (4.4)$$

**3b**

Tetraalkylphosphonium ions such as $PPh_4^+$ and $(n\text{-}Bu)_4P^+$ are unreactive towards compounds **2PM** and, in fact, aid in crystal growth of related *tri*anionic metallated Zintl ion compounds by replacing $[K(2,2,2\text{-crypt})]^+$ cations in the crystal lattice.[16] Compounds **4** are air and moisture sensitive and have been characterized by $^1H$, $^{13}C$ and $^{31}P$ NMR and IR spectroscopic studies, elemental analyses, and a representative single crystal X-ray diffraction study.

Because of the unusual nature of the above alkylation reaction, the use of alkylammonium salts to affect multiple alkylations of $P_7^{3-}$ in analogy to the alkyl halide chemistry described by Baudler and von Schnering was investigated.[4,7,20,21] Surprisingly, reactions of $P_7^{3-}$ with excess $R_4N^+$ gives quantitative conversions (one product by $^{31}P$ NMR) to the symmetrical *di*substituted $[R_2P_7]^-$ products (eq. 4.5) where R = Me (**5a**), Et (**5b**) and *n*-Bu (**5c**). These alkylation reactions proceed slowly at room temperature ($t_\infty \approx 6$ - 12 h) and do not require crypt or crown activators. However, the use of crypt or crown ethers appears to accelerate the reaction rates and all three compounds have been prepared as the $K^+$, $[K(18\text{-crown-6})]^+$, and $[K(2,2,2\text{-crypt})]^+$ salts. The use of only one equiv $R_4N^+$ in eq. 4.5 chemistry results in mixtures of compounds **5** and unreacted

$$P_7^{3-} + \text{excess } R_4N^+ \xrightarrow{\text{en}} [R_2P_7]^- + 2\,NR_3 \qquad (4.5)$$

**1P** **5a** (R = Me)

**5b** (R = Et)

**5c** (R = *n*-Bu)

starting material **1P**. Alkylphosphonium salts do not alkylate the $P_7^{3-}$ ion, however, $PPh_4^+$ affects an oxidative coupling to give $P_{16}^{2-}$ as mentioned in Chapter 1 (eq. 1.3).[22] Compounds **5** have been characterized by $^1H$, $^{13}C$, $^{31}P$ NMR and 2-D $^{31}P$-$^{31}P$ COSY NMR spectroscopic studies. Compounds **5** were isolated as oily solids that were contaminated with trialkyl amine byproducts and presumably potassium bromide. Repeated attempts to purify the compounds by crystallization / precipitation and sublimation were unsuccessful and we could therefore only characterize the compounds by spectroscopic methods and by derivatization (see below).

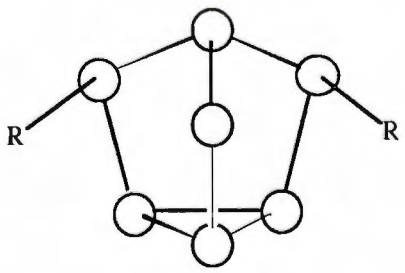


**5**

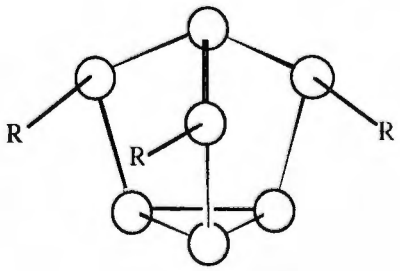


**6**

Compounds **5** can be alkylated further through reactions with alkyl halide reagents to give neutral $R_2R'P_7$ trialkyl compounds (**6**) (eq. 4.6). For example, **5c** reacts cleanly with *n*-BuBr in DMF to give $(n\text{-Bu})_3P_7$ (**6e**) in good yield.[21] Equation

$$[R_2P_7]^- + R'X \xrightarrow{en} R_2R'P_7 + X^- \qquad (4.6)$$

**5**

**6a** R = R' = Me

**6b** R = Me, R' = $CH_2Ph$

**6c** R = *n*-Bu, R' = Me

**6d** R = *n*-Bu, R' = $CH_2Ph$

**6e** R = R' = *n*-Bu

4.6 chemistry appears to give virtually quantitative conversions to mixtures of isomers, which requires inversion at one alkylated phosphorus position. Due to the extreme insolubility and thermal instability of most of compounds **6**, determination of percent conversions and diasteromeric distributions were quite difficult. Compounds **6a-6d** are pale orange to white solids that are moderately air sensitive, thermally unstable, and sparingly or insoluble in most solvents (THF, toluene, en, DMF). The *n*-Bu complex **6e** is appreciably soluble in DMF and en and is sparingly soluble in toluene. Compounds **6** have been characterized by $^{31}P$ NMR spectroscopies and fast atom bombardment mass spectroscopy (FAB-MS). The FAB-MS analyses of **6** showed protonated molecular ions ($[HR_2R'P_7]^+$) for all compounds along with secondary ions due to loss of various alkyl groups. The data are summarized in Table 4.1. Because of the thermal instability of these compounds, elemental analyses were not possible.

### 4.2.2 Structural Studies

The structure of the $[K(2,2,2\text{-crypt})]^+$ salt of $[EtP_7W(CO)_3]^{2-}$ (**4b**) was determined by single crystal X-ray diffraction. An ORTEP drawing of the anion is shown in Figure 4.1. A summary of the crystallographic data is given in Table 4.2 and a listing of selected bond distances and angles given in Table 4.3.

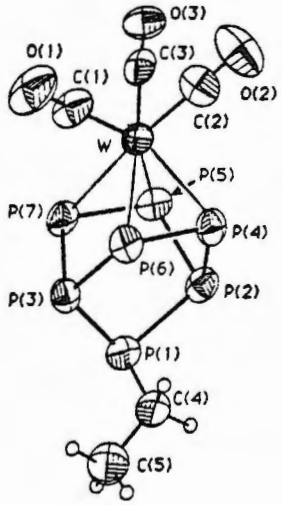


**Figure 4.1.** ORTEP drawing of the $[EtP_7W(CO)_3]^{2-}$ ion.

The structure contains a $\eta^4$-$P_7$ group attached to a $C_{3v}$ $W(CO)_3$ center and an ethyl group attached to the phosphorus atom furthest from the $W(CO)_3$ center. The attachment of the ethyl group lowers the virtual point symmetry of the ion from $C_s$ to $C_1$ in the solid state but virtual $C_s$ symmetry is observed in solution (see below). The W-P and P-P bond distances and angles are remarkably similar to those observed for types **2** and **3** compounds and range from 2.137 Å to 2.215 Å. The P(4)--P(5) and P(6)--P(7) separations of 2.923(3) Å and 3.299(3) Å, respectively, are highly asymmetric as is also observed in types **2** and **3** compounds.[13] The P-C bond of 1.858(7) Å is typical for compounds of this type and those in trialkyl phosphines.[23] The en solvate molecule and the $[K(2,2,2\text{-crypt})]^+$ ions were crystallographically well behaved and were well separated from the anion.

The $[K(2,2,2\text{-crypt})]^+$ salt of **4c** crystallizes with cubic crystal symmetry ($a$ = 19.0824(7) Å) but the structure was unsolved.

The alkyl groups of **5** reside on two of the three two-coordinate phosphorus atoms of the parent $P_7$ cage (see **1.II**). Only one two-coordinate P atom remains in **5**

(see **4.I** and previous drawing of **5**) and it bears a formal negative charge. There are three possible isomers for compounds **5** as illustrated in structures **4.I**-**4.III** below (viewed down the former $C_3$ axis of **1.II**). Structures **4.I** and **4.II** both have $C_s$ point symmetry with mirror planes bisecting the alkyl groups. In both structures, there are two pairs of equivalent phosphorus atoms with the remaining three being unique. In structure **4.III**, all seven phosphorus atoms are inequivalent. The NMR data show only one isomer in solution (see Section 4.2.3) and its spectral features are consistent with both structures **4.I** and **4.II**. Based on steric arguments, we believe that **4.I** is the structure adopted by **5**.

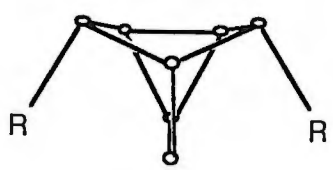


**4.I**

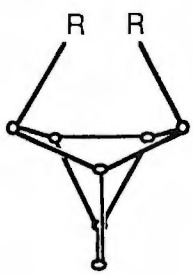


**4.II**

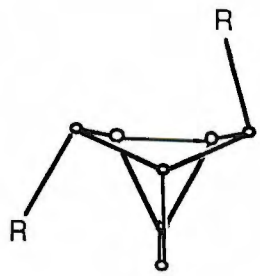


**4.III**

Compounds **6** possess three alkyl groups that are attached to the former two-coordinate phosphorus atoms of **1P**. There are two possible isomers of compounds **6**, **6-*sym*** and **6-*asym***, as illustrated below. $^{31}P$ NMR studies monitoring the formation of **6e** at -20 °C in DMF show that mixtures of isomers **6-*sym*** and **6-*asym*** are present in a 1:10 molar ratio at all stages of conversion. The 1:10 ratio of isomers is independent of termperature (-20 °C to +50 °C) and solvent (DMF, toluene, en).

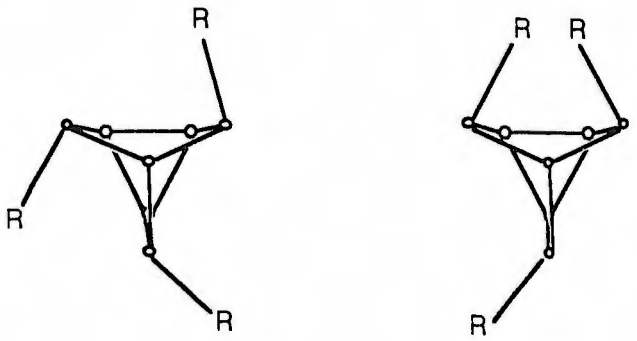


*6-sym* *6-asym*

### 4.2.3 Spectroscopic Studies

The spectroscopic data for compounds **4-6** are summarized in Table 4.4 and the remaining spectroscopic data are given in the Experimental Section (Section 4.4).

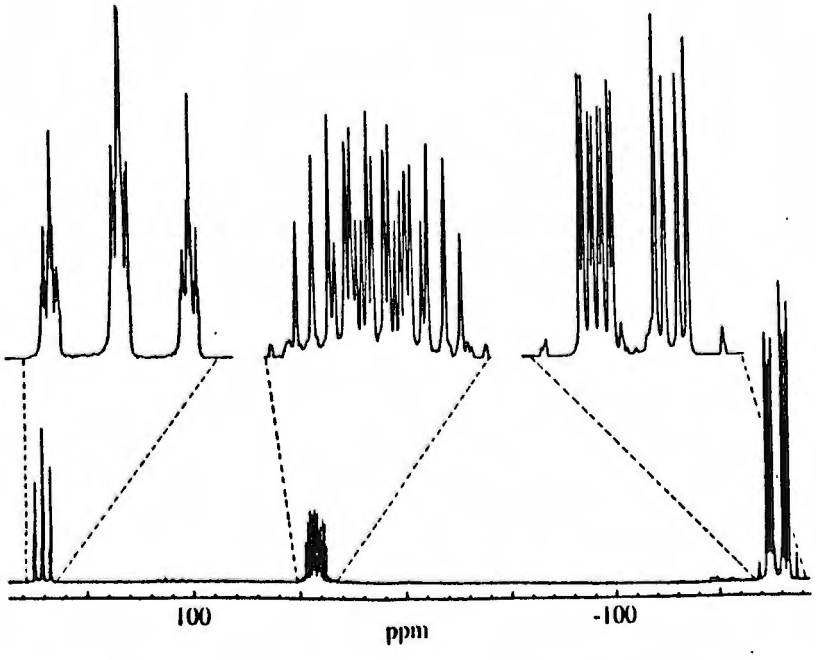


**Figure 4.2.** $^{31}P\{^{1}H\}$ NMR spectrum of $[EtP_7W(CO)_3]^{2-}$ recorded in DMF-$d_7$ at 28 $^{o}C$ and 81.0 MHz.

Based on the crystal structure of **4b**, one would anticipate seven $^{31}P$ resonances due to the seven inequivalent phosphorus atoms observed in the solid state. However, the $^{31}P$ NMR spectra for **4** (Fig. 4.2) show AA'BB'MM'X spin patterns due to a fluxional process that generates a virtual mirror plane of symmetry. The compounds remain fluxional at -60 °C in DMF-$d_7$. The data indicate that the $M(CO)_3$ fragments rotate rapidly in the $P_4$ face of compounds **4** as is common for similar $[E_xM(CO)_3]^{n-}$ [13,24,25] complexes and related organometallic compounds.[26-28] The data also indicate that the P(4)--P(5) / P(6)--P(7) asymmetries observed in the solid state are time averaged in solution (an intramolecular wagging process--Scheme 4.1) but inversion at P(1) is not observed on the NMR time scale. These conclusions are based on the following: (1) rapid inversion at P(1) without the wagging process would render P(2) and P(3) **in**equivalent, which is not observed, and (2) rapid wagging **and** inversion at P(1) would make P(4), P(5), P(6) and P(7) all chemically equivalent, which is also not observed.

**Scheme 4.1**

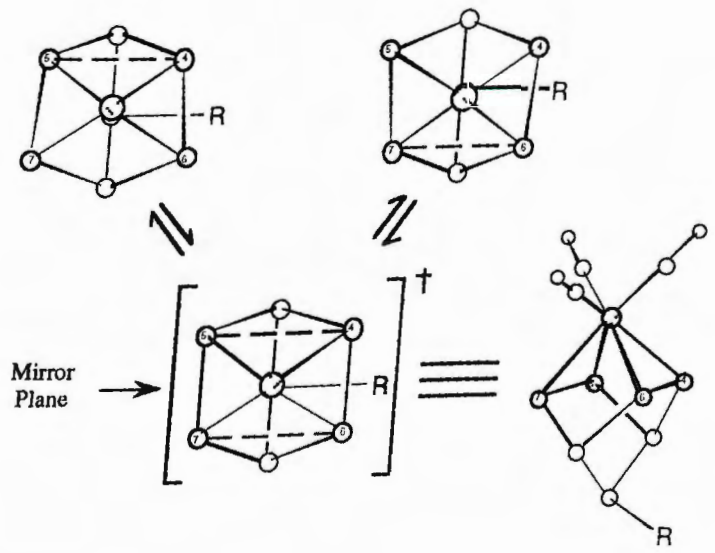

The $^{13}C$ NMR spectra show a single carbonyl resonanace at 229 ppm with $^{1}J_{W-C}$ = 167 Hz and $^{2}J_{P-C} \leq$ 4 Hz. Both coupling constants are only slightly diminished relative to **2PW** ($^{1}J_{W-C}$ = 180 Hz and $^{2}J_{P-C} \approx$ 5 Hz) which is surprising in view of the significant decrease in charge and the large blue shift in the ν (CO) bands (*ca.* 40 $cm^{-1}$). This P-C coupling indicates that $W(CO)_3$ / $P_7^{3-}$ dissociation is not occuring on the NMR time scale. The $^{1}J_{P-C}$ coupling constants to the α-carbons of the alkyl groups range 26 to 30 Hz which is also typical for alkyl polyphosphorous compounds but larger than coupling of 10-15 Hz observed in trialkylphosphines.[29] The α-hydrogens of **4b**, **4c** and **4d** are non-diastereotopic in that they are bisected by a mirror plane generated by the wagging process described above (Scheme 4.1).

The IR spectra for compounds **4** each contain three ν(CO) bands between 1874 and 1750 $cm^{-1}$. Due to the relative decrease in negative charge, these vibrations are blue shifted by *ca.* 40 $cm^{-1}$ from the parent trianion **2PW**.

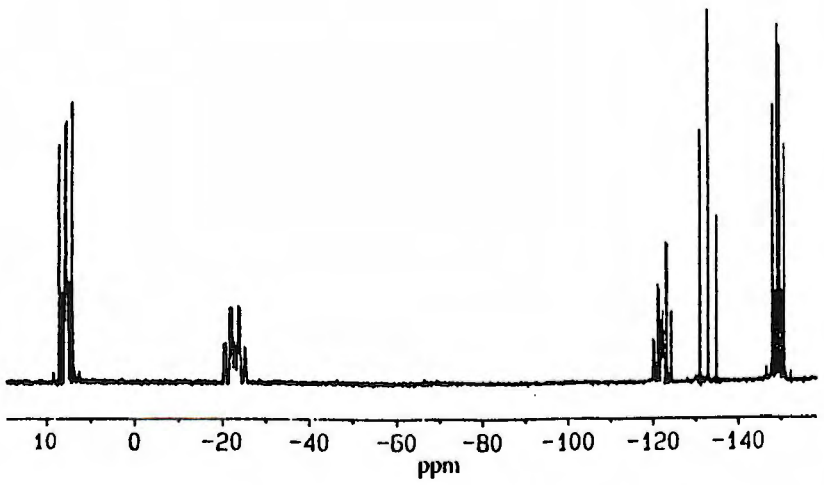


**Figure 4.3.** $^{31}P\{^{1}H\}$ NMR spectrum of $[Me_2P_7]^-$ from a crude reaction mixture of $P_7^{3-}$ and $Me_4N^+$ recorded in DMF-$d_7$ at 28 °C and 202.4 MHz.

The P-P coupling constants and the general features of the $^{31}P$ NMR spectra of compounds **5** are quite similar to those of the symmetrical $[H_2P_7]^-$ ion reported by Baudler *et al.*[6] The $^{31}P\{^1H\}$ NMR spectra for compounds **5** show five second-order resonanaces with relative intensities of 2:1:1:1:2 (Fig. 4.3). The solution structure is clearly that of a symmetrical isomer (**4.I** or **4.II**) in that seven equal intensity $^{31}P$ resonances would be expected for the unsymmetrical isomer (**4.III**). Through the use of proton coupled $^{31}P$ NMR and 2-D $^{31}P$-$^{31}P$ COSY NMR experiments, one can assign all five resonances in the $^{31}P$ NMR spectrum. The proton-coupled spectrum of **5a** shows broadening of the downfield resonance at 12 ppm due to coupling to the α-hydrogens of the alkyl groups. Thus, the two resonances of relative intensity two at 18 and -153 ppm can be assigned to alkylated and the non-alkylated equivalent pairs, respectively.

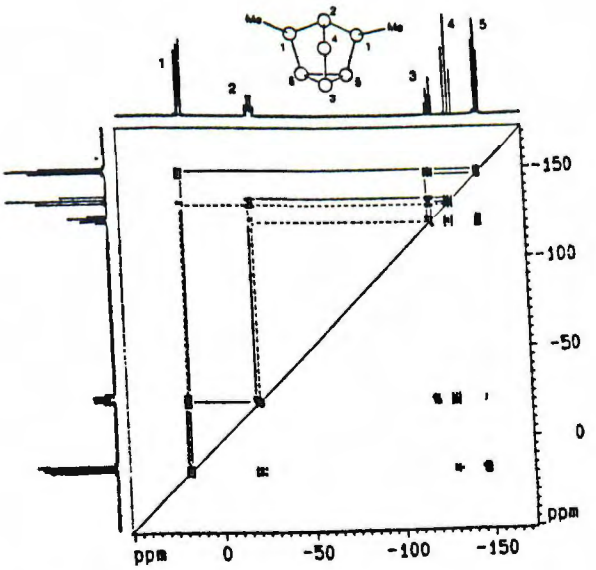


**Figure 4.4.** $^{31}P$ - $^{31}P$ COSY NMR spectrum of $[Me_2P_7]^-$ recorded in DMF-$d_7$ at 25 °C and 202.4 MHz. The atomic labelling scheme is shown in the inset. The solid lines denote cross peaks due to one-bond P-P couplings. The dashed lines represent the two-bond couplings.

The $^{31}P$-$^{31}P$ COSY NMR spectrum (Fig. 4.4) then allows for the assignments of the remaining resonances. Each resonance shows two principal cross peaks due to strong coupling between bound phosphorus neighbors and can be assigned as shown in Figure 4.4. Two additional weaker cross peaks are observed for the two-bond P(2)--P(3) and P(1)--P(4) interactions. Because bonds to two-coordinate phosphorus atoms are typically 0.1 Å shorter than those to three-coordinate phosphorus atoms, these two interactions are enhanced in that they couple to or through the two-coordinated P(4). Thus, the relatively large P(2)--P(3) and P(1)--P(4) two-bond couplings are quite consistent with the expected structural features.

The $^{13}C\{^{1}H\}$ NMR spectrum of **5a** shows a large $^{1}J_{C\text{-}P}$ value of 45 Hz with smaller $^{2}J_{C\text{-}P}$ coupling of $\leq 2$ Hz. As anticipated from structural considerations, the α-hydrogens of **5b** and **5c** are diastereotopic and give rise to AB patterns ($\delta = 0$ ppm) that are broadened due to coupling to phosphorus.

Spectroscopic characterization of compounds **6** was hampered by their limited solubility and thermal instability. In addition, both isomers of the mixed alkyl compounds **6b-6d** possess seven inequivalent phosphorus atoms (*i.e.*, both ***6-sym*** and ***6-asym*** have $C_1$ point symmetry) giving rise to 14 overlapping multiplets in their respective $^{31}P$ NMR spectra. In contrast, the symmetrical isomer ***6-sym*** for the homoleptic alkyl compounds (*e.g.*, **6a** and **6e**) have $C_3$ point symmetry with only three chemically distinct phosphorus nuclei in a 3:3:1 ratio. Thus, the symmetric and asymmetric isomers of **6a** and **6e** can easily be differentiated by $^{31}P$ NMR spectroscopy. Because of the extreme insolubility and thermal instability of **6a**,[30] only **6e** was studied in detail.

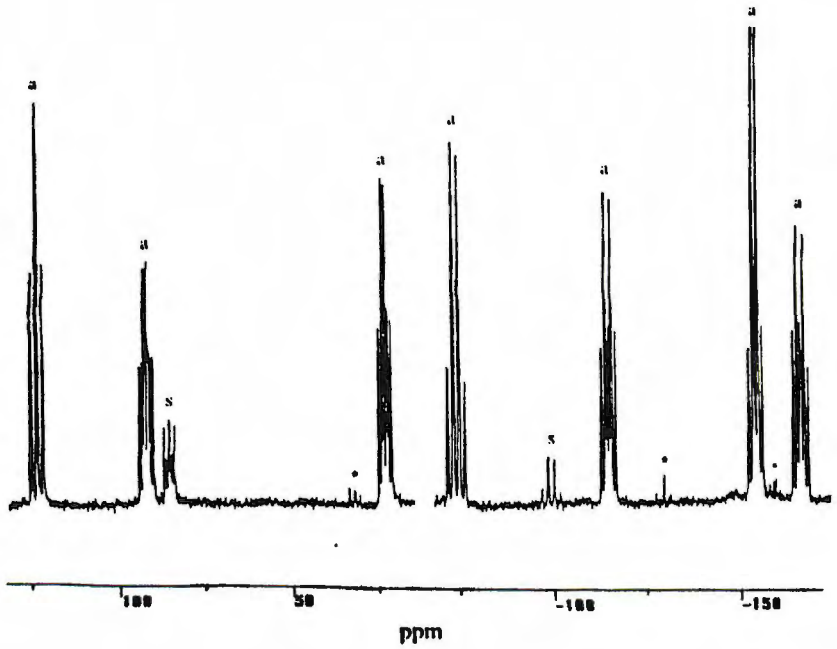


**Figure 4.5.** $^{31}P$ NMR spectrum of $(n\text{-Bu})_3P_7$ from a crude reaction mixture of $[(n\text{-Bu})_2P_7]^-$ and *n*-BuBr in DMF at -20 $^{o}$C and 202.4 MHz. The resonances marked with an "s" and "a" arise from the symmetrical isomer, **6-sym,** and asymmetrical isomer, **6-asym**, respectively. The asterisks denote unreacted $[(n\text{-Bu})_2P_7]^-$.

The $^{31}P\{^{1}H\}$ NMR spectrum of **6e** (Fig. 4.5) shows a preponderance of the asymmetric isomer as evidenced by the seven equal intensity multiplets between 122 and -167 ppm. The spectrum of the minor isomer ***6-sym*** is quite similar to those of related symmetrical $X_3P_7$ compounds[6,7,10] and is characterized by the three resonances at 84, -100 and -155 ppm. The latter resonance is hidden beneath a peak from isomer ***6-sym***. The -100 ppm resonance of intensity one arises from the unique apical phosphorus atom of isomer ***6-sym***. The proton coupled spectrum shows broadening of the 84 ppm resonance due to alkylated phosphorus atoms with the upfield peak at -155 ppm assignable to the basal atoms.

For the resonances associated with the asymmetric isomer, the proton coupled

spectrum shows significant broadening of the three downfield resonances at 122, 92 and 22 ppm indicating they arise from the alkylated phosphorus atoms. Through comparisons with related compounds (*e.g.*, isomer **6-*sym***), we can assign the -75 ppm resonance to the apical phosphorus and the three upfield resonances at -115, -155 and -167 ppm to the basal atoms. These assignments are in accord with those for $(i\text{-Pr})_3P_7$ previously reported by Fritz *et al.*[7]

## 4.3 Discussion

The transfer of $R^+$ from the $R_4N^+$ ions to the polyphosphide complexes described herein occurs by a nucleophilic displacement mechanism involving nucleophilic attack at the α-carbon of the $R_4N^+$ ions. Two other likely mechanisms that are encountered in related chemistry, the $S_{RN}1$ radical pathway and a Hofmann elimination / olefin insertion pathway, are not consistent with the observed experimental results. These findings are discussed individually below.

Because the steric congestion at the $(n\text{-Bu})_4N^+$ ion would hinder nucleophilic attack, the reactions might be occurring by a radical pathway such as an $S_{RN}1$ process.[31] A single-electron oxidation of $[P_7W(CO)_3]^{3-}$ appears to form a reactive radical that undergoes rapid abstractions of hydrogen atoms to form $[HP_7W(CO)_3]^{2-}$.[18] It was therefore of concern that the alkylammonium alkylations described herein might occur via a similar radical pathway: either a single-electron transfer reaction or an initiated radical process.[31] The formation of the Me complex **4a** from $Me(n\text{-}C_8H_{17})_3N^+$ (eq. 4.4) clearly shows that free alkyl radicals are **not** liberated from alkylammonium ions. The $n\text{-}C_8H_{17}$ radical is inherently more stable than the Me radical and the $[(n\text{-}C_8H_{17})P_7W(CO)_3]^{2-}$ complex would be the expected product from eq. 4.4 if free alkyl radicals were involved. Moreover, if alkyl transfer occurred from caged

radicals formed in tight-ion pairs (*i.e.*, a $R_4N^+\cdots[P_7W(CO)_3]^{3-}$ ion pair), transfer of the least sterically hindered alkyl group may be anticipated in a radical mechanism. The formation of the benzyl complex **4d** from $(CH_2Ph)Me_3N^+$ in eq. 4.5 suggests that ion pairing is not a determining factor in the formation of compounds **4** in that the most electrophilic alkyl group is transferred despite the unfavorable steric factors.

Dealkylations of $R_4N^+$ ions are known to occur by a Hofmann elimination process[32] involving an initial deprotonation of an alky β-hydrogen followed by an olefin elimination to give $H^+$, $R_3N$, and olefin. Although the formation of the Me and $CH_2Ph$ compounds **4a**, **4d**, **6a** and **6b** cannot proceed via this mechanism, the Et and *n*-Bu transfers could occur by way of a Hofmann elimination from the $R_4N^+$ ion (*i.e.*, formation of $[HP_7W(CO)_3]^{2-}$, olefin and $R_3N$) followed by an olefin insertion into the P-H bond of **3b**. This mechanism can be discounted in that olefins do not insert into the P-H bonds to form compounds **4** (see eq. 4.6). Although olefins appear to affect some type of transformation of compounds, **3b**, it is clear that compounds **4** are not formed in these reactions.

The data are consistent with a nucleophilic attack at the α-carbon of an $R_4N^+$ alkyl group in that the most electrophilic alkyl substituent is transferred in each case. Tetraalkylammonium ions are extremely weak electrophiles and are not known for their alklyating abilities. They are of course frequently used as "inert" spectator cations in various organic and inorganic reactions. In a related system, Haushalter and co-workers described the thermal decomposition of $(Me_4N)_4Sn_9$ to give $Me_3N$, $Sn_2Me_6$ and other methylated tin compounds that presumably result from $Me^+$ transfer from $Me_4N^+$ to $Sn_9^{4-}$.[33] An example of $RS^-$ methylation by $Me_4N^+$ under mild conditions has also been reported,[34-36] but nucleophilic alkyl transfer from $(n\text{-}Bu)_4N^+$ is, to our knowledge, unprecidented. Clearly, compounds **1** and **2** are potent nucleophiles, however, their basicity is relatively modest. As stated previously in Chapter 3, neither

**1** nor **2** will deprotonate MeOH and **3** is cleanly deprotonated by NaOMe in DMF to give **2**. A detailed discussion of the formation and properties of the $[HP_7M(CO)_3]^{2-}$ compounds was presented in Chapter 3.[18]

Because of the extremely weak electrophilicity of alkylammonium salts, the degree of alkylation and isomeric distributions can be controlled in these reactions. In particular the alkylations of **1** give quantitative conversions to single diasteromers. This selectivity is observed even for the least sterically demanding alkyl group, Me.

Preliminary investigations on other systems suggest that the alkylations of anionic polyphosphides is quite generic although exhaustive studies of the various R groups were not initiated. The chemical selectivity and the ease of subsequent alkylations gives this approach a decided advantage over the previously reported methods that utilize alkyl halides (eq. 4.7).[6,7,21,37] Equation 4.7 chemistry gives

$$P_7^{3-} + 3\ RBr \xrightarrow{en} R_3P_7 + 3\ Br^- \qquad (4.7)$$

R = Me, Et, *i*-Pr, *n*-Bu, *i*-Bu

mixtures of isomers and only certain alkyl groups are amenable to the synthetic conditions. For example, Et, $CH_2C_6H_5$, *n*-Bu and *i*-Bu derivatives cannot be prepared from alkly halide reactions and disubstituted products are unattainable with any R. The $R_3P_7$ (R = Me, Et, *i*-Pr) have been prepared by dehalogenation reactions according to eq 4.8.[21] However, through the combined use of $R_4N^+$ and RX alkylating agents, a large variety of mixed alkyl compounds can presumably be prepared in high yield.

$$(PR)_3 + 4\ PCl_3 + 6\ Mg \longrightarrow P_7R_3 + 6\ MgCl_2 \qquad (4.8)$$

R = Me, Et, *i*-Pr

Based on steric arguments, one must assume that the symmetrical structure **6-*sym*** is the thermodynamically favored isomer for the $R_2R'P_7$ compounds **6**. The $(R_3E)_3P_7$ compounds containing the bulky stannyl and silyl substituents $Me_3Sn$ and $(Me_3Si)_3Si$ gave exclusively the symmetric isomer **6-*sym***, (*e.g.*, $(Me_3Sn)_3P_7$,[7] $[(Me_3Si)_3Si]_3P_7$ [10]). The addition of R' to isomer **4.II** (or **4.I**) at the two-coordinate phosphorus site of compounds **5** in eq. 4.6 chemistry would require the formation of **6-*asym*** as the kinetic product. The formation of isomer **6-*sym*** in eq. 4.6 requires inversion at one of the alkylated phosphorus atoms of $[R_2P_7]^-$ during the course of reaction. Because the two do not interconvert after several hours at room temperature, one must assume that isomers **6-*sym*** and **6-*asym*** are formed competitively in a stereoselective reaction (eq. 4.6) and do not represent an equilibrium mixture.

In summary, the reactions described herein reveal a novel method for alkylating highly nucleophilic polyphophide compounds through the use of $R_4N^+$ alkylating agents. The reactions give virtually quantitative conversions to the alkylated products and appear to be quite generic for a variety of "$R^+$" electrophiles and polyphosphide nucleophiles. The use of this methodology in the formation of other alkylated polypnictides and heterosubstituted phosphines from phosphide anion precursors may be worthy of future investigations.

## 4.4 Experimental Section

### 4.4.1 General Data

General operating procedures used in our laboratory have been described in Chapter 2.[13] General data not found in Chapter 2 are presented below. Elemental analyses were performed under inert atmospheres by Desert Analytics, Tucson, AZ. Proton ($^1H$) NMR spectra were recorded at ambient temperature on both Bruker WP200

(200.133 MHz) and Bruker AM400 (400.136 MHz) spectrometers. Some phosphorus ($^{31}P$) NMR spectra were recorded on a Bruker AMX500 (202.458 MHz) spectrometer. The $^{31}P$-$^{31}P$ COSY NMR experiments were conducted on a Bruker AMX500 in DMF-$d_7$ at 28 °C. The mass spectra were obtained on a VG7070E magnetic sector mass spectrometer in the fast atom bombardment (FAB) mode utilizing a $Xe^+$ beam (8 kV) and a *m*-nitrobenzyl alcohol (mNBA) matrix.

The IR and NMR spectral data common to all compounds containing $[K(2,2,2\text{-crypt})]^+$ and/or en can also be found in Chapter 2.

### 4.4.2 Chemicals

The preparation of $K_3P_7$ was reported in Chapter 2. Chemicals not foud in Chapter 2 are presented below. Tetraalkylammonium halides, alkyl halides and 18-crown-6 were purchased from Aldrich and used without further purification. Dimethylformamide (DMF) was also purchased from Burdick & Jackson (High Purity), distilled at reduced pressure from $K_4Sn_9$ and stored under dinitrogen over molecular sieves. The preparation of **2PW** has been described in Chapter 2.

### 4.4.3 Syntheses

#### 4.4.3.1 Preparation of $[K(2,2,2\text{-crypt})]_2[MeP_7W(CO)_3]\cdot en$

Method A: $K_3P_7$ (29.6 mg, 0.089 mmol), 2,2,2-crypt (100.0 mg, 0.27 mmol), and $[C_6H_3(CH_3)_3]W(CO)_3$ (34.4 mg, 0.089 mmol) were dissolved in en (*ca.* 3 mL) and stirred for 12 h at ambient temperature yielding a red solution. An equivalent of solid $Me(n\text{-}C_8H_{17})_3NBr$ (39.9 ng, 0.089 mmol) was added. The reaction mixture was stirred for 1 h producing a dark red solution. Solvent was concentrated under vacuum to 2 mL and filtered through *ca.* 0.25 in. of tightly packed glass wool in a pipet. After

24 h, the reaction vessel contained rectangular maroon crystals that were removed from the mother liquor, washed with toluene, and dried under vacuum (crystalline yield, 49 mg, 39 %). Method B: A procedure identical to that described in Method A was followed except solid $Me_4NBr$ (13.8 mg, 0.089 mmol) was used and the reaction mixture was stirred for 4 h at *ca.* 40 °C, concentrated under vacuum to 2 mL and filtered through *ca.* 0.25 in. of tightly packed glass wool in a pipet. After 24 h, the reaction vessel contained rectangular maroon crystals that were removed from the mother liquor, washed with toluene, and dried under vacuum (crystalline yield, 39 mg, 32 %). IR (KBr pellet), $cm^{-1}$: 1871 (s), 1786 (s), 1757 (s). $^1H$ NMR (DMF-$d_7$) δ(ppm): 0.53 (dt, 3 H, $CH_3$). $^{13}C\{^1H\}$ NMR (DMF-$d_7$) δ(ppm): 229.4 (br s, *C*O), -3.3 (d, $^1J_{C-P}$ = 30.4 Hz; $CH_3$).

### 4.4.3.2 Preparation of $[K(2,2,2\text{-crypt})]_2[EtP_7W(CO)_3]\cdot en$

A procedure identical to that described for $[K(2,2,2\text{-crypt})]_2[MeP_7W(CO)_3]\cdot en$ (Method A) was followed except solid $(C_2H_5)_4NBr$ (18.7 mg, 0.089 mmol) was used. After 24 h, the reaction vessel contained rectangular maroon crystals which were removed from the mother liquor, washed with toluene and dried under vacuum (crystalline yield, 45.7 mg, 37 %). Anal. Calcd for $C_{43}H_{85}N_6O_{15}K_2P_7W$: C, 36.76; H, 6.10; N, 5.98. Found: C, 36.92; H, 6.09; N, 5.93. IR (KBr pellet), $cm^{-1}$: 1866 (s), 1787 (s), 1750 (s). $^1H$ NMR (DMF-$d_7$) δ(ppm): 0.96 (dq, $^2J_{H-P}$ = 14.2 Hz, $^3J_{H-H}$ = 7.1 Hz, 2 H; $CH_2CH_3$), 0.84 (dt, $^3J_{H-P}$ = 13.6 Hz, $^3J_{H-H}$ = 7.1 Hz; 3 H; $CH_2CH_3$). $^{13}C\{^1H\}$ NMR (DMF-$d_7$) δ(ppm): 229.4 (p, $^1J_{C-W}$ = 167 Hz, $^2J_{C-P}$ = 4 Hz, 3 C; *C*O), 15.6 (dt, $^1J_{C-P}$ = 10.8 Hz, $^2J_{C-P}$ = 5.4 Hz, 1 C; $CH_2CH_3$), 8.0 (d, $^2J_{C-P}$ = 26.0 Hz, 1 C; $CH_2CH_3$).

### 4.4.3.3 Preparation of $[K(2,2,2\text{-crypt})]_2[(n\text{-Bu})P_7W(CO)_3]\cdot en$

A procedure identical to that described for $[K(2,2,2\text{-crypt})]_2[MeP_7W(CO)_3]\cdot en$ (Method A) was followed except solid $(C_4H_9)_4NBr$ (28.7 mg, 0.089 mmol) was used. After 24 h, the reaction vessel contained octahedral maroon crystals that were removed from the mother liquor, washed with toluene and dried under vacuum (crystalline yield, 50 mg, 37 %). Anal. Calcd for $C_{47}H_{97}N_8O_{15}K_2P_7W$: C, 37.81; H, 6.55; N, 7.50; P, 14.52. Found: C, 37.73; H, 6.51; N, 7.91; P, 13.95. IR (KBr pellet), $cm^{-1}$: 1874 (s), 1785(s), 1752 (s). $^1H$ NMR (DMF-$d_7$) δ(ppm): 1.16 (m, 4H; *n*-Bu), 1.01 (m, 2 H; *n*-Bu), 0.74 (t, 3 H;*n*-Bu)). $^{13}C\{^1H\}$ NMR (DMF-$d_7$) δ(ppm): 229.4 (bs s, 3 C; *C*O), 33.7 (m, 1 C, *n*-Bu), 24.6 (d, $J_{C\text{-}P}$ = 8.1 Hz, 1 C; *n*-Bu), 14.6 (d, $J_{C\text{-}P}$ = 27 Hz, 1 C; *n*-Bu), 14.0 (s, 1 C; *n*-Bu).

### 4.4.3.4 Preparation of $[K(2,2,2\text{-crypt})]_2[(CH_2Ph)P_7W(CO)_3]\cdot en$

$[K(2,2,2\text{-crypt})]_2[(CH_2Ph)P_7W(CO)_3]\cdot en$ was prepared by two separate reactions from two different ammonium salts, $(CH_2Ph)Me_3NBr$ and $(CH_2Ph)Et_3NBr$. A procedure identical to that described for $[K(2,2,2\text{-crypt})]_2[MeP_7W(CO)_3]\cdot en$ (Method A) was followed except solid $(CH_2Ph)Me_3NBr$ (20.5 mg, 0.089 mmol) was added to one reaction and solid $(CH_2Ph)Et_3NBr$ (24.2 mg, 0.089 mmol) to the other. After 24 h, the reaction vessels contained rectangular maroon crystals that were removed from the mother liquors, washed with toluene and dried under vacuum. Crystalline yields were 42 mg (32 %) for each reaction. Anal. Calcd for $C_{46}H_{80}N_4O_{15}K_2P_7W$: C, 39.24; H, 5.73; N, 3.98. Found: C, 39.18; H, 5.73; N, 4.19. IR (KBr pellet), $cm^{-1}$: 1874 (s), 1792 (s), 1755 (s). $^1H$ NMR (DMF-$d_7$) δ(ppm): 7.17-7.00 ($CH_2$*Ph*), 2.38 (m, 2 H, *C*$H_2$Ph). $^{13}C\{^1H\}$ NMR (DMF-$d_7$) δ(ppm): 229.3 (br s, *C*O), 141.0 (s, $CH_2$*Ph*, ipso), 129.2, 128.4, 125.5 (s, ($CH_2$*Ph*), 21.2 (d, $^1J_{C\text{-}P}$ = 29.8 Hz; *C*$H_2$Ph).

#### 4.4.3.5 Preparation of $[Me_2P_7]^-$

In a drybox in a 5 dram vial, $K_3P_7$ (29.6 mg, 0.089 mmol) and $Me_4NBr$ (27.4 mg, 0.178 mmol) were combined in en (*ca.* 3 mL) and stirred for 12 h yielding a bright yellow solution. $^{31}P$ NMR spectra of the crude reaction mixtures showed quantitative conversion to a single product. The solvent was removed under vacuum leaving a yellow film on the vial that was redissolved in DMF-$d_7$ (*ca.* 1 mL). The NMR data for the dried films showed residual en. $^1H$ NMR (DMF-$d_7$) δ(ppm): -0.39 (m, C*H*$_3$). $^{13}C\{^1H\}$ NMR (DMF-$d_7$) δ(ppm): 42.1(d, $^1J_{C-P}$ = 44.6 Hz; *C*H$_3$).

#### 4.4.3.6 Preparation of $[Et_2P_7]^-$

A procedure identical to that described above for $[Me_2P_7]^-$ was followed except $Et_4NBr$ (37.3 mg, 0.178 mmol) was used. $^{31}P$ NMR spectra of the crude reaction mixtures showed quantitative conversion to a single product. The solvent was removed under vacuum leaving a yellow film on the vial that was redissolved in DMF-$d_7$ (*ca.* 1 mL). The NMR data for the dried films showed residual en. $^1H$ NMR (DMF-$d_7$) δ(ppm): 0.71 (m, $CH_2CH_3$), -0.07, -0.24 (br m, $CH_2CH_3$).

#### 4.4.3.7 Preparation of $[(n\text{-}Bu)_2P_7]^-$

A procedure identical to that described above for $[Me_2P_7]^-$ was followed except ($n$-Bu)$_4$NBr (57.3 mg, 0.178 mmol) was used. $^{31}P$ NMR spectra of the crude reaction mixtures showed quantitative conversion to a single product. The solvent was removed under vacuum leaving a yellow film on the vial that was redissolved in DMF-$d_7$ (*ca.* 1 mL). The NMR data for the dried films showed residual en. $^1H$ NMR (DMF-$d_7$) δ(ppm): 1.73 (m, 2 H, $n$-Bu), 1.37 (m, 2 H, $n$-Bu), 1.06 (m, 3 H, $n$-Bu), -0.12, -0.24 (br m, 1 H, $CH_2C_3H_7$).

#### 4.4.3.8 Preparation of $Me_3P_7$

$[Me_2P_7]^-$ (0.089 mmol) was prepared in en (*ca.* 3 mL) as described above except a 25 mL Schlenk flask was used. The en was removed under vacuum leaving a yellow film in the flask. This film was redissolved in DMF (*ca.* 4 mL). MeI (5.5 μL, 0.089 mmol) was syringed into the stirring reaction mixture yielding a colorless solution and white precipitant (ppt). An aliquot of the solution was immediately removed and taken for MS analysis while the remainder was used for $^{31}P$ NMR analysis.

#### 4.4.3.9 Preparation of $(CH_2Ph)Me_2P_7$

A procedure identical to that described earlier for $Me_3P_7$ was followed except $(CH_2Ph)Cl$ (10.2 μL, 0.089 mmol) was syringed into the stirring reaction mixture yielding a colorless solution and white ppt. An aliquot of the solution was immediately removed and taken for MS analysis.

#### 4.4.3.10 Preparation of $(n\text{-}Bu)_3P_7$

$K(n\text{-}Bu)_2P_7$ (0.089 mmol) was prepared in DMF (*ca.* 3 mL) as described above except a 25 mL Schlenk flask was used. $(n\text{-}Bu)Br$ (17.2 μL, 0.089 mmol) was syringed into the stirring reaction mixture yielding a red solution. An aliquot of the solution was immediately removed and taken for MS analysis while the remainder of the solution was used for $^{31}P$ NMR analysis.

#### 4.4.3.11 Preparation of $Me(n\text{-}Bu)_2P_7$

A procedure identical to that described earlier for $(n\text{-}Bu)_3P_7$ was followed except methyl iodide (5.5 μL, 0.089 mmol) was syringed into the stirring reaction mixture yielding a colorless solution and white ppt. An aliquot of the solution was immediately removed and taken for MS analysis.

#### 4.4.3.12 Preparation of $(CH_2Ph)(n\text{-}Bu)_2P_7$.

A procedure identical to that described earlier for $(n\text{-}Bu)_3P_7$ was followed except benzyl chloride (10.2 μL, 0.089 mmol) was syringed into the stirring reaction mixture yielding a colorless solution and white ppt. An aliquot of the solution was immediately removed and taken for MS analysis.

#### 4.4.3.13 Crystallographic Experimental Details for $[K(2,2,2\text{-crypt})]_2[EtP_7W(CO)_3]\cdot en$.

A single crystal X-ray diffraction study for $[K(2,2,2\text{-crypt})]_2[EtP_7W(CO)_3]\cdot en$ was done by Dr. James C. Fettinger, University of Maryland.

**Table 4.1.** FAB-MS Data for $R_2R'P_7$ Compounds (**6**).

| Compound | M/Z | % Intensity | Ion |
|---|---|---|---|
| $(n\text{-Bu})_2MeP_7$ | 347 | 61.6 | $HM^+$ |
| | 331 | 12.2 | $M^+ - CH_4$ |
| | 289 | 31.6 | $M^+ - C_4H_{10}$ |
| $(n\text{-Bu})_2(CH_2C_6H_5)P_7$ | 423 | 10.1 | $HM^+$ |
| | 365 | 8.39 | $M^+ - C_4H_{10}$ |
| | 331 | 12.5 | $M^+ - CH_3C_6H_5$ |
| $(Me)_2(CH_2C_6H_5)P_7$ | 339 | 54.7 | $HM^+$ |
| | 323 | 18.8 | $M^+ - CH_4$ |
| | 247 | 26.3 | $M^+ - CH_3C_6H_5$ |
| $Me_3P_7$ | 263 | 20.8 | $HM^+$ |
| | 247 | 11.7 | $M^+ - CH_4$ |

**Table 4.2.** Crystallographic Data for $[K(2,2,2\text{-crypt})]_2[EtP_7W(CO)_3]$.

| | | |
|---|---|---|
| Empirical formula | $C_{43}\ H_{85}\ K_2\ N_6\ O_{15}\ P_7\ W$ | |
| Formula weight | 1405.01 | |
| Temperature | 293(2) K | |
| Radiation | Mo $K_\alpha$ ($\lambda$ = 0.71073 Å) | |
| Space group | $P\bar{1}$ | |
| Cell dimensions | $a$ = 12.176(3) Å | $\alpha$ = 93.509(10) deg |
| | $b$ = 15.106(2) Å | $\beta$ = 98.833(13) deg |
| | $c$ = 18.975(2) Å | $\gamma$ = 111.472(12) deg |
| Volume | 3183.1(9) $Å^3$ (Z = 2) | |
| Density (calculated) | 1.466 $g/cm^3$ | |
| Absorption coefficient | 0.391 $mm^{-1}$ | |
| Crystal size | 0.50 x 0.25 x 0.20 mm | |
| Reflections collected | 8776 | |
| Independent reflections | 8301 [R(int) = 0.0224] | |
| Data / restraints / parameters | 8301 / 0 / 670 | |
| Goodness-of-fit on $F^2$ | 1.066 | |
| Final R indices [$I>2\sigma(I)$] | $R(F) = 0.0420$, $wR(F^2) = 0.1023$ [6746 data] | |
| Largest diff. peak and hole | 1.352 and -0.907 $e/Å^{-3}$ | |

---

$^aR(F) = \Sigma \mid F_o - F_c \mid / \Sigma F_o$. $^bR(wF) = (\Sigma w \mid (F_o)^2 - (F_c)^2 \mid^2 / \Sigma wF_o^2)^{1/2}$.

**Table 4.3.** Selected Distances ( Å ) and Angles ( $^{o}$ ) for the $[EtP_7W(CO)_3]^{2-}$ Ion.

Distances

| | | | |
|---|---|---|---|
| W-P(4) | 2.581(2) | W-P(5) | 2.584(2) |
| W-P(6) | 2.673(2) | W-P(7) | 2.676(2) |
| W-C(1) | 1.918(8) | W-C(2) | 1.911(9) |
| W-C(3) | 1.953(8) | C(1)-O(1) | 1.183(8) |
| C(2)-O(2) | 1.201(9) | C(3)-O(3) | 1.171(8) |
| P(4)-P(6) | 2.137(3) | P(5)-P(7) | 2.163(3) |
| P(4)--P(5) | 2.923(3) | P(6)--P(7) | 3.299(3) |
| P(4)-P(2) | 2.215(3) | P(5)-P(2) | 2.212(2) |
| P(6)-P(3) | 2.200(3) | P(7)-P(3) | 2.185(3) |
| P(1)-P(2) | 2.173(3) | P(1)-P(3) | 2.176(3) |
| P(1)-C(4) | 1.858(7) | C(4)-C(5) | 1.474(10) |

Angles

| | | | |
|---|---|---|---|
| C(2)-W-C(1) | 92.9(3) | C(2)-W-C(3) | 81.8(3) |
| C(1)-W-C(3) | 93.6(3) | C(1)-W-P(4) | 130.8(2) |
| C(3)-W-P(4) | 133.7(2) | C(2)-W-P(5) | 125.6(2) |
| C(1)-W-P(5) | 140.6(3) | C(3)-W-P(6) | 175.0(2) |
| C(2)-W-P(7) | 173.8(2) | P(5)-W-P(7) | 48.53(6) |
| P(6)-W-P(7) | 76.15(6) | P(4)-P(6)-W | 63.75(7) |
| P(3)-P(6)-W | 92.99(7) | P(6)-P(4)-W | 68.28(7) |
| P(2)-P(4)-W | 103.17(8) | P(7)-P(5)-W | 67.97(7) |
| P(2)-P(5)-W | 103.16(8) | P(4)-P(6)-P(3) | 103.77(10) |
| P(6)-P(4)-P(2) | 106.53(10) | P(1)-P(2)-P(5) | 99.07(10) |
| O(1)-C(1)-W | 177.4(8) | O(3)-C(3)-W | 177.0(6) |
| O(2)-C(2)-W | 177.4(7) | | |

## 4.5 References


(1) Corbett, J. D. *Chem. Rev.* **1985**, *85*, 383-397.

(2) von Schnering, H. G. *Angew. Chem. Int. Ed. Engl.* **1981**, *20*, 33-51.

(3) von Schnering, H. G. In *Rings, Chains, and Macromolecules of Main Group Elements*; A. L. Rheingold, Ed.; Elsevier: Amsterdam, 1977.

(4) Baudler, M.; Ternberger, H.; Faber, W.; Hahn, J. *Z. Naturforsch.* **1979**, *34B*, 1690-1697.

(5) Baudler, M. *Angew. Chem. Int. Ed. Engl.* **1982**, *21*, 492-512.

(6) Baudler, M. *Angew. Chem. Int. Ed. Engl.* **1987**, *26*, 419-441.

(7) Fritz, G.; Hoppe, K. D.; Hönle, W.; Weber, D.; Mujica, C.; Manriquez, V.; von Schnering, H. G. *J. Organomet. Chem.* **1983**, *249*, 63-80.

(8) Hönle, W.; von Schnering, H. G. *Z. Anorg. Allg. Chem.* **1978**, *440*, 171-182.

(9) von Schnering, H. G.; Hönle, W. *Chem. Rev.* **1988**, *88*, 243-273.

(10) Kovács, I.; Baum, G.; Fritz, G.; Fenske, D.; Wiberg, N.; Schuster, H.; Karaghiosoff, K. *Z. Anorg. Allg. Chem.* **1993**, *619*, 453-460.

(11) Eichhorn, B. W.; Haushalter, R. C.; Huffman, J. C. *Angew. Chem. Int. Ed. Engl.* **1989**, *28*, 1032-1033.

(12) Charles, S.; Eichhorn, B. W.; Bott, S. G. *J. Am. Chem. Soc.* **1993**, *115*, 5837-5838.

(13) Charles, S.; Eichhorn, B. W.; Rheingold, A. L.; Bott, S. G. *J. Am. Chem. Soc.* **1994**, *116*, 8077-8086.

(14) Charles, S.; Fettinger, J. C.; Eichhorn, B. W. *J. Am. Chem. Soc.* **1995**, *117*, 5303-5311.

(15) Charles, S.; Eichhorn, B. W.; Fettinger, J. C.; Bott, S. G. *Inorg. Chem.*

**1995**.

(16) Charles, S.; Eichhorn, B. W.; Bott, S. G.; Fettinger, J. C. *Angew. Chem. Int. Ed. Engl.* **1995**, submitted.

(17) Charles, S.; Eichhorn, B. W.; Fettinger, J. C.; Bott, S. G. **1995**, in preparation.

(18) Charles, S. C.; Eichhorn, B. W.; Fettinger, J. C. **1995**, in preparation.

(19) Bolle, U.; Tremel, W. *J. Chem. Soc., Chem. Commun.* **1994**, 217-219.

(20) Baudler, M.; Faber, W.; Hahn, J. Z. *Anorg. Allg. Chem.* **1980**, *469*, 15-21.

(21) Baudler, M.; Glinka, K. *Chem. Rev.* **1993**, *93*, 1623-1667.

(22) von Schnering, H. G.; Manriquez, V.; Hönle, W. *Angew. Chem. Int. Ed. Engl.* **1981**, *20*, 594-595.

(23) Bartell, L. S. *J. Chem. Phys.* **1960**, *32*, 832.

(24) Eichhorn, B. W.; Haushalter, R. C. *J. Chem. Soc., Chem. Commun.* **1990**, 937-938.

(25) Eichhorn, B. W.; Haushalter, R. C.; Pennington, W. T. *J. Am. Chem. Soc.* **1988**, *110*, 8704-8706.

(26) Kreiter, C. G.; Lang, M. *J. Organomet. Chem.* **1973**, *55*, C27-C29.

(27) Efraty, A. *Chem. Rev.* **1977**, *77*, 691-744.

(28) Mann, B. E. *Adv. Organomet. Chem.* **1974**, *12*, 135-193.

(29) Mann, B. E. *J. Chem. Soc., Perkin II* **1972**, 30-34.

(30) In our hands, the *in situ* preparation of $Me_3P_7$ gives very dilute solutions and weak NMR signals. The spectra reported by Baudler et al. (ref ) were clearly more concentrated presumably due to the difference in synthetic procedure. The $^{31}P$ chemical shifts were the same in both cases.

(31) Lowry, T. H.; Richardson, K. S. *Mechanism and Theory in Organic Chemistry;* 3rd ed.; Harper & Row: New York, 1987, pp 409-412, 645-648.

(32) Neckers, D. C.; Doyle, M. P. *Organic Chemistry*; John Wiley & Sons: New York, 1977, pp 546-548.

(33) Teller, R. G.; Krause, L. J.; Haushalter, R. C. *Inorg. Chem.* **1983**, *22*, 1809-1812.

(34) Shamma, M.; Deno, N. C.; Remar, J. F. *Tetrahedron Letters* **1966**, 1375-1379.

(35) Kametani, T.; Kigasawa, K.; Hiiragi, M.; Wagatsuma, N.; Wakisaka, K. *Tetrahedron Letters* **1969**, 635-638.

(36) Hutchins, R. O.; Dux, F. J. *J. Org. Chem.* **1973**, *38*, 1961-1962.

(37) Hönle, W.; von Schnering, H. G.; Fritz, G.; Schneider, H.-W. *Z. Anorg. Allg. Chem.* **1990**, *584*, 51.

# CHAPTER 5

## Reactivity of $[P_7M(CO)_3]^{3-}$ Ions in the Synthesis of $[P_7M(CO)_4]^{3-}$ and $[RP_7M(CO)_4]^{3-}$ (R = H, $CH_2Ph$; M = Mo, W) Complexes

### 5.1 Introduction

The synthesis and characterization of the $[E_7M(CO)_3]^{3-}$ complexes (where E = P, As, Sb and M = Cr, Mo, W) were described in Chapter 2. These complexes are easily prepared from ($\eta^6$-arene)$M(CO)_3$ precursors and $E_7^{3-}$ ions according to eq. 2.1. Tremel *et al.*[1,2] prepared the $[Sb_7Mo(CO)_3]^{3-}$ member of this class of compounds by using a $Mo(CO)_4$(bipy) precursor, which requires CO loss at some stage of the reaction.

The $[E_7M(CO)_3]^{3-}$ ions have norbornadiene-like $E_7$ fragments with a formal negative charge associated with the unique two-coordinate pnictogen atom furthest from the transition metal (the E(1) site). The pnictogen atom remains highly nucleophilic and is the site of attack by various electrophiles (*e.g.*, $H^+$, $R^+$, $W(CO)_3$(en), etc.) as described in Chapters 3, 4 and 6.[3-6] The reactivity of $[P_7W(CO)_3]^{3-}$ is depicted in Scheme 2.1.

The $[E_7M(CO)_3]^{3-}$ ions also react with nucleophiles. Contrary to the electrophilic attacks that were ligand-based, the nucleophiles attack at the metal-center. Under an atmosphere of carbon monoxide, the $[E_7M(CO)_3]^{3-}$ ions coordinate a fourth CO ligand to form the $[E_7M(CO)_4]^{3-}$ ions. The reactions of the $[P_7M(CO)_3]^{3-}$ (where M = Mo, W) with carbon monoxide have been investigated. The synthesis, structure and properties of the $[P_7M(CO)_4]^{3-}$ and $[HP_7M(CO)_4]^{2-}$ ions, as well as the alkylated complex, $[RP_7W(CO)_4]^{2-}$, are described.[7]

## 5.2 Results

### 5.2.1 Synthesis

Ethylenediamine (en) solutions of $[K(2,2,2\text{-crypt})]_3[P_7M(CO)_3]$ (M = Mo, W) react under one atmosphere of carbon monoxide to form $[K(2,2,2\text{-crypt})]_3[P_7M(CO)_4]$ complexes as crystalline powders according to eq. 5.1 in 18 % crystalline yield when M = Mo and 71 % crystalline yield

$$[\eta^4\text{-}P_7M(CO)_3]^{3-} + CO \rightleftharpoons [\eta^2\text{-}P_7M(CO)_4]^{3-} \qquad (5.1)$$

M = Mo (**2PMo**) M = Mo (**7a**)

M = W (**2PW**) M = W (**7b**)

when M = W.[7] The complexes are bright yellow and are very air and moisture sensitive in solution and the solid state. Both compounds are susceptible to CO loss under $N_2$ in solution and in the solid state. Additionally, both compounds are more soluble in DMF than in en, however, they lose CO more readily in DMF than they do in en. The $[P_7W(CO)_4]^{3-}$ ion, **7b**, is considerably more stable than the $[P_7Mo(CO)_4]^{3-}$ ion, **7a**, in both solid and solution. Because of this instability, **7a** is always contaminated by **2PMo** impurities when under $N_2$ and low pressures of CO. Compounds **7** were characterized by IR, $^{13}C$ and $^{31}P$ NMR spectroscopic studies. Microanaylsis was obtained for **7b**, but not for **7a** because it proved to be too unstable.

warmed (~ 35 °C) within minutes of initiation of the reaction, the relative amount of $[P_7Mo(CO)_3]^{3-}$ formed increases. If the reaction mixture is gently warmed after an hour into the reaction, the relative amount of $[HP_7Mo(CO)_3]^{2-}$ formed increases. The reaction of $P_7^{3-}$ with $(pyridine)_2W(CO)_4$ generates $[P_7W(CO)_4]^{3-}$ in an exceedingly slow reaction (eq. 5.3). Warming the solution to accelerate the reaction affects a decarbonylation of the product to form **2PW**.

$[P_7M(CO)_4]^{3-}$ reacts with methanol in en to quantitatively give $[HP_7M(CO)_4]^{2-}$ ions (**8**) according to eq. 5.4. Compounds **8** can also be prepared by carbonylation of $[HP_7M(CO)_3]^{2-}$, **3**, as shown in eq. 5.5.[7] The compounds are yellow to golden yellow and the solids and solutions are very air and moisture sensitive. The compounds are susceptible to CO loss under $N_2$ in solution and the solid state.

$$\underset{\textbf{7}}{[P_7M(CO)_4]^{3-}} + MeOH \longrightarrow \underset{M = Mo\ (\textbf{8a});\ M = W\ (\textbf{8b})}{[HP_7M(CO)_4]^{2-}} + MeO^- \qquad (5.4)$$

$$\underset{\textbf{3}}{[HP_7M(CO)_3]^{2-}} + CO \longrightarrow [HP_7M(CO)_4]^{2-} \qquad (5.5)$$

The $[K(2,2,2\text{-crypt})]_2[HP_7M(CO)_4]\cdot en$ salts were isolated in 40 % (M = Mo) and 76 % (M = W) crystalline yields. The compounds are golden yellow in color and moderately air and moisture sensitive in solution and the solid state. Compounds **8a** and **8b** slowly lose one CO ligand under $N_2$ atmospheres in solution but are much more stable than 7.

Compounds **8a** and **8b** were characterized by microanalyses and IR, $^1H$, $^{13}C$, and $^{31}P$ NMR spectroscopies. The $[K(2,2,2\text{-crypt})]^+$ salts of **8a** and **8b** were studied by single crystal X-ray diffraction.

Unlike the tricarbonyl complexes **3** (see Scheme 5.1, eq. **C**), $MeO^-$ is not a strong enough base to deprotonate **8** in en or DMF. However, **8b** is efficiently deprotonated by $LiNHCH_2CH_2NH_2$ in en to give **7b** according to eq. 5.6. For **8a**, deprotonation with $LiNHCH_2CH_2NH_2$ presumably gives **7a** as a transient intermediate, however **2PMo** is the only detectable product (eq. 5.7). Identical experiments in which

$$\underset{\textbf{8b}}{[HP_7W(CO)_4]^{2-}} + NH_2CH_2CH_2NH^- \longrightarrow \underset{\textbf{7b}}{[P_7W(CO)_4]^{3-}} + en \qquad (5.6)$$

$$\underset{\textbf{8a}}{[HP_7Mo(CO)_4]^{2-}} + NH_2CH_2CH_2NH^- \longrightarrow "[P_7Mo(CO)_4]^{3-}" + en \longrightarrow \underset{\textbf{2PMo}}{[P_7Mo(CO)_3]^{3-}} + CO \qquad (5.7)$$

$$\underset{\textbf{8a}}{[HP_7Mo(CO)_4]^{2-}} \not\longrightarrow \underset{\textbf{3c}}{[HP_7Mo(CO)_3]^{2-}} + CO \xrightarrow{MeO^-} \underset{\textbf{2PMo}}{[P_7Mo(CO)_3]^{3-}} + MeOH \qquad (5.8)$$

**8a** and excess NaOMe (instead of $LiNHCH_2CH_2NH_2$) are stirred in en show unreacted **8a** after 48 h at room temperature. These experiments show that the **2PMo** formed by deprotonating **8a** with $LiNHCH_2CH_2NH_2$ proceeds through **7a** as outlined in eq. 5.7 and not through **3c** as shown in eq. 5.8. If **3c** were the intermediate in the formation of **2PMo**, the reaction with NaOMe would have been equally effective in the preparation of **2PMo** from **8a** (*i.e.*, $MeO^-$ readily deprotonated **3c**). In addition, the corresponding tungsten chemistry yields **7b** as an isolable intermediate in the deprotonation reactions.

Ethylenediamine solutions of $[(CH_2Ph)P_7W(CO)_3]^{2-}$, **4d**, react under an atmosphere of CO to form the yellow $[(CH_2Ph)P_7W(CO)_4]^{2-}$ complex, **8c**, according to eq. 5.9. The reaction between $Me_3(CH_2Ph)N^+$ and $[P_7W(CO)_4]^{3-}$ also affords **8c**

according to eq. 5.10. This reaction appears to proceed faster ($t_{\infty} \leq 4$ h) than the alkylations reactions of **2PM** ($t_{\infty} \approx 12$ h) at room temperature, however, neither reaction rates were quantitatively measured. Through the use of eq. 5.9 chemistry, transparent

$$[(CH_2Ph)P_7W(CO)_3]^{2-} + CO \rightleftharpoons [(CH_2Ph)P_7W(CO)_4]^{2-} \qquad (5.9)$$

**4d** **8c**

$$[P_7W(CO)_4]^{3-} + Me_3(CH_2Ph)N^{+} \longrightarrow [(CH_2Ph)P_7W(CO)_4]^{2-} + Me_3N \qquad (5.10)$$

**7b** **8c**

yellow crystals of **8c** were isolated in 61 % crystalline yield as the [K(2,2,2-crypt)]$_2$[$(CH_2Ph)P_7W(CO)_4$]·en salt and have been characterized by microanalysis and IR, $^1$H, $^{13}$C and $^{31}$P NMR spectroscopic studies. Repeated attempts to grow X-ray quality crystals were unsuccessful, however the spectroscopic studies show that **8c** contains an $\eta^2$-$P_7$ unit and is isostructural to the protonated analog **8b**. Carbonylations of other $[RP_7W(CO)_3]^{2-}$ complexes where R = Me, Et, *n*-Bu appear to proceed similarly but were not studied in detail.

### 5.2.2 Structural Studies

Crystals of **7** suitable for X-ray diffraction were not obtained, however, NMR spectroscopic studies and structural comparison between **2PM**, **4** and **8** indicate an $\eta^2$-$P_7$ ligand with overall $C_s$ point symmetry with the mirror plan defined by P(1), mutually *trans* carbonyl ligands (see drawing of the $[P_7M(CO)_4]^{3-}$ ion).

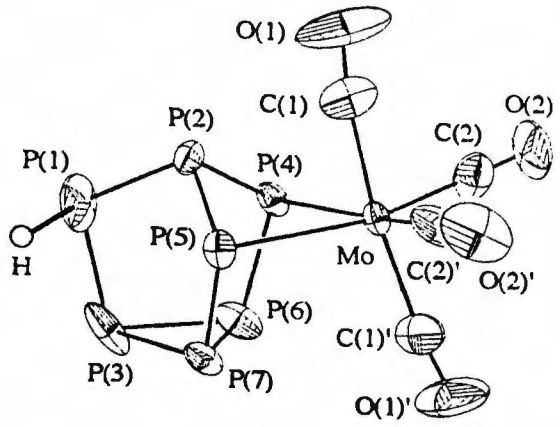


**Figure 5.1.** ORTEP drawing of the $[HP_7Mo(CO)_4]^{2-}$ ion (**8a**). The hydrogen atom was not crystallographically located.

The structures of the $[K(2,2,2\text{-crypt})]^+$ salts of the $[HP_7M(CO)_4]^{2-}$ ions [M = Mo (**8a**), M = W (**8b**)] were determined by single crystal X-ray diffraction. The compounds are isotypic and crystallize in space group *C2/c*, however, have overall $C_1$ point symmetry. An ORTEP drawing of the anion **8a** is shown in Figure 5.1. A summary of the crystallographic data is given in Table 5.1 and a listing of selected bond distances and angles given in Table 5.2.

The anions have rotational disorder in the solid state. The $P_7$ unit is rotationally disordered about the crystallographic two-fold axis that places the P(2) atom "up" fifty percent of the time, and "down" [P(2)'] the other fifty percent. The two-fold disorder of the $[HP_7M(CO)_4]^{2-}$ ions is illustrated in Figure 5.2.

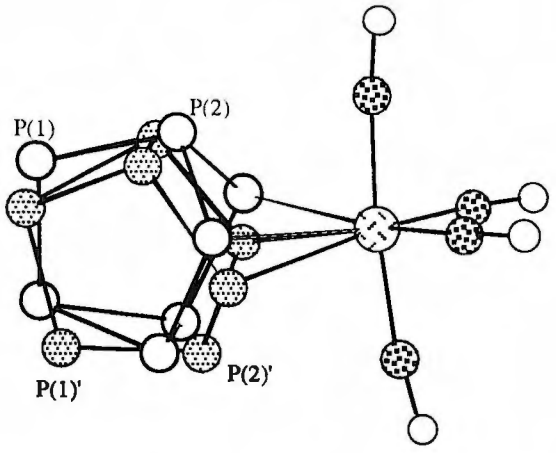


**Figure 5.2.** Ball-and-stick drawing of the disordered $[HP_7W(CO)_4]^{2-}$ ion (**8b**). The two-fold disorder is illustrated by the differently shaded $P_7$ units.

The $[HP_7M(CO)_4]^{2-}$ structure type contains a $P_7$ core that is virtually unperturbed from the parent $P_7^{3-}$ anion. A $P_7$ core is bound $\eta^2$ to an $M(CO)_4$ fragment and a hydrogen atom is bound to a phosphorous atom giving the anion overall $C_1$ molecular symmetry. Four carbonyl groups and two phosphorus atoms form a distorted octahedron of ligands about the central transition metal with the phosphorus atoms necessarily *cis*. Two of the carbonyl groups [C(2), C(2)'] are *trans* to phosphorus atoms [P(5) and P(4) respectively] and two are *trans* to one another [C(1), C(1)']. The en solvates and $[K(2,2,2\text{-crypt})]^+$ ions are well separated from the anions in the crystal lattice.

The average M-C(1) distances [2.025(10) Å (**8a**), 2.000(13) Å (**8b**)] are typical of M-C distances of metal carbonyls *trans* to carbonyl groups of neutral compounds.[8-11] The average M-C(2) distances [1.919(10) Å (**8a**), 1.920(12) Å (**8b**)] are shorter than the M-C(1) distances as one would expect due to the higher *trans* influence of carbonyl groups relative to P. These contacts are also shorter than M-C distances of metal carbonyls *trans* to phosphorus atoms of neutral compounds.[8-11]

The average C(1)-O(1) distances [1.141(10) Å (**8a**), 1.116(14) Å (**8b**)] are typical of C-O distances of metal carbonyls *trans* to carbonyl groups of neutral compounds.[8-10,12] The average C(2)-O(2) distances [1.173(10) Å (**8a**), 1.178(12)) Å (**8b**)] are longer than the C(1)-O(1) distances as one would expect and also longer than C-O distances of metal carbonyls *trans* to phosphorus atoms of neutral compounds.[8-10,12]

The average M-P bonding distances to P(4) and P(5) [2.719(6) Å (**8a**), 2.702(11) Å (**8b**)] are significantly longer than distances typically found for M-P bonds *trans* to carbonyls [*e.g.*, 2.462(2) Å (*cis*-$Mo(CO)_4[P(OCH_3)_3]NHC_5H_{10}$);[8] 2.502(7) Å (*cis*-$W(CO)_4(PCH_3)_6$)[13]]. Although these long bonds may imply weak M-P interactions, this was not found. The $P_7$ ligands do not dissociate on the NMR time scale and are not displaced by en or dppe. The lack of correlation between M-P bond length and bond strength was recently described.[10] The average distances from the transition metal to P(6) and P(7) [3.673 Å (**8a**), 3.678 Å (**8b**)] are well beyond bonding distances.[14]

The range of P-P bonding distances of **3** (2.15-2.29 Å) is similar to that of the bare $P_7^{3-}$ ion in $Sr_3P_{14}$ (2.17-2.25 Å)[15] and $[P_7Cr(CO)_3]^{3-}$ (2.114-2.237 Å).[16] The P(1)-P(2) distance in **8b** (2.09 Å) is very short for a P-P single bond but may be the consequence of the various disorders within the crystal lattice.

The **8c** ion contains seven inequivalent phosphorus atoms as determined by $^{31}P$ NMR spectroscopic studies (see below) which is indicative of $C_1$ point symmetry. The spectroscopic similarities to **8a** and **8b** suggest the three are isostructural.

### 5.2.3 IR Spectroscopic Studies

The IR spectra (KBr pellet) for compounds **7** show four ν(CO) bands between 1940 and 1743 $cm^{-1}$ with the usual appearance characteristic of *cis*-$L_2M(CO)_4$

compounds.[17,18] The carbonyl stretching frequencies are ~ 85 $cm^{-1}$ lower energy than neutral *cis*-$L_2M(CO)_4$ structures signaling significant charge transfer from the $P_7$ cluster to the $M(CO)_4$ center.

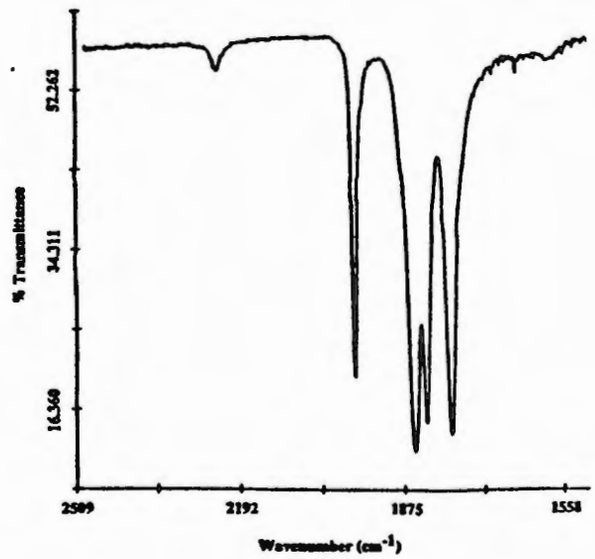


**Figure 5.3.** Solid-state IR spectrum (KBr pellet) showing the P-H and carbonyl regions of the $[HP_7Mo(CO)_4]^{2-}$ (**8a**) ion.

The $\nu$(PH) and $\nu$(CO) regions of **8a** are shown in Figure 5.3. The IR spectra for **8a** and **8b** show $\nu$(PH) modes at 2240 to 2238 $cm^{-1}$. The IR spectra of compounds **8** show four $\nu$(CO) bands between 1969 and 1778 $cm^{-1}$ that are blue shifted 24-37 $cm^{-1}$ relative to the respective compounds **7**. The IR spectrum for **8c** is virtually identical to that of **8b**.

### 5.2.4 NMR Spectroscopic Studies

The $^{31}P$ NMR spectra for compounds **7** show five second-order resonances between 65 and -130 ppm of integrated relative intensities 1:1:1:2:2. The $^{31}P$ NMR spectrum of **7b** is shown in Figure 5.4 as an example. The samples showed minor

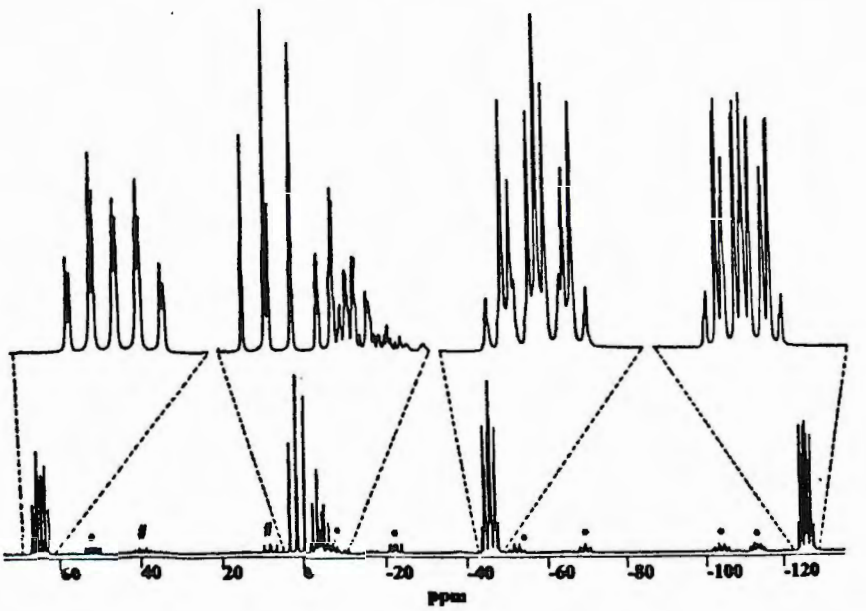


**Figure 5.4.** $^{31}P$ NMR spectrum for the $[P_7W(CO)_4]^{3-}$ ion (**7b**) recorded at 27 $^{o}C$ and 202.458 MHz from DMF-$d_7$ solution. The resonances marked with * are for the $[HP_7W(CO)_4]^{2-}$ ion (**8b**) and the resonances marked with # were due to impurities.

amounts of **2PM**, $[HP_7M(CO)_4]^{2-}$ and unknown impurities. The solution structure of **7** show $C_s$ point symmetry with a mirror plane of symmetry defined by the transition metal, P(2), P(1) and P(3). This mirror plane bisects the two sets of phosphorus atoms P(4)-P(6) and P(5)-P(7) rendering them pairwise equivalent. Based on comparisons to related compounds, the following assignments are proposed. For **7b**, the -127 ppm (-130 ppm, **7a**) resonance is assigned to the two equivalent basal phosphorus atoms,[19-23] P(6) and P(7), and the -46 ppm (-53 ppm, **7a**) resonance is assigned to the two phosphorus atoms bound to the transition metal, P(4) and P(5) (see drawing $[P_7W(CO)_4]^{3-}$). The resonance at 3 ppm (-11 ppm, **7a**) is a disordered doublet of doublets and can be confidently assigned to the lone two-coordinate phosphorus atom P(1). The splitting is consistent to that observed for the lone two-coordinate

phosphorus atom of $[Me_2P_7]^-$.[5] The resonances at 65 ppm (60 ppm, **7a**) and -3 ppm (-16 ppm, **7a**) can be assigned to P(3) and P(2) respectively. The P(3) assignment is unusual in that basal phosphorus resonances usually appear upfield from nonbasal phosphorus resonances.[19-21,24,25]

The $^{13}C$ NMR spectrum for **7b** shows three resonances in the 218-208 ppm range in a 2:1:1 ratio. The downfield resonance of intensity 2 shows a splitting of 13 Hz. The other two CO resonances are broad singlets. In general, there is a downfield shift of the carbonyl resonances relative to the $M(CO)_6$ compounds (204-194 ppm)[26] and an upfield shift relative to the $[P_7M(CO)_3]^{3-}$ ions (239-232 ppm) where M = Mo, W.[16]

The $^1H$ NMR spectra of **8a** and **8b** (Figure 5.5) show P-H resonances that appear as doublets of doublets of multiplets at 1.78 ppm with one-bond H-P couplings of 174 Hz and two-bond H-P coupling of 16.7 Hz. Additional couplings to atoms P(2) and P(3) are also observed.

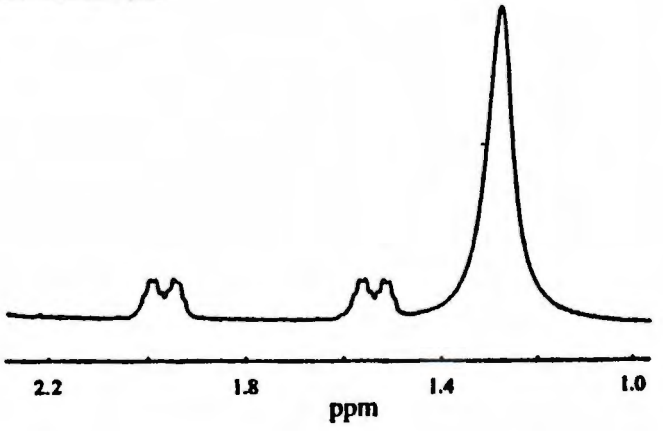


**Figure 5.5.** $^1H$ NMR spectrum for the $[HP_7W(CO)_4]^{2-}$ ion (**8b**) recorded at 27 $^oC$ and 400.1 MHz from DMF-$d_7$ solution. The resonance at 1.28 ppm is ethylenediamine.

The $^{31}P$-$^{31}P$ COSY NMR spectrum of **8a** is shown in Figure 5.6. The $^{31}P$ NMR spectra of **8** show seven resonances of equal intensity corresponding to each of

the seven inequivalent phosphorus atoms. This chemical inequivalence is consistent with the $C_1$ point symmetry observed in the solid state that is caused by the hydrogen atom bound to P(1). In the proton coupled $^{31}P$ NMR spectra, the resonance furthest downfield [35.5 ppm (**8a**), 49.5 ppm (**8b**)] shows coupling to hydrogen and can therefore be assigned to P(1) (see Figure 5.1).

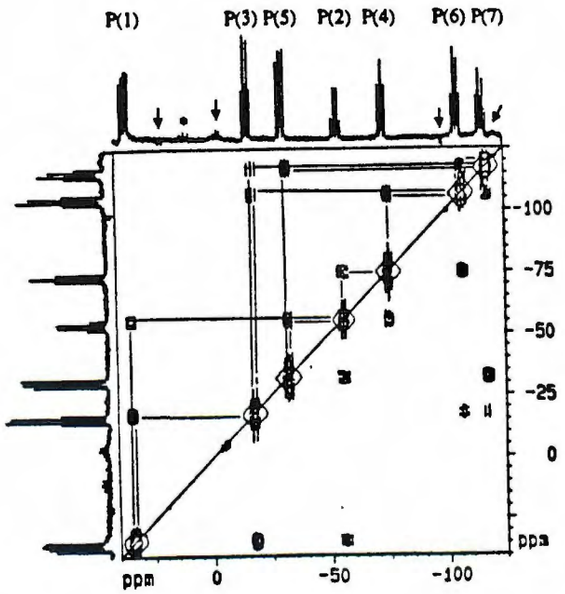


**Figure 5.6.** $^{31}P$-$^{31}P$ COSY NMR spectrum for the $[HP_7Mo(CO)_4]^{2-}$ ion (**8a**) recorded at 27 $^{o}C$ and 202.5 MHz from DMF-$d_7$ solution. The arrows point to resonances of the $[HP_7Mo(CO)_3]^{2-}$ ion, **3c**. The asterisk denotes a resonance from an unidentified product.

With this assignment of P(1), one can interpret the $^{31}P$-$^{31}P$ COSY NMR spectrum of **8a** without difficulty. The threshold level was selected so that only the crosspeaks due to normal one-bond P-P coupling would be exhibited. The resonance furthest downfield (120 ppm) for **8c** can then also be assign to P(1). The P(1) resonance for **8c** is considerably further downfield than for **8a** and **8b**, presumably because of the attached benzyl group.

The $^{13}C$ NMR spectra for compounds **8** show four resonances in the 200-225 ppm range. Two of these resonances are doublets with coupling of ~ 10 Hz. Another is a doublet that shows a larger coupling of 28.7 Hz. The remaining resonance in this chemical shift range is a broad singlet. As was observed for compounds **7**, there is a downfield shift of the carbonyl resonances relative to the $M(CO)_6$ compounds and an upfield shift relative to the $[P_7M(CO)_3]^{3-}$ ions where M = Mo, W. For **8c**, the benzyl α-carbon resonance appears as a doublet at 26.9 ppm with $^2J_{P\text{-}C}$ = 30 Hz. The $^1H$ NMR spectrum of **8c** shows resonances between 7.3 to 7.0 ppm due to the phenyl hydrogens of the benzyl group and "AB multiplets" at 1.83 and 1.53 ppm resulting from the diastereotopic α-hydrogens.

## 5.3 Discussion

Our initial discovery of the $[HP_7M(CO)_4]^{2-}$ complexes, **8**, involved an attempted $Mo(CO)_3$ / $W(CO)_3$ exchange reaction between $[P_7W(CO)_3]^{3-}$ and (cycloheptatriene)$Mo(CO)_3$. Although no exchange occurred in the absence of protio impurities after several days, in the presence of $H^+$ the [K(2,2,2-crypt)]$^+$ salts of $[HP_7Mo(CO)_4]^{2-}$ and $[HP_7W(CO)_4]^{2-}$ were isolated as well as an ill-defined "K-Mo-P"

$$[P_7W(CO)_3]^{3-} + \text{"}Mo(CO)_3\text{"} \rightarrow [HP_7W(CO)_4]^{2-} + [HP_7Mo(CO)_4]^{2-} + \text{"K-Mo-P"} \quad (5.11)$$

**2PW** **8b** **8a**

solid state compound with a $BaVS_3$ related structure (eq. 5.11).[27] While this reaction is quite reproducible, it gives inseparable mixtures of products thus prompting the develop the rational routes to the complexes described herein.

**Scheme 5.1**

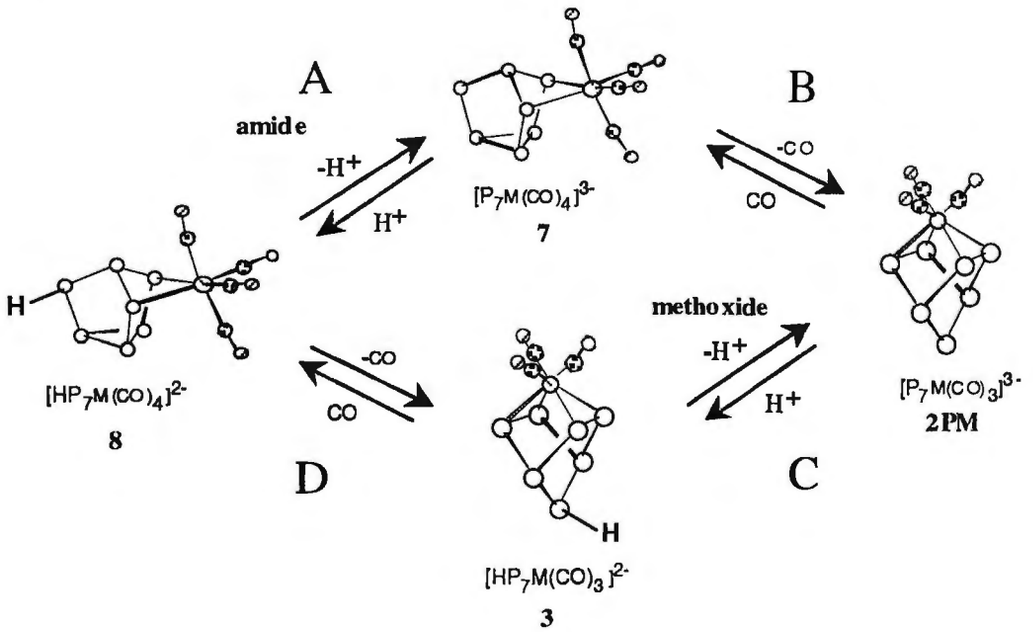


The $[\eta^4\text{-}P_7M(CO)_3]^{3-}$ ions (**2**) react with carbon monoxide in ethylenediamine to form the $[\eta^2\text{-}P_7M(CO)_4]^{3-}$ ions (**7**) (M = Mo, W) (Scheme 5.1). In contrast, complexes **8** are isolable and relatively stable towards CO loss in solution and the solid sate. Compounds **7** readily lose CO under $N_2$ atmospheres and only the tungsten complex **7b** has been prepared in pure form. The enhanced relative stability of the protonated tetracarbonyl complexes **8** in comparison to the unprotonated complexes **7** is somewhat curious. Upon protonation of the $P_7$ cage, the C-O bond strengths increase [higher $\nu$(CO)] which is usually accompanied by a *decrease* in the M-C bond strengths. However, the protonated compounds **8** are *less* prone to CO loss than **7**. These relative stabilities are consistent with the following two scenarios:

1) If the tetracarbonyl complexes (**7** or **8**) rapidly (and reversibly) lose CO to give $\eta^2\text{-}P_7M(CO)_3$ 16-electron intermediates, two reaction pathways can be envisaged and are shown in eq. 5.12. The intermediate can either coordinate CO to reform the

tetracarbonyl complexes (no net reaction) or undergo a haptatropic shift of the $P_7$ ligand ($\eta^2$ --> $\eta^4$) to form the stable tricarbonyl compounds (**2PM** or **3**). Partitioning of products in eq. 5.12 results from a competition between CO and the $P_7$ cage for the vacant coordination site at the 16-electron intermediate. The *un*protonated $P_7$ cage of **7** is more nucleophilic and competes more effectively with CO than does the protonated $HP_7$ cage of **8**. The result is that the net loss of CO is faster for **7** than **8**.

$$[\eta^2\text{-}P_7M(CO)_4]^{n-} \rightleftharpoons [\eta^2\text{-}P_7M(CO)_3]^{n-} + CO \longrightarrow [\eta^4\text{-}P_7M(CO)_3]^{n-} \quad (5.12)$$

**7** (or **8**) **2PM** (or **3**)

2) Alternatively, the haptatropic shift could be part of a concerted nucleophilic displacement of a CO ligand to form the tricarbonyl complexes without pre-dissociation of CO. In this case, the relative nucleophilicities of the protonated versus unprotonated $P_7$ cages would still give rise to the same relative stabilities of **7** versus **8**.

In either scenario, the *un*protonated $P_7^{3-}$ ligand of **7** is more nucleophilic than the protonated $HP_7^{2-}$ cage of **8** and will favor formation of the tricarbonyl complexes (CO loss).

The series of compounds also show unusual trends in basicity and nucleophilicity. For example, addition of a CO ligand to **2PM** in the formation of **7** increases the basicity and nucleophilicity of the coordinated $P_7$ cage. These enhancements are evidenced qualitatively by the faster alkylation reactions of **7** (*i.e.*, eq. 5.10) relative to **2PM** (*i.e.*, Scheme 2.1, eq. **B**) and quantitatively in the acid-base reactions outlined in Scheme 5.1. Protonation of **7** in en solutions is easily accomplished using MeOH (eq. 5.4) and the deprotonation of **8** requires a stronger base than $MeO^-$ (*i.e.*, an amide, eq. 5.7). In contrast, protonation of **2PM** requires stronger acids than MeOH (*i.e.*, 9-phenylfluorene) to form **3** and subsequent deprotonations are

accomplished using $MeO^-$ (see Scheme 5.1).[4] The enhanced basicity and nucleophilicity of **7** can be understood through the following considerations. First, the $P_7^{3-}$ ligand is functioning as a four-electron density from the $P_7^{3-}$ fragment in **7** relative to **2PM**. Second, the molecular orbital calculations indicate a large degree of charge transfer from the $P_7^{3-}$ ligand to the $M(CO)_3$ fragments in the electronic structure of **2PM**. In a limiting valence bond model for **2PM**, one could partition the charge in the form $P_7^{1-}$ -- $M(CO)_3^{2-}$ thus making it electronically equivalent to $Fe(CO)_3$(norbornadiene)[28] and adequately describing the $\nu$(CO) energies. In contrast, the IR data for **7** show a lesser overall charge transfer suggesting a limiting valence bond description of $P_7^{3-}$ -- $M(CO)_4$. Both of these factors could lead to enhanced basicity and nucleophilicity of the $P_7$ cage in **7** relative to **2PM**.

A similar pathway may be proposed for Tremel's synthesis of the $[Sb_7Mo(CO)_3]^{3-}$ ion from the (bipy)$Mo(CO)_4$ and $Sb_7^{3-}$ precursors.[1,2] The $[Sb_7Mo(CO)_4]^{3-}$ ion may be formed initially followed by the loss of a CO ligand.

## 5.4 Experimental Section

### 5.4.1 General Data

General operating procedures and data have been described in Chapter 2. General data not included in Chapter 2 follow. Proton ($^1H$) NMR spectra were recorded at ambient temperature on a Bruker AM400 (400.136 MHz) spectrometer. Some carbon ($^{13}C$) NMR spectra were recorded at ambient temperature on a Bruker AF200 (50.324 MHz) spectrometer. Some of the $^{13}C$ NMR chemical shifts and couplings were confirmed by recording the spectra at different magnetic field strengths. Some phosphorus ($^{31}P$) NMR spectra were recorded on a Bruker AMX500 (202.458

MHz) spectrometer. The $^{31}P$-$^{31}P$ COSY NMR experiment was conducted on a Bruker AMX500 in DMF-$d_7$ at 27 °C.

The IR and NMR spectral data common to all compounds containing [K(2,2,2-crypt)]$^+$ and/or en can be found in Chapter 2.

### 5.4.2 Chemicals

All materials not included in Chapter 2 follow. Tetracarbonylbis(piperidine)molybdenum and benzyltrimethylammonium bromide were purchased from Aldrich and used without further purification. Carbon monoxide (CO) was purchased from Air Products and used without further purification. The preparation of **2PMo**, **2PW** and **4d** were previously reported.[5,16]

### 5.4.3 Syntheses

#### 5.4.3.1 Preparation of $[K(2,2,2\text{-crypt})]_3[P_7Mo(CO)_4]$.

In a 25 mL Schlenk flask, crystalline $[K(2,2,2\text{-crypt})]_3[P_7Mo(CO)_3]\cdot$en (114 mg, 0.067 mmol) was dissolved in en (~ 3 mL) yielding a red solution. The head gases were removed under vacuum and the flask back filled with CO (~ 1 atm). The flask was left open to the bubbler with a flow of CO for 30 s. The reaction mixture was vigorously stirred for 12 h producing a yellow-orange solution and yellow-orange powder. The mother liquor was removed, the yellow-orange powder washed with tol and dried under vacuum (powder yield, 57 mg). IR spectroscopic analysis of the powder showed **8a** contaminates and $^{31}P$ NMR spectroscopic analysis of the mother liquor showed both **2PMo** and **8a** contaminates. IR data (KBr pellet), cm$^{-1}$: 1943 (s), 1830 (s), 1799 (s), 1748 (s). $^{31}P$ NMR (DMF-$d_7$) δ(ppm): 60 (m, 1 P), -11 (dd, 1 P), -16 (m, 1 P), -53 (m, 2 P), -130 (m, 2 P).

### 5.4.3.2 Preparation of $[K(2,2,2\text{-crypt})]_3[P_7W(CO)_4]\cdot en$.

In a 25 mL Schlenk flask, $K_3P_7$ (29.6 mg, 0.089 mmol), 2,2,2-crypt (100.0 mg, 0.27 mmol) and $[C_6H_3\text{-}(CH_3)_3]W(CO)_3$ (34.4 mg, 0.089 mmol) were combined in en (~ 3 mL). The reaction mixture was stirred for 12 h yielding a red solution. The head gases were removed under vacuum and the flask back filled with CO (~ 1 atm). The flask was left open to the bubbler with a flow of CO for 30 s. The reaction mixture was vigorously stirred for 12 h producing a yellow solution and yellow powder. The mother liquor was removed, the yellow powder washed with tol and dried under vacuum (powder yield, 115 mg, 71 %). Anal. Calcd for $C_{60}H_{116}N_8O_{22}K_3P_7W$: C, 39.61; H, 6.43; N, 6.16. Found: C, 39.79; H, 6.25; N, 6.31. IR data (KBr pellet), $cm^{-1}$: 1939 (s), 1819 (s), 1793 (s), 1744 (s). $^{13}C\{^1H\}$ NMR (DMF-$d_7$) δ(ppm): 218 (d, $J_{C\text{-}P}$ = 13 Hz, CO), 215 (br s, CO), 212 (br s, CO). $^{31}P$ NMR (DMF-$d_7$) δ(ppm): 65 (m, 1 P), 3 (m, 1 P), -3 (m, 1 P), -46 (m, 2 P), -127 (m, 2 P).

### 5.4.3.3 Preparation of $[K(2,2,2\text{-crypt})]_2[HP_7Mo(CO)_4]\cdot en$.

In a vial in a drybox, $K_3P_7$ (29.6 mg, 0.089 mmol), 2,2,2-crypt (100.0 mg, 0.27 mmol) and $[(C_5H_{10}NH)_2Mo(CO)_4]$ (33.7 mg, 0.089 mmol) were dissolved in en (~ 2 mL) and gently stirred for 3 h yielding a red-orange solution. The reaction mixture was filtered through *ca.* one quarter inch of tightly packed glass wool in a pipet. After 24 h, the reaction vessel contained rectangular yellow-orange crystals that were removed from the mother liquor, washed with toluene and dried under vacuum (crystalline yield, 47 mg, 40 %). Anal. Calcd for $C_{42}H_{81}N_6O_{16}K_2P_7Mo$: C, 38.30; H, 6.20; N, 6.38. Found: C, 37.42; H, 5.89; N, 6.07. IR data (KBr pellet), $cm^{-1}$: 2238 (w), 1969 (s), 1854 (s), 1831 (s), 1783 (s). $^1H$ NMR (DMF-$d_7$) δ(ppm): 1.78 (ddm, $^1J_{H\text{-}P}$ = 172 Hz, $^2J_{H\text{-}P}$ = 16.7 Hz). $^{13}C\{^1H\}$ NMR (DMF-$d_7$) δ(ppm): 223 (d, $^2J_{C\text{-}P}$ = 11 Hz,

CO), 222 (d, $^2J_{C\text{-}P}$ = 10 Hz, CO), 215 (d, $^2J_{C\text{-}P}$ = 29 Hz, CO), 214 (br s, CO). $^{31}P\{^1H\}$ NMR (DMF-$d_7$) δ(ppm): 35.5 (m, 1 P), -18.5 (m, 1 P), -31.5 (m, 1 P), -55.0 (m, 1 P), -74.0 (m, 1 P), -106.0 (m, 1 P), -118.0 (m, 1 P).

### 5.4.3.4 Preparation of $[K(2,2,2\text{-crypt})]_2[HP_7W(CO)_4]\cdot en$.

Method A: $[K(2,2,2\text{-crypt}]_3[P_7W(CO)_4]\cdot en$ (0.089 mmol) was generated *in situ* as described above (Method A). The powder was not isolated from the mother liquor. Instead, methanol (10 μL) was added under a flow of CO and the mixture stirred vigorously for 8 h. The color of the solution remained yellow. After stirring, the mother liquor was removed leaving a yellow, powdery solid that was washed with toluene and dried under vacuum (powder yield, 96 mg, 76 %). Method B: In a 25 mL Schlenk flask, crystalline $[K(2,2,2\text{-crypt})]_2[HP_7W(CO)_3]\cdot en$ (41 mg, 0.031 mmol) was dissolved in en (~ 2 mL) yielding a dark red solution. The head gases were removed under vacuum and the flask back filled with CO (~ 1 atm). The flask was left open to the bubbler with a flow of CO for 30 s. The reaction mixture was vigorously stirred for 12 h producing a yellow solution and yellow powder. $^{31}P$ NMR spectroscopic analysis of the mother liquor showed quantitative yield of **8b**. Anal. Calcd for $C_{42}H_{81}N_6O_{16}K_2P_7W$ prepared by Method A: C, 35.91; H, 5.81; N, 5.98. Found: C, 35.37; H, 5.64; N, 5.96. IR data (KBr pellet), $cm^{-1}$: 2240 (w), 1964 (s), 1843 (s), 1825 (s), 1778 (s). $^1H$ NMR (DMF-$d_7$) δ(ppm): 1.78 (ddm, $^1J_{H\text{-}P}$ = 172 Hz, $^2J_{H\text{-}P}$ = 16.7 Hz). $^{13}C\ \{^1H\}$ NMR (DMF-$d_7$) δ(ppm): 215 (d, $^2J_{C\text{-}P}$ = 11 Hz, CO), 214 (d, $^2J_{C\text{-}P}$ = 11 Hz, CO), 211 (br s, CO), 210 (d, $^2J_{C\text{-}P}$ = 29 Hz, CO). $^{31}P\{^1H\}$ NMR (DMF-$d_7$) δ(ppm): 49.5 (m, 1 P), -9.3 (m, 1 P), -24.2 (m, 1 P), -54.7 (m, 1 P), -71.3 (m, 1 P), -106.2 (m, 1 P), -116.0 (m, 1 P).

### 5.4.3.5 Preparation of $[K(2,2,2\text{-crypt})]_2[(CH_2Ph)P_7W(CO)_4]\cdot en$.

Method A: In a vial in a drybox, $K_3P_7$ (29.6 mg, 0.089 mmol), 2,2,2-crypt (100.0 mg, 0.27 mmol) and $[C_6H_3\text{-}(CH_3)_3]W(CO)_3$ (34.4 mg, 0.089 mmol) were combined in en (~ 3 mL) and stirred for 12 h producing a red solution. Solid $(CH_2Ph)Me_3NBr$ (20.5 mg, 0.089 mmol) was added and the reaction mixture stirred for an additional 12 h yielding a maroon solution. The reaction mixture was transferred from the vial to a 25 mL Schlenk flask, and the head gases were removed under vacuum. The Schlenk flask was then back filled with CO (~ 1 atm). The flask was left open to the bubbler with a flow of CO for 30 s. The reaction mixture was vigorously stirred for 12 h producing a yellow solution and yellow powder. The mother liquor was removed yielding a yellow powder that was washed with tol and dried under vacuum (powder yield, 81 mg, 61 %). Method B: $[K(2,2,2\text{-crypt})]_3[P_7W(CO)_4]\cdot en$ (0.089 mmol) was prepared as described above (Method A). Solid $(CH_2Ph)Me_3NBr$ (20.5 mg, 0.089 mmol) was added and the reaction mixture stirred for 8 h. $^{31}P$ NMR spectroscopic analysis of the mother liquor showed quantitative yield of **8c**. Anal. Calcd for $C_{49}H_{88}N_6O_{16}K_2P_7W$ prepared by Method B: C, 39.34; H, 5.93; N, 5.62. Found: C, 38.50; H, 5.69; N, 5.44. IR data (KBr pellet), $cm^{-1}$: 1964 (s), 1840 (s), 1824, (s), 1774 (s). $^1H$ NMR (DMF-$d_7$) δ(ppm): 7.3-7.0 (m, $CH_2$*Ph*), 1.83, 1.53 (C*H*$_2$Ph). $^{13}C\{^1H\}$ NMR (DMF-$d_7$) δ(ppm): 215 (m, CO), 214 (m, CO), 211 (br s, CO), 210 (d, $^2J_{C\text{-}P}$ = 30 Hz), CO), 144 (br s, ipso C), 130, 128, 125 ($CH_2$*Ph*), 26.9 (d, $^1J_{C\text{-}P}$ = 30 Hz, *C*H$_2$Ph). $^{31}P\{^1H\}$ NMR (DMF-$d_7$) δ(ppm): 120 (m, 1 P), -1 (m, 1 P), -38 (m, 1 P), -58 (m, 1 P), -80 (m, 1 P), -119 (m, 2 P).

### 5.4.3.6 Reaction of $[P_7W(CO)_3]^{3-}$ and "$Mo(CO)_3$".

In vial 1 in a drybox, $K_3P_7$ (29.6 mg, 0.089 mmol), 2,2,2-crypt (100.0 mg, 0.27 mmol) and $[C_6H_3\text{-}(CH_3)_3]W(CO)_3$ (34.4 mg, 0.089 mmol) were dissolved in en

(~ 3 mL) and stirred for 12 h producing a red solution. In vial 2, $(C_7H_8)Mo(CO)_3$ (24.1 mg, 0.089 mmol) was suspended in toluene (~ 1 mL) then added dropwise to the contents of vial 1 and stirred for 2 h. The solution color remained red. After 24 h, the reaction vessel contained golden yellow crystals that were removed from the mother liquor, washed with toluene and dried under vacuum (crystalline yield, 46 mg). A crystal was selected for single crystal X-ray diffraction analysis giving the structure as $[K(2,2,2\text{-crypt})]_2[HP_7W(CO)_4]\cdot en$. IR and $^{31}P$ NMR spectroscopic analysis of the crystals revealed **8a** and **8b** in a 1:10 ratio. Visual inspection of the crystals also showed five that were red in color. Single crystal X-ray diffraction revealed a "K-Mo-P" compound with a $BaVS_3$-type structure.[27]

### 5.4.3.7 Attempts at Deprotonation.

$K(2,2,2\text{-crypt})]_2[HP_7M(CO)_4]\cdot en$ (M = Mo, W) (0.089 mmol) was prepared as described above (Method A for **8b**). Solid NaOMe (7.2 mg, 0.134 mmol) was added and the reaction mixture stirred for 8 h. $^{31}P$ NMR spectroscopic analyses of the mother liquors showed a 1:4 ratio for **2PMo**:**8a** when M = Mo and **8b** when M = W.

$[K(2,2,2\text{-crypt})]_2[HP_7M(CO)_4]\cdot en$ (M = Mo, W) (0.089 mmol) was prepared as described above (Method A for **8b**). Solid $H_2NCH_2CH_2NHLi$ (8.9 mg, 0.134 mmol) was added and the reaction mixture stirred for 8 h. $^{31}P$ NMR spectroscopic analyses of the mother liquors showed quantitative conversion to **2PMo** when M = Mo and **7b** and **2PW** when M = W.

### 5.4.4 X-ray Crystallographic Studies.

Single crystal X-ray diffraction studies of $[K(2,2,2\text{-crypt})]_2[HP_7Mo(CO)_4]\cdot en$ and $[K(2,2,2\text{-crypt})]_2[HP_7W(CO)_4]\cdot en$ were done by Dr. James C. Fettinger, University of Maryland.

**Table 5.1.** Crystallographic Data for $[K(2,2,2\text{-crypt})]_2[HP_7M(CO)_4]\cdot en$ Where M = Mo, W.

| formula | $C_{42}H_{81}K_2MoN_6O_{16}P_7$ | $C_{42}H_{81}K_2WN_6O_{16}P_7$ |
|---|---|---|
| fw | 1317.10 | 1405.01 |
| space group | *C2/c* | *C2/c* |
| *a*, Å | 22.848(2) | 23.067(20) |
| *b*, Å | 12.528(2) | 12.6931(13) |
| *c*, Å | 21.460(2) | 21.433(2) |
| α, deg | 90 | 90 |
| β, deg | 91.412(12) | 90.758(7) |
| γ, deg | 90 | 90 |
| V, $Å^3$ | 6140.9(12) | 6274.9(10) |
| Z | 4 | 4 |
| cryst dimens, mm | 0.50 x 0.20 x 0.20 | 0.50 x 0.20 x 0.20 |
| cryst color | yellow | golden yellow |
| D(calcd), $Mg/m^3$ | 1.419 | 1.455 |
| μ(Mo Kα), $mm^{-1}$ | 0.595 | 0.395 |
| temp, K | 153(2) | 293(2) |
| 2θ scan range, deg | 2.57 - 22.50 | 20.6 - 22.50 |
| no. of reflns, colld | 4125 | 4478 |
| no. of ind reflns [$R_{int}$=0.0220] | 4008 [$R_{int}$ = 0.0505] | 4096 |
| Data/restraints/parameters | 4008 / 0 / 357 | 4096 / 0 / 363 |
| no. of ind obsd reflns $F_o > 4\sigma(F_o)$ | 2697 | 2833 |
| R(F), %[a] | 0.0681 | 0.0573 |

| | | |
|---|---|---|
| $R_w(F^2)$, %[b] | 0.1399 | 0.1409 |
| $\Delta/\sigma$(max) | $\leq$ 0.001 | $\leq$ 0.001 |
| GOF | 1.135 | 1.004 |

[a] $R(F) = \Sigma \mid F_o - F_c \mid / \Sigma F_o$. [b] $R_w(F^2) = (\Sigma w \mid F_o - F_c \mid^2 / \Sigma w F_o^2)^{1/2}$.

**Table 5.2.** Selected Distances ( Å ) and Angles ( ° ) for the $[HP_7M(CO)_4]^{2-}$ Ions.

| Distances | M = Mo | M = W | Distances | M = Mo | M = W |
|---|---|---|---|---|---|
| M-C(1) | 2.025(10) | 2.000(13) | M-C(2) | 1.919(10) | 1.920(12) |
| C(1)-O(1) | 1.141(10) | 1.116(14) | C(2)-O(2) | 1.173(10) | 1.178(12) |
| Mo-P(4) | 2.722(6) | 2.691(11) | Mo-P(5) | 2.717(6) | 2.714(11) |
| P(1)-P(2) | 2.15(2) | 2.09(2) | P(1)-P(3) | 2.190(12) | 2.18(2) |
| P(2)-P(4) | 2.148(8) | 2.174(13) | P(2)-P(5) | 2.180(8) | 2.151(12) |
| P(3)-P(6) | 2.24(2) | 2.29(2) | P(3)-P(7) | 2.25(2) | 2.29(2) |
| P(4)--P(5) | 3.268(8) | 3.238(13) | P(4)-P(6) | 2.175(7) | 2.155(10) |
| P(5)-P(7) | 2.169(7) | 2.155(12) | P(6)-P(7) | 2.195(7) | 2.178(9) |
| Angles | M = Mo | M = W | Angles | M = Mo | M = W |
| P(1)-P(2)-P(4) | 99.2(5) | 105.4(7) | P(1)-P(2)-P(5) | 102.5(6) | 100.8(7) |
| P(1)-P(3)-P(6) | 99.3(10) | 103.1(10) | P(1)-P(3)-P(7) | 102.3(11) | 100.1(10) |
| P(2)-P(1)-P(3) | 103.7(12) | 102.8(10) | P(2)-P(4)-P(6) | 99.8(3) | 99.3(5) |
| P(2)-P(5)-P(7) | 99.8(3) | 99.3(5) | P(3)-P(6)-P(4) | 108.2(5) | 106.3(6) |
| P(3)-P(6)-P(7) | 60.9(4) | 61.6(5) | P(3)-P(7)-P(5) | 107.7(5) | 105.9(6) |
| P(3)-P(7)-P(6) | 60.6(4) | 61.7(5) | P(4)-P(2)-P(5) | 98.1(2) | 97.0(3) |
| P(4)-P(6)-P(7) | 104.3(2) | 104.2(4) | P(5)-P(7)-P(6) | 104.3(3) | 104.3(4) |
| P(6)-P(3)-P(7) | 58.5(4) | 56.8(4) | P(2)-P(4)-M | 81.8(2) | 82.1(4) |
| P(2)-P(5)-M | 81.4(2) | 81.9(4) | P(4)-M-P(5) | 73.86(12) | 73.6(2) |
| P(4)-M-C(1) | 83.6(3) | 86.6(4) | P(4)-M-C(2) | 169.6(3) | 168.1(4) |
| P(5)-M-C(1) | 86.6(3) | 84.5(4) | P(5)-M-C(2) | 169.1(3) | 169.0(4) |
| P(6)-P(4)-M | 96.8(2) | 98.0(4) | P(7)-P(5)-M | 96.6(3) | 97.5(4) |
| C(1)-M-C(1)' | 172.3(6) | 172.6(8) | C(1)-M-C(2) | 91.0(4) | 91.3(5) |
| C(2)-M-C(2)' | 87.7(5) | 90.6(7) | M-C(1)-O(1) | 171.6(11) | 173(2) |
| M-C(2)-O(2) | 178.8(9) | 175.3(12) | | | |

## 5.5 References


(1) Bolle, U.; Tremel, W. *J. Chem. Soc., Chem. Commun.* **1992**, 91-93.

(2) Bolle, U.; Tremel, W. *J. Chem. Soc., Chem. Commun.* **1994**, 217-219.

(3) Charles, S.; Eichhorn, B. W.; Bott, S. G. *J. Am. Chem. Soc.* **1993**, *115*, 5837-5838.

(4) Charles, S. C.; Eichhorn, B. W.; Fettinger, J. C. **1995**, in preparation.

(5) Charles, S.; Fettinger, J. C.; Eichhorn, B. W. *J. Am. Chem. Soc.* **1995**, *117*, 5303-5311.

(6) Charles, S.; Eichhorn, B. W.; Fettinger, J. C.; Bott, S. G. **1995**, in preparation.

(7) Charles, S.; Eichhorn, B. W.; Fettinger, J. C.; Bott, S. G. *Inorg. Chem.* **1995**,

(8) Atwood, J. L.; Darensbourg, D. J. *Inorg. Chem.* **1977**, *16*, 2314-2317.

(9) Elmes, P. A.; Gatehouse, B. M.; Lloyd, D. J.; West, B. O. *J. Chem. Soc., Chem. Commun.* **1974**, 953-954.

(10) Ernst, R. D.; Freeman, J. W.; Stahl, L.; Wilson, D. R.; Arif, A. M.; Nuber, B.; Ziegler, M. L. *117* **1995**, 5055-5064.

(11) Sheldrick, W. S. *Chem. Ber.* **1975**, *108*, 2242-2246.

(12) Sullivan, P. J.; Rheingold, A. L. *Organometallics* **1982**, *1*, 1547-1549.

(13) Elmes, P. S.; Gatehouse, B. M.; West, B. O. *J. Organomet. Chem.* **1974**, *82*, 235-241.

(14) Alcock, N. W. *Adv. Inorg. Chem. Radiochem.* **1972**, *15*, 1-53.

(15) Dahlmann, W.; von Schnering, H. G. *Naturwissenschaften* **1972**, *59*, 420.

(16) Charles, S.; Eichhorn, B. W.; Rheingold, A. L.; Bott, S. G. *J. Am. Chem. Soc.* **1994**, *116*, 8077-8086.

(17) Darensbourg, D. J.; Kump, R. L. *Inorg. Chem.* **1978**, *17*, 2680-2682.

(18) Grim, S. O.; Briggs, W. L.; Barth, R. C.; Tolman, C. A.; Jesson, J. P. *Inorg. Chem.* **1974**, *13*, 1095-1100.

(19) Baudler, M.; Ternberger, H.; Faber, W.; Hahn, J. Z. *Naturforsch.* **1979**, *34B*, 1690-1697.

(20) Baudler, M.; Faber, W.; Hahn, J. Z. *Anorg. Allg. Chem.* **1980**, *469*, 15-21.

(21) Fritz, G.; Hoppe, K. D.; Hönle, W.; Weber, D.; Mujica, C.; Manriquez, V.; von Schnering, H. G. *J. Organomet. Chem.* **1983**, *249*, 63-80.

(22) Hönle, W.; von Schnering, H. G.; Fritz, G.; Schneider, H.-W. *Z. Anorg. Allg. Chem.* **1990**, *584*, 51.

(23) von Schnering, H. G. *Angew. Chem. Int. Ed. Engl.* **1981**, *20*, 33-51.

(24) Hönle, W.; von Schnering, H. G. *Z. Anorg. Allg. Chem.* **1978**, *440*, 171-182.

(25) von Schnering, H. G.; Manriquez, V.; Hönle, W. *Angew. Chem. Int. Ed. Engl.* **1981**, *20*, 594-595.

(26) Braterman, P. S.; Milne, D. W.; Randall, E. W.; Rosenberg, E. *J. Chem. Soc., Dalton Trans.* **1973**, 1027-1031.

(27) Charles, S.; Eichhorn, B. W., K-Mo-P.

(28) Albright, T. A.; Burdett, J. K.; Whangbo, M.-H. *Orbital Interactions in Chemistry*; John Wiley & Son, Inc.: New York, 1985, pp 218, 387.

# CHAPTER 6

## The Synthesis and Characterization of the $[(en)(CO)_3WP_7M(CO)_3]^{3-}$ ions Where M = Cr, W. Inversion at Phosphorus!

### 6.1 Introduction

The synthesis and characterization of the $[E_7M(CO)_3]^{3-}$ complexes (where E = P, As, Sb and M = Cr, Mo, W) were described in Chapter 2. The $[E_7M(CO)_3]^{3-}$ ions (**2EM**) have norbornadiene-like $E_7$ fragments bound $\eta^4$ to the $M(CO)_3$ fragment. The compounds possess high-lying lone pairs associated with the unique two-coordinate pnictogen atom furthest from the transition metal (the E(1) site). The pnictogen atom remains highly nucleophilic and is the site of attack by various electrophiles (*e.g.*, $H^+$, $R^+$) as described in Chapters 3 and 4.[1-3] In this chapter, the preparation and characterization of the $[(en)(CO)_3WP_7M(CO)_3]$ (M = Cr, W) bimetallic complexes are described in which a neutral $WL_5$ fragment is appended to the P(1) site.[4]

### 6.2 Results

#### 6.2.1 Synthesis

Ethylenediamine solutions of $[K(2,2,2\text{-crypt})]_3[P_7M(CO)_3]$ (M = Cr, W) react with one equiv of $(mesitylene)W(CO)_3$ to form $[K(2,2,2\text{-crypt})]_3[(en)(CO)_3WP_7M(CO)_3]$ in good yields (eq. 6.1). Eq. 6.1 chemistry also occurs in DMF to presumably give $[(DMF)_2(CO)_3WP_7M(CO)_3]^{3-}$ although this anion has not been isolated.

$$[P_7M(CO)_3]^{3-} + (\text{mesitylene})W(CO)_3 \xrightarrow{\text{en or DMF}} [(L_2)(CO)_3WP_7M(CO)_3]^{3-} \quad (6.1)$$

**2PM**

M = Cr, $L_2$ = en (**9a**)

M = W, $L_2$ = en (**9b**)

Monitoring by $^{31}P$ NMR spectroscopy shows modest rates of reaction ($t_\infty$ = 3 h) and virtually quantitative conversion to **9** at ambient temperatures. Like the protonations and alkylations, the attachment of the $(L_2)(CO)_3W$ moiety ($L_2$ = en or $DMF_2$) is at the P(1) site of the precursor **2PM**.[2,3] Equation 6.1 chemistry affords good crystalline yields of **9** (**9a**, 53 %; **9b**, 60 %) with small quantities of co-crystallized **2PM**. Compounds **9** are dark red in color and are moderately air and moisture sensitive in solution and solid state. Compounds **9** have been characterized by IR, $^1H$, $^{13}C$ and $^{31}P$ NMR spectroscopies, elemental analyses, and a representative single crystal X-ray diffraction study.

The reaction between **9b** and 2 equiv of $PMe_3$ in DMF showed no sign of $PMe_3$ coordination (eq. 6.2). However, the reaction between **9a** and one equiv of $K_3P_7$ in DMF displaces the $L_2(CO)_3W$ fragment to form one equiv each of $[P_7Cr(CO)_3]^{3-}$ and $[P_7W(CO)_3]^{3-}$ (eq. 6.3).

$$[(en)(CO)_3WP_7W(CO)_3]^{3-} + 2\ PMe_3 \xrightarrow{\text{DMF}} [(PMe_3)_2(CO)_3WP_7W(CO)_3]^{3-} \quad (6.2)$$

**9b**

$$[(en)(CO)_3WP_7Cr(CO)_3]^{3-} + P_7^{3-} \xrightarrow{\text{DMF}} [P_7W(CO)_3]^{3-} + [P_7Cr(CO)_3]^{3-} \quad (6.3)$$

**9a** **2PW** **2PCr**

### 6.2.2 Structural Studies

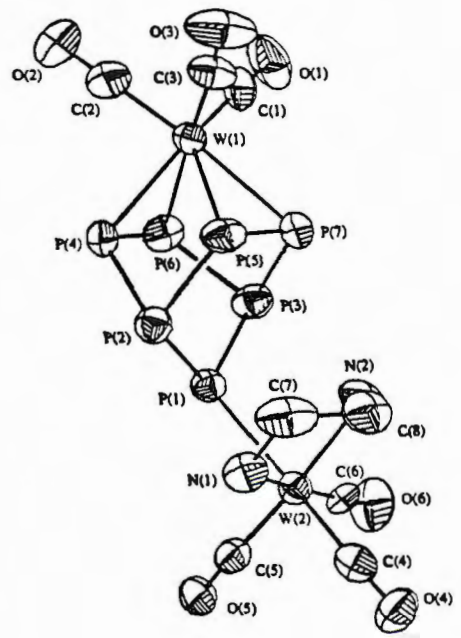


Figure 6.1. ORTEP drawing of the $[(en)(CO)_3WP_7W(CO)_3]^{3-}$ ion.

The structure of the $[K(2,2,2\text{-crypt})]^+$ salt of $[(en)(CO)_3WP_7W(CO)_3]^{3-}$ (**9b**) was determined by single crystal X-ray diffraction. An ORTEP drawing of the $[(en)(CO)_3WP_7W(CO)_3]^{3-}$ anion is shown in Figure 6.1. A summary of the crystallographic data is given in Table 6.1 and a listing of selected bond distances and angles given in Table 6.2. The structure contains an $\eta^4$-$P_7$ group attached to a $C_{3v}$ $M(CO)_3$ center and a $(en)(CO)_3W$ fragment attached to the phosphorus atom furthest from the $M(CO)_3$ center [P(1)] (see Fig. 6.1). The structural study shows that P(1) is pyramidal so that only one pair of electrons on P(1) participates in sigma bonding to the tungsten atom (see Table 6.3). The W(1)-P (ave 2.634 Å) and P-P (2.135 to 2.232 Å) bond distances are virtually identical to those observed for $[HP_7W(CO)_3]^{2-}$ (**3b**) and

$[EtP_7W(CO)_3]^{2-}$ (**4b**) (Chapters 3 and 4).[2,3] A selection of distances and angles of **3b**, **4b** and **9b** is presented in Table 6.3 below. As was seen in **3b** and **4b**, there is a slight lengthening of the W-P contacts to the phosphorus atoms *trans* to the CO ligands due to the high *trans* influence of carbon monoxide [P(6)-W(1)-C(3) = 174.4(4)°, P(7)-W(1)-C(2) = 172.7(4)°, and P(1)-W(2)-C(4) = 177.1(4)°]. The W(2)-C bonds *trans* to the W-N bonds are significantly longer [1.950(13) Å and 1.94(2) Å] than those of the other W-C contacts. However, the average W(2)-N bond distance of 2.324 Å is typical for W-N bonds *trans* to CO ligands [*i.e.*, $N_4P_4(NMe_2)_8W(CO)_4$ {2.33(2) Å and 2.37(1) Å}].[5] The W(2)-P(1) bond distance of 2.643(3) Å is virtually identical to the average of those of W(1) to the four metal-bound phosphorus atoms (2.634(3) Å ave.), but long for a typical W-P single bond [*i.e.*, $W(CO)_4(PMe_3)_6$ {2.502(7) Å}].[6]

**Table 6.3**. Select distances (Å) and angles (°) associated with appended fragment of $[HP_7W(CO)_3]^{2-}$ (**3b**), $[EtP_7W(CO)_3]^{2-}$ (**4b**) and $[(en)(CO)_3WP_7W(CO)_3]^{3-}$ (**9b**).

| | **3b** | **4b** | **9b** |
|---|---|---|---|
| P(1)-appendage | ---- | 1.858(7) | 2.643(3) |
| P(1)-P(2) | 2.163(4) | 2.173(3) | 2.144(4) |
| P(1)-P(3) | 2.162(4) | 2.176(3) | 2.149(4) |
| P(2)-P(1)-P(3) | 100.8(7) | 100.0(2) | 97.3(2) |
| P(2)-P(1)-appendage | ---- | 103.4(3) | 115.0(2) |
| P(3)-P(1)-appendage | ---- | 101.5(2) | 116.9(2) |
| W(1)-P(1)-appendage | ---- | 115.9(3) | 135.5(4) |

### 6.2.3 Spectroscopic Studies

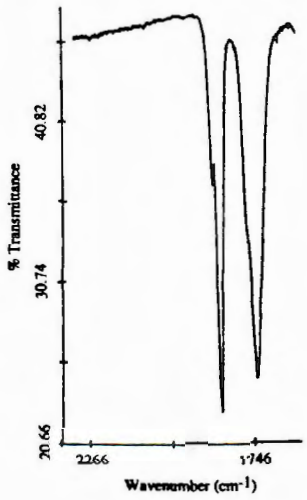


Figure 6.2. Solid-state IR spectrum (KBr pellet) showing the carbonyl region of the $[(en)(CO)_3WP_7W(CO)_3]^{3-}$ anion (**9b**).

The IR spectra for **9** show four ν(C-O) bands between 1869 and 1734 $cm^{-1}$ and have similar energies and intensities as found for $M(dien)(CO)_3$ (1884-1727 $cm^{-1}$) where M = Cr and W.[7] The $\nu$(CO) region of **9b** (KBr pellet) is shown in Figure 6.2 as an example. The blue shift of ~ 35 $cm^{-1}$ from the bands of the parent **2PM** is approximately the same as seen for the $[HP_7M(CO)_3]^{2-}$ (**3**) and $[RP_7W(CO)_3]^{2-}$ (**4**) compounds relative to **2PM**.[1-3]

The time-lapse $^{31}P\{^1H\}$ NMR spectra from a crude reaction mixture of the parent **2PW** with $(mesitylene)W(CO)_3$ is shown in Figure 6.3. The spectrum at t = 0 h is of $[P_7W(CO)_3]^{3-}$ in DMF-$d_7$. $(Mesitylene)W(CO)_3$ was added to the sample and stirred for 1.5 hours. The spectrum at t ≈ 1.5 h is of an aliquot removed from the crude reaction mixture at 1.5 h and shows both the $[P_7W(CO)_3]^{3-}$ and $\{(DMF)_2(CO)_3WP_7W(CO)_3\}^{3-}$ ions. The spectrum at t ≈ 3 h is of an aliquot removed

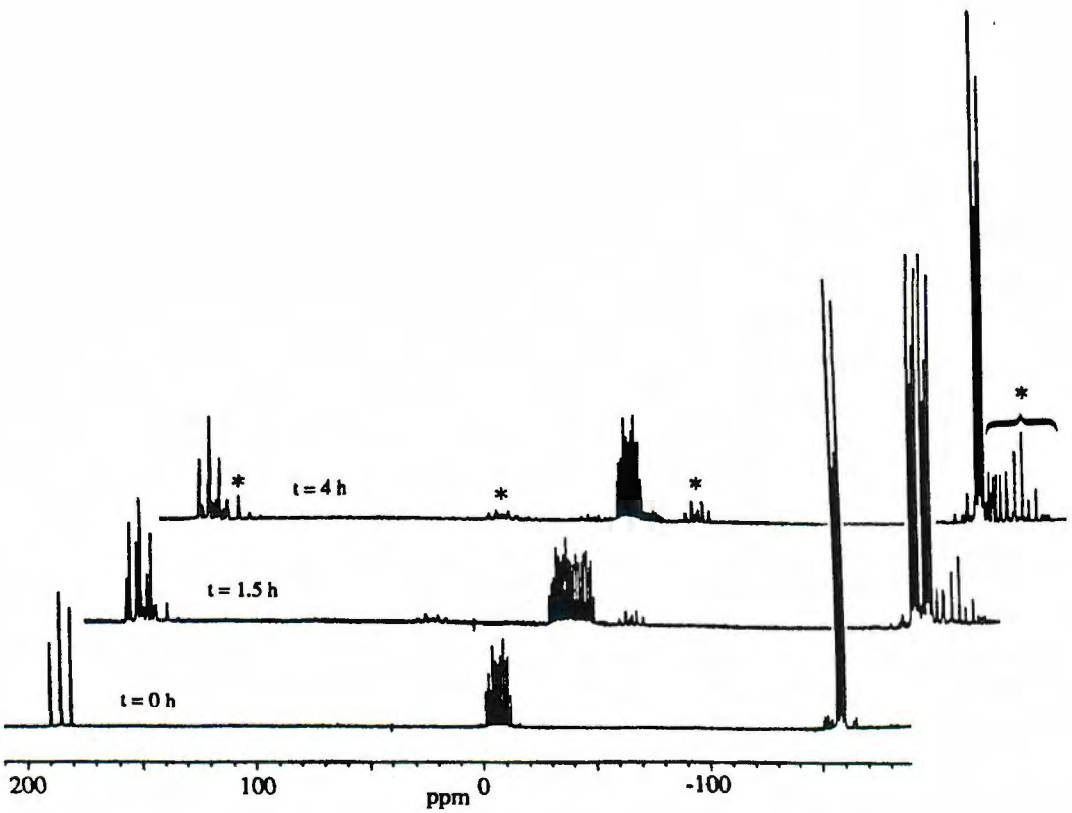


Figure 6.3. $^{31}P\{^{1}H\}$ NMR spectra from a crude reaction mixture of $[P_7W(CO)_3]^{3-}$ and mesityleneW(CO)$_3$ giving $[(DMF)_2(CO)_3WP_7W(CO)_3]^{3-}$ in DMF-$d_7$ recorded at t = 0 h, t ≈ 1.5 h and t ≈ 3 h (bottom to top, respectively) at 27 °C and 81.0 MHz. The asterisks denote unidentified by-products. The spectra at t ≈ 1.5 h and t ≈ 3 h are offset by ~ 35 ppm.

from the crude reaction mixture after 4 h and shows the $[(en)(CO)_3WP_7W(CO)_3]^{3-}$ ion. The $^{31}P$ NMR spectra for **9** show three resonances in a 4:2:1 integral ratio corresponding to the four metal-bound atoms [P(4), P(5), P(6), P(7)], the two bridging atoms [P(2), P(3)] and the unique phosphorus atom P(1), respectively. A summary of NMR data is given in Table 6.4. These spectra are similar to those of the parent **2PW** compounds in that the four metal-bound atoms appear chemically equivalent on the NMR time scale.[1] This is in sharp contrast from what is observed for the protonated

(Chapter 3)[2] and the alkylated (Chapter 4)[3] compounds that also have appended moieties at P(1). Based on the crystal structure of **9b**, one would anticipate seven $^{31}P$ resonances due to the seven inequivalent phosphorus atoms observed in the solid state. However, the spectra are consistent with AA'A"A'"MM'X spin systems, indicating that the compounds are fluxional on the NMR time scale at room temperature. That is, the asymmetries in the P(4)--P(5) / P(6)--P(7) separations observed in the solid state are time averaged in solution due to an intramolecular wagging process, generating a virtual mirror plane that bisects the P(4)-P(6) and P(5)-P(7) bonds making atoms P(4) and P(5) chemically equivalent to atoms P(6) and P(7), respectively. This mirror plane does **not**, however, make atoms P(4) and P(6) chemically equivalent to atoms P(5) and P(7), respectively. These atoms are made chemically equivalent by pyramidal inversion at P(1) of the $(en)(CO)_3W$ moiety generating another virtual mirror plane that bisects the P(4)--P(5) / P(6)--P(7) separations (see Section 6.3).

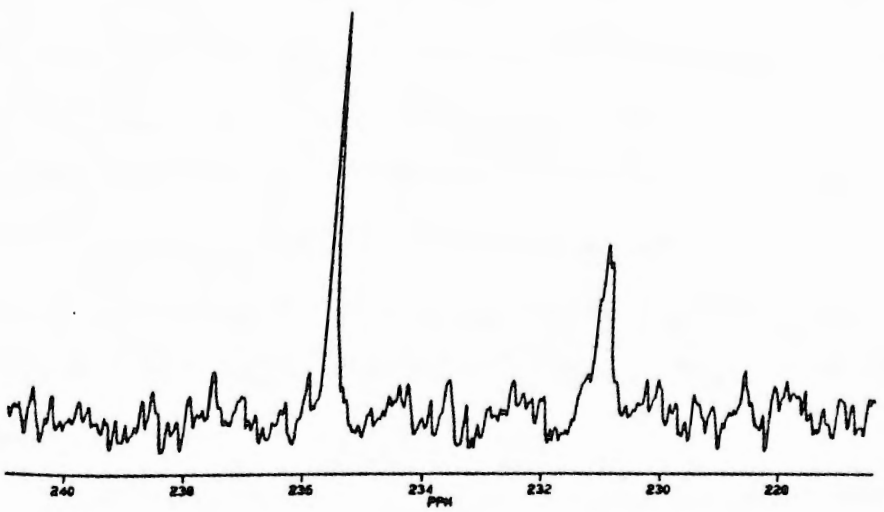


Figure 6.4. $^{13}C\{^1H\}$ NMR spectrum of $[(en)(CO)_3WP_7Cr(CO)_3]^{3-}$ recorded at 27 °C and 50.3 MHz from DMF-$d_7$ solution.

The $^{13}C\{^1H\}$ NMR spectrum of **9a** is exhibited in Figure 6.4 and the data are presented in Table 6.3. The $^{13}C\{^1H\}$ NMR spectra for **9** show two carbonyl resonances between 236 to 226 ppm for both compounds. For this discussion, the metal center with the $\eta^4$-$P_7$ ligand will be denoted as $M(CO)_3$ and the metal center with the $\eta^1$-$P_7$ ligand will be denoted as $W(en)(CO)_3$. The $^{13}C$ NMR spectrum for the mixed metal ion, $[(en)(CO)_3WP_7Cr(CO)_3]^{3-}$ (**9a**), provided the information necessary for the decisive assignments of the $^{13}C$ NMR resonances. For **9a**, the upfield resonance (231 ppm) is a multiplet ($^2J_{C\text{-}P} \approx 6$ Hz) with tungsten satellites ($^1J_{C\text{-}W} = 171$ Hz). Therefore, this resonance is assignable to the carbonyls of the $W(en)(CO)_3$ fragment and the broad singlet at 236 ppm is assignable to the carbonyls of the $Cr(CO)_3$ fragment. The C-P coupling indicates that $\eta^1$-$P_7$ / $W(en)(CO)_3$ dissociation is not occurring on the NMR time scale. Because of the similarities of the $^{13}C$ NMR spectra of **9a** and **9b**, the assignment of resonances of **9a** can be directly inferred from **9b**. It follows then that for **9b** the resonance at 230 ppm is assigned to the carbonyls of $W(CO)_3$ and the resonance at 226 ppm is assigned to the carbonyls of $W(en)(CO)_3$. As stated earlier, the carbonyl resonances of **9b** are similar to those observed for **9a** with the exception that the downfield carbonyl resonance (230 ppm) exhibits C-P ($^2J_{C\text{-}P} = 2.5$ Hz) coupling reminiscent of the carbonyl resonance of the parent **2PW**. The upfield carbonyl resonance (226 ppm) is a multiplet and also exhibits C-P coupling ($^2J_{C\text{-}P} \approx 3$ Hz). Again, the C-P coupling indicates that $\eta^1$-$P_7$ / $W(en)(CO)_3$ dissociation is not occurring on the NMR time scale.

The single resonance for the carbonyls of the $M(CO)_3$ fragments indicate that the $M(CO)_3$ fragments rotate rapidly in the $P_4$ face of **9** as is also observed for the compounds **2EM**, **3** and **4**.[1-3] The single resonance for the carbonyls of the $W(en)(CO)_3$ fragments indicates fluxtionality of the fragment relative to the $P_7M(CO)_3$

core **and** ligand rearrangement at the W center. There is a downfield shift of the carbonyl resonances of **9** relative to the $M(CO)_6$ compounds (M = Cr, $\delta$ = 212 ppm; M = W, $\delta$ = 192 ppm)[8] and an upfield shift relative to the parent **2PM** (M = Cr, $\delta$ = 246 ppm; M = W, $\delta$ = 232 ppm).

## 6.3 Discussion

Perhaps the most interesting feature of **9** is the fluxional behavior of the compounds in solution. The data are indicative of rapid inversion at P(1). This conclusion is based on the following observations: 1) the $^{31}P$ NMR data show that the four phosphorus atoms bound to W(1) of **9** remain chemically equivalent on the NMR time scale from -60 °C to 27 °C and 2) the $^{13}C$ NMR data show that the three carbonyls of the $(en)(CO)_3W$ fragment are chemically equivalent on the NMR time scale and exhibit C-P coupling.

Numerous papers and reviews have been presented on such mechanisms involving inversion at nitrogen, phosphorus and sulfur.[9,10] Typical ranges for barriers of inversion are 4-8 kcal/mol for trialkylamines, 29-40 kcal/mol for trialkylphosphines, 25-29 kcal/mol for sulfonium ions and 35-42 kcal/mol for sulfoxides.[9,10] Noteworthy is the dramatic reduction in barrier height conveyed by the presence of *d* orbitals on an adjacent substituent, as in the silylphosphines that have barriers of ~ 19 kcal/mol and some sulfur containing transition metal complexes that have barriers of 5-18 kcal/mol.[9-12]

The first detection of inversion of configuration at phosphorus in a polycyclophosphane was reported by Baudler *et al.* for the compounds $P_9R_3$ (R = Et, *t*-Bu). The inversion barrier for $P_9$*t*-$Bu_3$ was determined to be 18.5 kcal/mol which lies in the range of the inversion barriers for open-chain organophosphanes with P-P bonds in their molecular skeletons.[10,13-15] It was noted that $P_9Et_3$ inverted at a lower rate than

$P_9t$-$Bu_3$, but no value was reported. Inversion is also observed for other polycyclophosphanes including $P_{11}i$-$Pr_3$, $P_{12}i$-$Pr_4$, $P_{13}i$-$Pr_5$, and $P_{14}i$-$Pr_4$. Barriers to inversion for these compounds were found to be higher than that of $P_9t$-$Bu_3$ but no values were reported.

To explain the observed $^{13}C$ and $^{31}P$ NMR data, two mechanisms for phosphorus inversion (at the P(1) site) were considered: a dissociation-recombination pathway and inversion through a trigonal planar state. The inversion at P(1) of $[(en)(CO)_3WP_7W(CO)_3]^{3-}$ cannot be occuring by the dissociation-recombination pathway. The carbon-phosphorus coupling exhibited by the carbonyls of the $(en)(CO)_3W$ fragment clearly shows that this fragment remains associated to the $P_7$ core in solution and that $[P_7W(CO)_3]^{3-}$ and $[(en)(CO)_3WP_7W(CO)_3]^{3-}$ are not in equilibrium on the NMR time scale (see Figure 6.3).

With the $(en)(CO)_3W$ fragment remaining attached in solution, *both* the rearrangement of ligands of the $(en)(CO)_3W$ fragment *and* the inversion at P(1) must be occurring to explain the observed NMR data. If the ligands were rearranging and inversion were not occurring, one would observe four resonances in the $^{31}P$ NMR spectra with an integral ratio of 2:2:2:1 equated with P(5, 7), P(4, 6), P(2, 3), and P(1), respectively. If the inversion were occurring and the ligands were not rearranging, one would observe two resonance in the $^{13}C$ NMR spectra for the carbonyls of the $(en)(CO)_3W$ fragments with an integral ratio of 2:1.

The $^1H$ and $^{13}C$ NMR data for the ethylenediamine of the $[(en)(CO)_3WP_7W(CO)_3]^{3-}$ ions (in DMF-$d_7$) show resonances that are of "free" ethylenediamine. This indicates that ethylenediamine is dissociating from the tungsten atom. This dissociation allows the subsequent rearrangement of the carbonyls on the tungsten atom affording a single resonance as seen in the $^{13}C$ NMR spectra for the $(en)(CO)_3W$ fragment.

The ethylenediamine dissociation from the $(en)(CO)_3W$ fragment (presumably one "arm" at a time) leaves a 5-coordinate, 16-electron tungsten atom open to coordination by either a solvent molecule or the second lone pair on P(1). A reasonable hypothesis is that the second lone pair coordinates to the tungsten atom and that midway in the inversion process, double bond character is present between tungsten and phosphorus lowering the barrier to inversion (see Figure 6.5). The NMR data are consistent with this mechanism. This mechanism has been also been proposed for other cases of pyramidal inversion involving transition metals [*i.e.*, *cis*-bis(dibenzyl sulfide)dichloroplatinum(II) ($E_a$ = 18.0 kcal/mol)].[11]

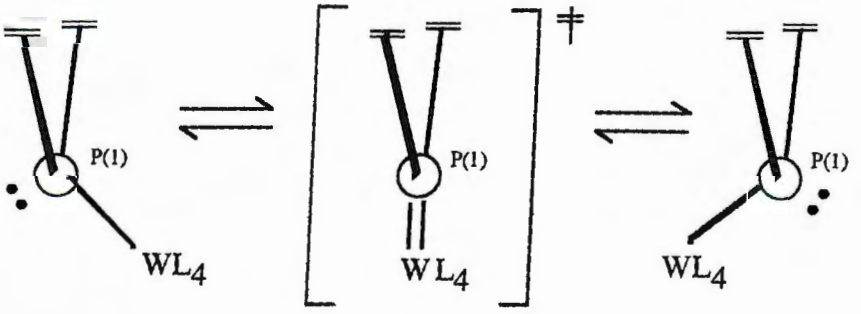


**Figure 6.5.** The proposed process of inversion for the $[(en)(CO)_3WP_7W(CO)_3]^{3-}$ ion depicting the double bond character of the intermediate.

The IR data for **9** show $\nu$(CO) bands blue shifted ~ 35 $cm^{-1}$ from the parent **2PM** indicating "effective oxidation" of $[P_7W(CO)_3]^{3-}$ upon attachment of the $(en)(CO)_3W$ fragment.[1] As stated earlier, this is approximately the same shift exhibited by **3** and **4**.[2,3] Structural comparison of **9b** with **3b** and **4b** shows the $P_7W(CO)_3$ core of **9b** virtually identical to the $P_7W(CO)_3$ cores of **3b** and **4b** (see Table 6.3) giving no structural indication why **9** exhibits inversion and **3** and **4** do not.[2,3]

## 6.4 Experimental

### 6.4.1 General Data

General operating procedures used in our laboratory have been described in Chapter 2.[1] General data not included in Chapter 2 follow. Proton ($^1$H) NMR spectra were recorded at ambient temperature on a Bruker AM400 (400.136 MHz) spectrometer. Carbon ($^{13}$C) NMR spectra were recorded at ambient temperature on Bruker AF200 (50.324 MHz) and Bruker AM400 (100.614 MHz) spectrometers. Some of the $^{13}$C NMR chemical shifts and couplings were confirmed by recording the spectra at different magnetic field strengths. Elemental analyses were performed under inert atmospheres by Desert Analytics, Tucson, AZ.

The IR and NMR spectral data common to all compounds containing [K(2,2,2-crypt)]$^+$ and/or en can be found in Chapter 2.

### 6.4.2 Material

The only material not included in Chapter 2 is trimethylphosphine that was purchased from Aldrich and used without further purification.

### 6.4.3 Synthesis

#### 6.4.3.1 Preparation of $[K(2,2,2\text{-crypt})]_3[(en)(CO)_3WP_7Cr(CO)_3]\cdot 2en$

$K_3P_7$ (29.6 mg, 0.089 mmol), 2,2,2-crypt (100.0 mg, 0.27 mmol) and (mesitylene)$Cr(CO)_3$ (22.7 mg, 0.089 mmol) were combined in en (~ 3 mL) and stirred for 12 h producing an orange solution. (Mesitylene)$W(CO)_3$ (34.4 mg, 0.089 mmol) was added as a solid and the reaction mixture was stirred for an additional 4 h yielding a dark red solution with a dark red powder precipitant. The solution was warmed gently

(~ 35 °C) to redissolve the precipitant, then allowed to slowly cool to ambient temperature. After 24 h, the reaction vessel contained a dark red microcrystalline solid. The solid was removed from the mother liquor, washed with toluene, and dried under vacuum (microcrystalline yield, 76 mg, 53 %). IR (KBr pellet), $cm^{-1}$: 1869 (m), 1848 (s), 1760 (sh), 1734 (s). $^{13}C\{^1H\}$ NMR (DMF-$d_7$) δ(ppm): 236 [s, $Cr(CO)_3$], 231 [m, $^1J_{C-W}$ = 171 Hz, $^2J_{C-P}$ = 6 Hz, $W(CO)_3$]. $^{31}P\{^1H\}$ NMR (DMF-$d_7$) δ(ppm): 187 [t, $^1J_{P-P}$ = 364 Hz, 1 P, P(1)], -5 [m, 2 P, P(2, 3)], -157 [m, 4 P, P(4, 6) and P(5, 7)]. Anal. Calcd for $C_{66}H_{132}K_3N_{12}O_{24}P_7CrW$: C, 38.71; H, 6.50 N, 8.21. Found: C, 37.39; H, 6.46; N, 8.21.

### 6.4.3.2 Preparation of $[K(2,2,2\text{-crypt})]_3[(en)(CO)_3WP_7W(CO)_3]\cdot 2en$

A procedure identical to that described for $[K(2,2,2\text{-crypt})]_3[(en)(CO)_3WP_7Cr(CO)_3]\cdot 2en$ was followed except (mesitylene)$W(CO)_3$ (34.4 mg, 0.089 mmol) was used in the reaction instead of (mesitylene)$Cr(CO)_3$. After 24 h, the reaction vessel contained a dark red microcrystalline solid. The solid was removed from the mother liquor, washed with toluene, and dried under vacuum (microcrystalline yield, 116 mg, 60 %). IR (KBr pellet), $cm^{-1}$: 1869 (m), 1849 (s), 1759 (sh), 1736 (s). $^{13}C\{^1H\}$ NMR (DMF-$d_7$) δ(ppm): 230 [m, $^2J_{C-P}$ = 3 Hz, $W(CO)_3$], 226 [m, $^2J_{C-P}$ = 3 Hz, $W(en)(CO)_3$]. $^{31}P\{^1H\}$ NMR (DMF-$d_7$) δ(ppm): 187 [tm, $^1J_{P-P}$ = 353 Hz, $^2J_{P-P}$ = 16 Hz, 1 P, P(1)], 2 [m, 2 P, P(2, 3)], -153 [m, 4 P, P(4, 6) and P(5, 7)]. Anal. Calcd for $C_{66}H_{132}K_3N_{12}O_{24}P_7W_2$: C, 36.37; H, 6.10; N, 7.71. Found: C, 36.29; H, 5.95; N, 7.96.

### 6.4.4. Exchange Reaction

$[K(2,2,2\text{-crypt})]_3[(en)(CO)_3WP_7Cr(CO)_3]\cdot 2en$ was prepared as described above. $K_3P_7$ (29.6 mg, 0.089 mmol) was added *in situ* as a solid and the reaction mixture stirred for an additional 12 h. An aliquot was removed and analyzed by $^{31}P$ NMR spectroscopy.

### 6.4.5. Crystallographic Experimental Details for $[K(2,2,2\text{-crypt})]_3[(en)(CO)_3WP_7W(CO)_3]\cdot 2en$

The single crystal X-ray diffraction study of $[K(2,2,2\text{-crypt})]_3[(en)(CO)_3WP_7W(CO)_3]\cdot 2en$ was done by Dr. James C. Fettinger, University of Maryland .

**Table 6.1.** Crystallographic data for $[K(2,2,2\text{-crypt})]_3[(en)(CO)_3WP_7W(CO)_3]\cdot 2en$.

| | |
|---|---|
| Empirical formula | $C_{66}H_{132}K_3N_{12}O_{24}P_7W_2$ |
| Formula weight | 2179.63 |
| Temperature, K | 293(2) |
| Radiation | Mo $K_\alpha$ ($\lambda$ = 0.71073 Å) |
| Crystal system | Triclinic |
| Space group | $P\bar{1}$ |
| Cell dimensions | $a$ = 14.396(4) Å $\alpha$ = 82.419(11) deg<br>$b$ = 17.543(3) Å $\beta$ = 76.830(14) deg<br>$c$ = 20.518(2) Å $\gamma$ = 69.16(2) deg |
| Volume, $Å^3$ | 4708(2) |
| Z | 2 |
| Density (calcd), $Mg/m^3$ | 1.538 |
| Absorption coefficient, $mm^{-1}$ | 0.343 |
| Crystal size, mm | 0.35 x 0.25 x 0.20 |
| Theta range for data collection | 2.01 to 22.48 deg |
| Index ranges | $0 \le h \le 15$, $-17 \le k \le 18$, $-21 \le l \le 22$ |
| Reflections collected | 12852 |
| Independent reflections | 12261 [R(int) = 0.0577] |
| Data / restraints / parameters | 12261 / 0 / 1017 |
| Goodness-of-fit on $F^2$ | 1.027 |
| Final R indices [$I > 2\sigma(I)$] [7741 data] | $R(F) = 0.0552$,[a]<br>$wR(F^2) = 0.1431$[b] |
| Largest diff. peak and hole, $e\cdot A^{-3}$ | 1.246 and -0.816 |

[a] $R(F) = \Sigma \mid F_o - F_c \mid / \Sigma F_o$. [b] $wR(F^2) = (\Sigma w \mid (F_o)^2 - (F_c)^2 \mid^2 / \Sigma wF_o^2)^{1/2}$.

**Table 6.2.** Selected Distances ( Å ) and Angles ( deg ) for the $[(en)(CO)_3WP_7W(CO)_3]^{3-}$ ion.

Distances

| | | | |
|---|---|---|---|
| P(1)-P(2) | 2.144(4) | P(1)-P(3) | 2.149(4) |
| P(2)-P(4) | 2.217(4) | P(2)-P(5) | 2.232(5) |
| P(3)-P(6) | 2.214(5) | P(3)-P(7) | 2.219(5) |
| P(4)--P(5) | 2.873(5) | P(6)--P(7) | 3.192(5) |
| P(4)-P(6) | 2.136(5) | P(5)-P(7) | 2.135(5) |
| P(1)-W(2) | 2.643(3) | P(4)-W(1) | 2.601(3) |
| P(5)-W(1) | 2.591(3) | P(6)-W(1) | 2.670(3) |
| P(7)-W(1) | 2.675(3) | W(1)-C(1) | 1.91(2) |
| W(1)-C(2) | 1.91(2) | W(1)-C(3) | 1.917(14) |
| W(2)-C(4) | 1.892(14) | W(2)-C(5) | 1.950(13) |
| W(2)-C(6) | 1.94(2) | C(1)-O(1) | 1.18(2) |
| C(2)-O(2) | 1.19(2) | C(3)-O(3) | 1.17(2) |
| C(4)-O(4) | 1.216(14) | C(5)-O(5) | 1.153(13) |
| C(6)-O(6) | 1.17(2) | W(2)-N(1) | 2.321(9) |
| W(2)-N(2) | 2.327(9) | N(1)-C(7) | 1.50(2) |
| N(2)-C(8) | 1.44(2) | C(7)-C(8) | 1.55(2) |

Angles

| | | | |
|---|---|---|---|
| P(1)-P(2)-P(4) | 104.0(2) | P(1)-P(3)-P(7) | 107.3(2) |
| P(2)-P(1)-P(3) | 115.0(2) | P(2)-P(4)-P(6) | 104.3(2) |
| P(3)-P(7)-P(5) | 103.3(2) | P(4)-P(2)-P(5) | 80.5(2) |
| P(6)-P(3)-P(7) | 92.2(2) | P(4)-W(1)-P(5) | 67.19(11) |
| P(4)-W(1)-P(6) | 47.79(11) | P(6)-W(1)-P(7) | 73.37(11) |
| P(2)-P(4)-W(1) | 105.0(2) | P(3)-P(7)-W(1) | 97.0(2) |

| | | | |
|---|---|---|---|
| P(4)-P(6)-W(1) | 64.43(12) | P(7)-P(5)-W(1) | 68.17(13) |
| P(4)-W(1)-C(1) | 137.7(4) | P(5)-W(1)-C(1) | 134.2(4) |
| P(6)-W(1)-C(3) | 174.4(4) | P(7)-W(1)-C(2) | 172.7(4) |
| W(1)-C(1)-O(1) | 176.5(13) | W(1)-C(2)-O(2) | 179.5(14) |
| W(1)-C(3)-O(3) | 174.7(13) | P(1)-W(2)-C(4) | 177.1(4) |
| P(1)-W(2)-N(1) | 86.3(2) | W(2)-C(4)-O(4) | 178.6(11) |
| W(2)-C(5)-O(5) | 178.0(10) | W(2)-C(6)-O(6) | 178.3(11) |
| W(2)-N(1)-C(7) | 112.4(8) | C(4)-W(2)-C(5) | 88.9(5) |
| C(5)-W(2)-C(6) | 83.9(5) | N(1)-W(2)-C(4) | 91.0(4) |
| N(1)-W(2)-N(2) | 74.9(4) | N(1)-C(7)-C(8) | 109.6(11) |

**Table 6.4.** Spectroscopic data of **2PM** and **9** complexes.

| Compound | IR[a] | NMR[b] | | | | | |
|---|---|---|---|---|---|---|---|
| | | $^{31}P$ | | | $^{13}C$ | | |
| | $\nu_{C-O}$ ($cm^{-1}$) | δ (ppm) | J (Hz) | | δ (ppm) | J (Hz)[c] | |
| | | | $^{1}J_{P(1)-P(2,3)}$ | $^{2}J_{P(1)-P(4,5,6,7)}$ | | $^{1}J_{C-W}$ | $^{2}J_{C-P}$ |
| **2PCr** | 1829,1738,1716 | 204,-20, -139 | 370 | 11.7 | 246 | | <2 |
| **9a** | 1869, 1848, 1760, 1734 | 185, -6, -157 | 369 | 12.4 | 236<br>231 | 171 | 6 |
| **2PW** | 1837, 1728 | 184,-7, -159 | 369 | 12.4 | 232 | 180 | 5 |
| **9b** | 1869, 1849, 1759, 1736 | 187, 2, -153 | 353 | 15.5 | 230<br>226 | | 2<br>3 |

[a] KBr pellets. [b] $^{31}P$ NMR (DMF-$d_7$), ambient temperature, 81.015 MHz; $^{13}C$ NMR (DMF-$d_7$), ambient temperature, 100.614 MHz.
[c] Some coupling constants were determined with negative line broadening.

## 6.5 References


(1) Charles, S.; Eichhorn, B. W.; Rheingold, A. L.; Bott, S. G. *J. Am. Chem. Soc.* **1994**, *116*, 8077-8086.

(2) Charles, S. C.; Eichhorn, B. W.; Fettinger, J. C. **1995**, in preparation.

(3) Charles, S.; Fettinger, J. C.; Eichhorn, B. W. *J. Am. Chem. Soc.* **1995**, *117*, 5303-5311.

(4) Charles, S.; Eichhorn, B. W.; Fettinger, J. C.; Bott, S. G. **1995**, in preparation.

(5) Trotter, J.; Paddock, N. L.; Calhoun, H. P. *J. Chem. Soc., Dalton Trans.* **1973**, 2708-2712.

(6) Buhro, W. E.; Chisholm, M. H.; Folting, K.; Huffman, J. C.; Matrin, J. D.; Streib, W. E. *J. Am. Chem. Soc.* **1992**, *114*, 557-570.

(7) Cotton, F. A.; Kraihanzel, C. S. *Inorg. Chem.* **1963**, *2*, 533-540.

(8) Braterman, P. S.; Milne, D. W.; Randall, E. W.; Rosenberg, E. *J. Chem. Soc., Dalton Trans.* **1973**, 1027-1031.

(9) Lambert, J. B. *Top. Stereochem.* **1971**, *6*, 19-105.

(10) Rauk, A.; Allen, L. C.; Mislow, K. *Angew. Chem. Int. Ed. Engl.* **1970**, *9*, 400-414.

(11) Haake, P.; Turley, P. C. *J. Am. Chem. Soc.* **1967**, *89*, 4617-4621.

(12) Abel, E. W.; Bush, R. P.; Hopton, F. J.; Jenkins, C. R. *J. Chem. Soc., Chem. Commun.* **1966**, 58-59.

(13) Baudler, M.; Hahn, J.; Arndt, V.; Koll, B.; Kazmierczak, K.; Därr, E. *Z. Anorg. Allg. Chem.* **1986**, *538*, 7-20.

(14) Baudler, M.; Glinka, K. *Chem. Rev.* **1993**, *93*, 1623-1667.

(15) Baechler, R. D.; Mislow, K. *J. Am. Chem. Soc.* **1971**, *93*, 773.